

41 0640154 3



ProQuest Number: 10183450

All rights reserved

INFORMATION TO ALL USERS

The quality of this reproduction is dependent upon the quality of the copy submitted.

In the unlikely event that the author did not send a complete manuscript and there are missing pages, these will be noted. Also, if material had to be removed, a note will indicate the deletion.



ProQuest 10183450

Published by ProQuest LLC (2017). Copyright of the Dissertation is held by the Author.

All rights reserved.

This work is protected against unauthorized copying under Title 17, United States Code
Microform Edition © ProQuest LLC.

ProQuest LLC.
789 East Eisenhower Parkway
P.O. Box 1346
Ann Arbor, MI 48106 – 1346

328413

THE NOTTINGHAM TRENT UNIVERSITY LLR	
Short Loan	PHD/ BNS/ OS
Ref	KAS

**PRIME Surface Coating:
A Novel Method for Making Thick
Ceramic Coatings**

Mehrdad Kashefi
B. Eng, M. Eng

*A thesis submitted in partial fulfilment of the requirements of The
Nottingham Trent University for the degree of Doctor of Philosophy*

2005

Abstract

The use of coatings to protect or enhance the performance of a component manufactured from a different material is well recognised as a cost effective solution in many engineering situations. This approach is particularly appropriate for ceramic materials deposited as coatings. However, in general such coatings are either relatively thin (<0.1mm) with very good properties, or thicker but with mechanical properties that are somewhat less good.

The present study has investigated the development of a novel coating technique, primarily concentrating on ceramics in the first instance, with the aim of producing relatively thick uniform coatings with good mechanical properties. This novel method is based on initially depositing a coating mixture based on a fine ceramic powder in a cyanoacrylate binder. This experimental investigation has concentrated on the selection and examination of several possible materials for the coatings and substrates and has developed procedures for the mixing, application, debinding and sintering of the coating mixtures.

It was determined that ceramic powders could be well dispersed in an alkoxyethyl cyanoacrylate binder to a maximum volume fraction of 0.45 for uni-modal powders with mean particle sizes $\sim 8 \mu\text{m}$, and 0.58 for a bi-modal alumina powder. Para-toluene sulphonic acid and caffeine have been identified as suitable polymerization inhibitors and initiators respectively. Coatings with controlled thicknesses between 0.4 and 1.0 mm have been successfully deposited onto metallic and ceramic substrates. SEM micrographs show good uniformity of the coating and that successful adhesion can be achieved, as also shown by the joint shear strength test results. The versatile properties of the cyanoacrylates suggest that there are potential applications for the coatings at the cured stage.

This study also describes and discusses the debinding and sintering of alumina and zirconia coatings. Using 96% alumina substrates resulted in successful sintering of the debonded layers to full density. The microstructural studies show good uniformity in the coatings with good adhesion to the substrate. The indentation hardness and toughness values measured in the sintered coatings were comparable with the results obtained on the commercial alumina used as the substrate.

Acknowledgments

I would like to express my gratitude to my supervisor, Professor Les Henshall, for his support throughout this research program. His expertise, understanding, and patience, added considerably to my knowledge and experience. I appreciate his vast knowledge and skill in many areas and his assistance in writing reports and papers as well as proof reading this dissertation. I would also like to thank the other member of my committee, Professor Barry Hull for the assistance provided at all levels of the research project. I greatly appreciate Dr Ahmad Lotfi for taking time out from his busy schedule to serve as a moral mentor for giving motivation and encouragements at times of need. I must also acknowledge Professor Birkinshaw for his suggestions on cyanoacrylate and supporting thermo gravimetric testing on mixtures.

Very special thanks go to Miss Judith Kipling, who provided me with direction, technical support and Mr Allen Chambers for making the rigs and technical assistance; both became more of a friend than a member of staff. My thanks are also given to Mr Gary Griffiths for all of his computer and technical advice throughout this study. I would also like to thank my friend in the materials team Mr Siak Hong Ng, for the exchanges of knowledge, skills, and venting of frustration during these several years of the program.

I recognize that this research would not have been possible without the financial assistance of the Nottingham Trent University, College of Science and Technology and express my gratitude to them.

Last, but not least, I want to express my loving appreciation to my mother for the support she provided me through my entire life.

Table of Contents

Chapter 1:	Introduction	
1-1	General.....	1
1-2	Aim/Objectives.....	2
1-3	Research methodology.....	3
1-4	Publications/Presentations.....	3
Chapter 2:	Literature Review	
	<i>Introduction</i>	5
2-1	Classification and properties of ceramics.....	5
2-1-1	General.....	5
2-1-2	Mechanical properties.....	6
2-1-3	Electronic and magnetic properties.....	6
2-1-4	Thermal and chemical properties.....	7
2-2	Ceramic processing techniques.....	8
2-2-1	General.....	8
2-2-2	Dry processing.....	8
2-2-3	Wet processing.....	9
2-2-3-1	Slip casting.....	9
2-2-3-2	Tape casting.....	9
2-2-4	Plastic forming.....	10
2-2-4-1	Ceramic injection moulding (CIM).....	10
2-2-4-2	Powder reaction injection moulding technique (PRIME)...	11
2-3	Ceramic coating techniques.....	13
2-3-1	General.....	13
2-3-1	Thin film.....	14
2-3-1-1	Sol gel.....	14
2-3-1-2	CVD.....	14
2-3-1-3	PVD.....	15
2-3-2	Thick film.....	15
2-3-2-1	Ink jet technique.....	15
2-3-2-2	Thermal spray.....	15

2-4	Coating characterisation techniques.....	16
2-4-1	General.....	16
2-4-2	Micro-hardness Test.....	17
2-4-3	Scratch test.....	19
2-4-4	Bend test.....	20
2-4-5	Friction and wear tests.....	21
2-5	Ceramic powder manufacture.....	21
2-5-1	General.....	21
2-5-2	Alumina powder.....	22
2-5-3	Zirconia powder.....	24
2-6	Cyanoacrylate.....	26
2-6-1	General.....	26
2-6-2	Cyanoacrylate chemistry and polymerization.....	28
2-7	Liquid/Solid mixing.....	30
2-7-1	General.....	30
2-7-2	Powder.....	30
2-7-3	Binder.....	32
2-7-4	Additives.....	34
2-7-5	Powder to binder ratio.....	34
2-7-6	Rheology of liquid-solid mixtures.....	35
2-8	Debinding.....	36
2-8-1	General.....	36
2-8-2	Debinding Processes.....	36
2-8-2-1	Solvent extraction.....	37
2-8-2-2	Thermal debinding.....	37
2-8-3	Thermal degradation of cyanoacrylate.....	39
2-9	Sintering.....	41
2-9-1	General.....	41
2-9-2	Solid state sintering.....	42
2-9-3	Liquid state sintering.....	46
2-9-4	Sintering of alumina.....	49
2-9-5	Sintering of zirconia.....	52

Chapter 3: Materials Processing & Mixing

<i>Introduction</i>	54
3-1 Materials Specification.....	55
3-1-1 Binders.....	55
3-1-2 Ceramic powders.....	56
3-1-3 Inhibitor.....	62
3-1-4 Initiator.....	62
3-1-5 Indicator.....	63
3-1-6 Surfactant.....	63
3-1-7 Sintering aid.....	63
3-1-8 Substrate.....	63
3-2 Coating mixture preparation.....	64
3-2-1 Pre-processing treatments.....	64
3-2-2 Mixing procedures.....	65
3-3 Mixing component composition and concentration effects..	66
3-3-1 Inhibition of the cyanoacrylate polymerization.....	66
3-3-2 Effect of powder.....	67
3-3-3 Effect of binder.....	68
3-3-4 Solid loading.....	68
3-3-5 Effect of surfactant.....	70
3-4 Influence of coating mixture composition on viscosity.....	71
3-5 pH measurements.....	75
3-6 Summary.....	76

Chapter 4: Coating Application & Properties

<i>Introduction</i>	78
4-1 Application of the coating.....	79
4-2 Curing of the Mixture.....	81
4-2-1 Curing methods.....	81
4-2-1-1 Water vapour.....	81
4-2-1-2 Substrate surface activation.....	82
4-2-1-3 Caffeine treatment.....	82
4-2-2 Effect of caffeine on curing.....	84
4-2-3 Gas release during curing.....	86

4-3	Powder-Substrate-Cyanoacrylate chemical compatibility...	87
4-3-1	Sample preparation.....	87
4-3-2	Surface treatment of Aluminium substrate.....	88
4-3-3	Effect of powder chemistry.....	88
4-4	Property testing procedures.....	95
4-4-1	Shear strength test.....	95
4-4-2	Hardness test.....	100
4-5	Irregular substrate.....	101
4-6	Summary.....	102
Chapter 5: Debinding		
	<i>Introduction</i>	104
5-1	'Pure' cyanoacrylate debinding characterisation.....	105
5-2	Binder thermal analysis.....	106
5-2-1	Thermal gravimetric analysis.....	107
5-2-2	Differential scanning calorimetry.....	108
5-3	Heating methods.....	109
5-3-1	Debinding procedure.....	109
5-3-2	Influence of fast heating rate.....	110
5-3-3	Step heating of the coating layer.....	111
5-4	Debinding prior to full curing.....	117
5-5	Summary.....	118
Chapter 6: Sintering		
	<i>Introduction</i>	120
6-1	Equipment used for sintering.....	121
6-1-1	Induction furnace.....	121
6-1-2	Temperature measurement and control.....	123
6-1-3	Preparation of samples for SEM study and mechanical tests	125
6-2	Solid state sintering.....	126
6-2-1	Procedure for making the coating.....	126
6-2-2	Sintering of the coatings.....	126
6-3	Liquid state sintering.....	130
6-3-1	Procedure for making coatings.....	130

6-3-2	Sintering of the modified coating.....	131
6-4	96% alumina tile.....	135
6-4-1	96% alumina substrates.....	135
6-4-2	Procedure for making the coating.....	138
6-4-3	Study of the coatings.....	139
6-4-3-1	Uni-modal alumina powder coating.....	139
6-4-3-2	Bi-modal alumina powder coating.....	144
6-4-3-3	Stabilized zirconia powder coating.....	147
6-5	Summary.....	149
Chapter 7: Summary & Discussion		
	<i>Introduction</i>	151
7-1	Materials processing & mixing.....	152
7-2	Application & curing.....	155
7-3	Debinding.....	150
7-4	Sintering.....	158
7-5	Summary.....	162
Chapter 8: Conclusions & Recommendations for Future Research		
	<i>Introduction</i>	163
8-1	Conclusions.....	163
8-1-1	Materials processing & Curing.....	164
8-1-2	Debinding.....	165
8-1-3	Sintering.....	166
8-2	Recommendations for future research.....	167
8-2-1	Process developments.....	167
8-2-2	Properties measurements.....	167
8-2-3	Applications.....	167
	References	169

1

Introduction

1-1 General

The ability to change the surface properties of components independently of the bulk material properties by use of surface coatings is widely utilised by industry in sectors such as aerospace, automotive, biomedical and tooling. Ceramic coatings include oxide, nitride, carbide, boride, cermet, diamond and diamond-like carbon coatings (Freitag 1998). They have been used for many years to solve problems of wear and corrosion or provide resistance to high temperatures (Foresight report 2002). A range of coating technologies from thermal and plasma spray to vapour deposition (both chemical and physical) and sol gel are used to deposit such coatings (Bunshah 2001). They have opened up many new and diverse applications and have undergone considerable development.

Although new ceramic coating materials are likely to be developed for specialist applications, it is perceived that much of the growth in the ceramics coating industry would lie in developing new coating technologies. In particular there is significant current research into the deposition of ceramic coatings onto metals or other materials, which are more economical or offer flexibility or performance unmatched by existing processes or major developments in the improvement of existing coating methods (Foresight report 2002, Freitag 1998). These requirements cannot be delivered by a single coating material. There is thus a trend to develop multi-layer, multifunctional coatings that combine useful

properties. Nanostructured coatings can show properties greatly enhanced from the average properties predicted by the individual constituents of the coating.

1-2 Aim and Objectives

The aim and objectives of the present research were, in outline:

Aim:

- To investigate the use of cyanoacrylate loaded with solid particulates to develop a novel method for the production of thick coatings, which adhere well to a variety of substrates after the curing and sintering stages.

Objectives:

- To determine suitable powders, binders and additives that can be successfully used in the developed method.
- To formulate a procedure for mixing cyanoacrylate and particulates for deposition as a coating onto flat and irregular substrates.
- To study the reproducibility of the mixing process in terms of uniformity and effective viscosity.
- To investigate the factors affecting the bonding between the cyanoacrylate carrier and the particulate materials and also substrates.
- To select a curing method for the coating on metallic and ceramic substrates over a period of time such that handling and deposition could be satisfactorily performed, and with the goal of reproducibility of the curing process.
- To study the microstructural and mechanical properties of the cured coatings.
- To study the thermal degradation behaviour (temperature range and rate) of the cyanoacrylate, and coating mixtures containing cyanoacrylate as a binder after curing.
- To investigate methods to ensure that the debonded layer will retain its integrity after debinding, and establish a thermal debinding cycle which leads to macro-defect free debonded layers.
- To sinter defect free ceramic coatings of controlled thickness with good adhesion to a suitable ceramic or metallic substrate in a controlled and reproducible procedure.

- To study the microstructures of the sintered coatings, substrate and substrate-coating interface and determine the final microhardness of the sintered coatings.

1-3 Research Methodology

The methodology adopted in this study was primarily experimental. The approach taken was to proceed in a sequential manner through considered and controlled investigations of the following:

- The starting point is the determination of suitable component materials to be able to produce a homogeneous particulate dispersion in a cyanoacrylate matrix. This will involve the consideration of the effects of cyanoacrylate base formulation, powder chemistry, shape and size distribution, polymerization, inhibitors and initiators, and other additions such as surfactants or pH indicators to monitor the state of the mixtures. These topics are covered in Chapter 3.
- The next phase of the research was to develop procedures and processes for the successful deposition of thick, 0.2 – 2 mm, layers of cyanoacrylate bonded particulates onto flat and shaped substrates. The microstructures of the layers and interface regions, and the properties of these would require investigation, as described in Chapter 4.
- Debinding of the deposited layers will be studied to enable macro-defect free adherent powder coatings to be obtained, as outlined in Chapter 5.
- This was followed by an investigation into the sintering to full density of the deposited, debonded layers, combined with microstructural study and hardness testing, Chapter 6.

1-4 Publications/Presentations

[1] “PRIME Coatings”, SET for Britain (Science, Engineering and Technology for Britain) House of Commons, UK, March 2004. (poster presentation)

[2] “PRIME Surface Coatings”, International Congress for Particle Technology, PARTEC 2004, Nuremberg, Germany, March 2004. (oral presentation)

[3] “PRIME Surface Coating - A Novel Technique of Applying Thick Ceramic Coatings”, 3rd ASM International Surface Engineering congress, Orlando, USA, August 2004. (oral presentation)

[4] “PRIME Coatings- a Novel Thick Ceramic Coating”, UK Coating Forum – Characterisation and Performance of Thick Coatings, National Physical Laboratory (NPL), London, UK, November 2004. (poster presentation)

2

Literature Review

Introduction

The word ceramic derives from the Greek KERAMOS, meaning “a pottery” or from an older root “to burn” (Haber and Smith 1991). However, modern usage of the term broadens the meaning to include all inorganic and non-metallic materials. Today, ceramic products touch our lives in many ways. Their applications include magnetic, optical and electronic as well as wear and heat resistant applications.

2-1 Classification and Properties of Ceramics

2-1-1 General

There are many possible approaches to classifying ceramics. They can be grouped by their chemical composition, their properties or their uses. Table 2.1 summarizes the classification of ceramics by their chemical composition (Somiya 1989).

The properties of ceramics can be generally divided into three major groups: mechanical: electronic and magnetic: and thermal and chemical.

Table 2.1 Classification of ceramics by chemical composition (Somiya 1989)

Oxides	SiO ₂ , Al ₂ O ₃ , Fe ₂ O ₃ , FeO, Fe ₃ O ₄ , CaO, MgO, Mn ₂ O ₄ , TiO ₂ , ZrO ₂ , HfO ₂ , ThO ₂ , BeO, Y ₂ O ₃ , La ₂ O ₃ , CeO ₂
Binary compounds	3Al ₂ O ₃ ·2SiO ₂ -2Al ₂ O ₃ ·SiO ₂ , Al ₂ SiO ₅ , MgSiO ₃ ,
Ternary compounds	Mg ₂ SiO ₄ , CaO·MgO, Ca ₂ SiO ₃ , Ca ₃ Si ₂ O ₇ , MgAl ₂ O ₄ , FeCr ₂ O ₄ , MgFe ₂ O ₄ , MgCr ₂ O ₄ , FeTiO ₃ , CaTiO ₃ , 3Y ₂ O ₃ , 5Fe ₂ O ₂ (Y ₆ Fe ₁₀ O ₂₄), BaO·6Fe ₂ O ₃ (BaFe ₁₂ O ₁₉), Ba ₂ SiO ₄ (phenacite)
Quaternary compounds	3CaO·MgO·2SiO ₂ (merwinite), 2CaO·MgO·2SiO ₂ (akermanite), 3BeO·Al ₂ O ₂ , 6SiO ₂ (beryl), 2MgO·2Al ₂ O ₃ ·5SiO ₂ (cordierite), Li ₂ O·Al ₂ O ₃ ·2SiO ₂ (eucryptite), 2CaO·Al ₂ O ₃ ·SiO ₂ (gehlenite), 3CaO·Al ₂ O ₃ ·2SiO ₂ (grossuralite), Na ₂ O·Al ₂ O ₃ ·SiO ₂ (nephelite), 3MgO·Al ₂ O ₃ ·3SiO ₂ (pyrope), Li ₂ O·Al ₂ O ₃ ·4SiO ₂ (spodumene)
Carbides	SiC, WC, TiC, TaC, ZrC, B ₄ C
Nitrides	Si ₃ N ₄ , BN, TiN, ZrN, AlN
Oxynitrides	Sialon

2-1-2 Mechanical Properties

Ceramics have several major advantages over metals and other materials: i.e. superior hardness, wear and abrasion resistance. On the other hand it is true that ceramics are inferior in term of brittleness especially with their low impact and thermal shock resistance. A striking breakthrough was the development of fully dense silicon carbide (SiC), silicon nitride (Si₃N₄), Sialon (a solid solution of β-Si₃N₄ and Al₂O₃) and high toughness partially stabilized zirconia (PSZ). Generally, interest in the mechanical strength of ceramics is increasing to give full access to their functional characterization (Nunomura et al. 1989).

It is worth mentioning that because of the unique combination of properties that ceramics possess they have found roles in other fields of technology. For example, although alumina has been developed extensively as a structural ceramic, high-purity alumina ceramics have also played an important role as a bone substitute for orthopaedic and dental implants, as well as in the field of maxillary and oral surgery (Inamori 1989).

2-1-3 Electronic and Magnetic Properties

Electronic ceramics have a wide range of usage. The insulators in spark plugs, used in internal combustion engines in vehicles, are usually made from 90-96% alumina (Al₂O₃) porcelain with small amounts of CaO, MgO and SiO₂ added to lower the sintering temperature. Boron nitride (BN) is low in density and has

excellent electrical insulating properties. Ceramics also show semiconductor characteristics. Some examples include thermistors, varistors, capacitors and sensors. Examples of ceramics used for these purposes are SrTiO_3 and BaTiO_3 .

Another example of the use of an advanced ceramic is that of stabilized zirconia, which is used in oxygen sensors that must be used under very severe conditions; such as in furnaces or automobile exhaust equipment (Wakino 1989). Another very important family of ceramic materials is ferrite (Fe_2O_3), and its solid solutions such as Mn-Zn ferrite along with Ba and Sr ferrite which form the mainstream of magnetic materials. For example barium ferrite ($\text{BaO}\cdot 6\text{Fe}_2\text{O}_3$) is used as a permanent magnet (Hiraga 1989).

2-1-4 Thermal and Chemical Properties

The thermal properties of ceramics include heat resistance, thermal conductivity, thermal insulation and low thermal expansion.

To produce a high thermal conductivity the following conditions are necessary: the crystal structure must be simple; the constituent atoms must be light elements with relatively low packing density and their diameters uniform; the bond strength between atoms must be high; and pores, impurities or other defects must be few (Kawakaubo and Yamamoto 1989). The volume fraction, size and shape of any second phase, such as pores, affect the thermal conductivity of polycrystalline ceramics. In addition, when impurities exist in a solid solution or a secondary phase, they reduce the thermal conductivity. SiC, BeO, MgO, alumina and cubic boron nitride are good thermal conductors. In contrast, silicates and stabilized zirconia are poor thermal conductors.

Low thermal expansion ceramics usually have strongly covalent interatomic bonds and form crystals with loosely packed anions such as oxygen. Silicon ceramics, such as Si_3N_4 , with comparatively low coefficients of thermal expansion are outstanding in mechanical properties at high temperature and offer great promise as engine parts; for instance, as part of a gas turbine engine

The chemical properties of ceramics may be used in a wide variety of applications such as humidity sensors, ceramic chemical sensors or surface electrometer gas

sensors, ion concentration sensors, and batteries for high temperature use (Hayakawa and Sekida 1989).

2-2 Ceramic Processing Techniques

2-2-1 General

Although there is a wide range of methods for making ceramic parts, most ceramic fabrication processes begin with finely ground powder. The objective is usually to achieve the greatest degree of particle packing and a good degree of homogeneity. Purity, particle size and distribution, reactivity and polymorphic form can all affect the final properties and thus must be considered from the outset. Forming transforms the ceramic powders and additives into a green product. Drying and binder elimination are the possible following procedures with sintering as the final step in ceramic processing. Table 2.2 summarizes the major techniques for the consolidation of powders and producing shapes (Richardson 1992).

Table 2.2 Major techniques used for ceramic fabrication (Richardson 1992)

<i>Pressing</i>	<i>Fugitive- mold casting</i>
Uniaxial	Gel casting
Hot isostatic pressing	Electrophoretic deposition
	<i>Tape casting</i>
<i>Slip casting</i>	Doctor blade
Drain casting	Waterfall
Solid casting	<i>Plastic forming</i>
Vacuum casting	Extrusion
Pressure casting	Injection moulding
Centrifugal casting	Compression moulding

2-2-2 Dry Processing

The majority of ceramic parts are made by dry consolidation techniques, principally pressing. This shaping method is inexpensive and suitable for high-volume production of simple shapes (limited geometrical possibilities) such as

refractories, tiles, electronic ceramics, etc. High production rates and close tolerances can be achieved by using a high pressure. The powders that are used must be agglomerated in order to evenly fill the die and moulds (Matsumoto 1991). The pressure can be asserted uniaxially or isostatically. Uniaxial pressing involves the compaction of powder into a rigid die by applying pressure in a single axial direction through a rigid punch or piston. Isostatic pressing uses a fixed elastomeric mould that is pressurised externally by a fluid. In hot pressing, the die/fluid is heated at the same time as the pressure is exerted, which sinters the powder during the pressing operation.

2-2-3 *Wet Processing*

Wet consolidation methods are usually techniques used to fabricate complex structures. In these methods the powder is placed in an aqueous carrier. Wet colloidal processing provides exceptional microstructural uniformity of the resulting ceramic "green body". Additionally, submicron grains inherently involved in colloidal processing increase the driving force for densification, to result in desirable fine-grained microstructures at relatively low temperatures.

2-2-3-1 *Slip Casting*

This method is one of the oldest methods for forming ceramics, especially hollow shapes. The basic process involves the suspension of a powdered material in a fluid. The colloidal suspension is poured into a porous mould and the fluid is removed from the mixture by capillary action. As a result, a layer of powder consolidates at the mould surface and grows as more liquid enters the mould wall. The green part can be removed from the mould and sintered (Ainsley and Gong 1999).

2-2-3-2 *Tape Casting*

The tape casting, or doctor blade process, is a shape forming technique for powders, which produces thin, flat sheets. A powder containing slurry layer is formed on a carrier film by a shearing action on a stationary or moving ceramic slurry. After drying, the tape contains a binder system, which gives it enough 'green strength' to be removed from the carrier film without damage. The binder is

burnt out and the tape is usually sintered. Typical thicknesses are in the range 300-1000 μm . Applications cover a wide range including thin alumina substrates for the electronics industry (Albano and Garrido 2005) and ferromagnetic and dielectric uses (Jantunen et al 2004).

2-2-4 Plastic Forming

Plastic forming involves producing shapes from a mixture of powder and additives that are deformable under pressure. Among the methods in this group, ceramic injection moulding (CIM) has been regarded as a preferred method for making many precision engineering and electrical components. This particular method is discussed in more detail in the following section.

2-2-4-1 Ceramic Injection Moulding (CIM)

This technique is one of the newest methods for ceramic forming. The advantage of the process is that it produces near net shape parts with higher density and improved mechanical properties compared to the traditional methods.

A schematic diagram of the production sequence is given in Fig. 2.1 (German and Bose 1997). The process consists of four basic parts; mix preparation, part formation, binder removal and sintering (Janney et al 1995). After having mixed fine ceramic powders and a thermoplastic binder to form a pelletised moulding compound, this mixture, called "feedstock", is then injected into a mould cavity. The plastic binder is used only as a carrier for the ceramic powder in order to obtain the desired geometry by injection. After injection, the binder is no longer needed and is removed (debinding) and the remaining powder structure sintered; these last two steps can be combined into a single thermal cycle.

The process has many variants, reflecting different combinations of powders, binders, moulding techniques, debinding routes and sintering conditions. Detailed reviews of the process have been written by German and Bose (1997), Mutsuddy and Ford (1995) and more technologically by Binner (1990) and King (2002).

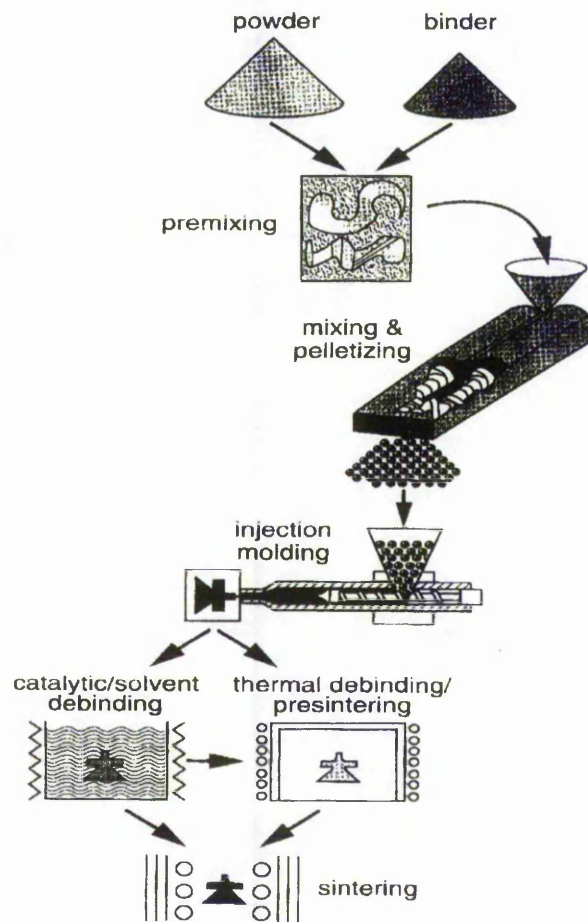


Fig. 2.1 Schematic diagram of powder injection moulding
(German and Bose 1997)

2-2-4-2 Powder Reaction Injection Moulding Technique (PRIME)

Despite its rapid commercial success, there are still several technically recognized problems for conventional CIM processing techniques, using polymers as binders. The most commonly cited difficulty is with the binder. A binder that makes for easy moulding is very difficult to control in debinding. On the other hand, a binder that proves easy to extract in debinding is usually difficult to mould without defects (German and Hens 1991). Another problem regarding binders is the long debinding time. This can take hours or even days (Ridgway et al 1997, Li 2003).

A method to overcome this problem by using cyanoacrylate as a reactive binder and carrier based on powder reaction moulding technology was first developed by Hull et al (1996). The reactive binder can be removed in minutes from the powder

compact by thermal depolymerization and recovered for use (Ridgway et al 1998). Birkinshaw et al (1996), using stainless steel and silicon nitride powders, studied the effect of powder volume fraction and inhibitor concentration on inhibition time. They suggested that dissolving measured quantities of para-toluene sulphonic acid in cyanoacrylate monomer would inhibit the polymerization reaction. The results demonstrated that the inhibition characteristics vary with the kind of powder and reduce as the powder concentration increases, confirming the importance of the powder surface area and its surface chemistry in controlling the inhibition of polymerization. It has also been claimed that acid washing and drying of the ceramic powder does not reduce its reactivity.

Using pyridine, t-butylamine or caffeine as an initiator, small moulded balls of the monomer-powder mixture were brought into contact with the initiator. The first two were effective but caffeine was not, probably because of the hindered diffusion condition. They also mentioned the role of some premature surface polymerization on increasing the viscosity.

In addition to Birkinshaw's observations (1996), which were undertaken on a laboratory scale, another approach to making a novel seamless conduit ceramic heart valve was developed by Ridgway (2000). Using butyl cyanoacrylate as the binder and alumina powder, he investigated the process parameters such as powder and inhibitor volume fraction, initiator and debinding conditions. Alumina powder was mixed with the binder to a volume fraction as high as 0.5. To prevent polymerization while mixing, p-toluene sulphonic acid was used as an inhibitor and batches of feedstock were polymerized in hot water, cold water, steam and a hot oven. It was found that the steam or hot water media provided the most suitable neutralisation of the acid within a five hour period. It was also found that the cyanoacrylate would debind most efficiently between 210°C and 230°C. This conclusion was based on data obtained from a differential scanning calorimeter. The actual parts were debonded within two hours at a heating rate of 5°C/min up to 220°C. The parts were finally sintered at 1750°C with a hold time of either 60 or 100 minutes.

More recently, the machinability of the green compacts made by this method has been examined (Ng et al 2003, 2004).

2-3 Ceramic Coating Techniques

2-3-1 General

Coating is used for an enormous range of applications including electronic, optical, protection at high temperature, corrosion and thermal protection and wear resistance. Many of these applications require the properties associated with non-metallic materials; i.e. ceramics.

The protective coating of metallic components, especially by the application of ceramic films, is one of the most rapidly changing technologies involving a wide range of recently developed techniques. Many techniques have been developed and commercialised during the past 30 years for applying a ceramic coating with thickness ranging from less than 1 μm to greater than 1 mm. Table 2.3 shows a summary of the areas of application with some typical examples for each (Wachtman and Haber 1993).

Table 2.3 Uses of ceramic films and coatings (Wachtman and Haber 1993)

Use	Typical Ceramic Material
Wear Reduction	Al_2O_3 , B_4C , Cr_2O_3 , Cr B_2 Cr Si_2 , Cr_2Si_2 , DLC^* , Mo_2C MoSi_2 , SiC , TiB_2 , TiC , WC
Friction Reduction	MoS_2 , BN , BaF_2
Corrosion Reduction	Cr_2O_3 , Al_2O_3 , Si_3N_4 , SiO_2
Thermal Protection	Ca_2Si_4 , MgAl_2O_4 , MgO , ZrO_2 (Mg or Ca stabilized)
Electrical conductivity	$\text{In}_2\text{O}_3/\text{SnO}_2$, $\text{YBa}_2\text{Cu}_3\text{O}_{7-x}$
Semiconductors	GaAs , Si
Electrical Insulation	SiO_2
Ferroelectricity	$\text{Bi}_4\text{Ti}_3\text{O}_{12}$
Electromechanical	AlN
Selective optical transmission and reflectivity	BaF_2/ZnS , CeO_2 , CdS , $\text{CuO}/\text{Cu}_2\text{O}$, Ge/ZnS , SnO_2
Optical wave guides	SiO_2
Optical processing (electrooptic, etc.)	GaAs , InSb
Sensors	SiO_2 , SnO_2 , ZrO_2

* DLC = Diamond-like carbon

The special properties of ceramics lead to a wide range of applications. Because of the availability of a wide range of ceramic compounds, and the ability to introduce additives into their structures, their electronic and optical properties can

be tailored to make them semiconductors or electro-optic materials. Because of their basic bonding some possess large and useful amounts of ferroelectricity, ferromagnetism or piezoelectricity. Finally, many ceramics have great hardness and strength.

Ceramic coating technology has been affected by many lines of progress in related technologies. This progress includes developments in film processing, film characterization, and the materials science of ceramics. Practical ceramic films vary greatly in function and thickness and each coating is required to satisfy the specific needs of a given application (Laux et al 1998).

There are a number of methods such as sol-gel (Klien 1988) and several physical vapour deposition (PVD) processes (Bunshah 2001), which produce excellent thin films on a substrate, but are not usable for thick films on complex geometry surfaces. Other techniques which can be used to form thick coatings, such as electro-deposition or flame spraying (Wachtman and Haber 1993) provide either lower quality coatings or are limited in the range of materials and/or substrate geometry.

2-3-1 *Thin Film*

2-3-1-1 *SolGel*

Sol gel can be defined as the making of ceramic materials by preparation of a sol, gelling of the sol, and removal of the solvent (Brinker and Scherrer 1990). A sol is a colloid of solid particle in a liquid. A gel is composed of a single 3-dimensional interconnected rigid network of a highly dispersed solid containing a highly dispersed liquid. The resulting gel can be fired to crystallize and/or densify the material (Wachtman and Haber 1993).

Sol-gel processing is largely limited to objects, which are small in at least one direction, e.g. coatings, fibres or particles. Sol-gel processing of ceramics is used because of the degree of microstructural and compositional control available as well as homogeneity, which is impossible to obtain using other techniques.

2-3-1-2 *CVD*

Chemical Vapour Deposition (CVD) is generally defined as a deposition of solid materials on the surface of a substrate, which is normally heated, as a result of a

chemical reaction in the gaseous phase (Bunshah 2001). This atomistic deposition technique can produce high purity materials with atomic structural control. It can produce single layer, multi layer composite, and functionally graded coatings for a wide range of applications including hard coating, protection against corrosion, diffusion barrier, and semiconductor (Choy 2003).

2-3-1-3 PVD

Physical vapour deposition (PVD) involves the creation of material vapour (by evaporation or sputtering), transporting the vapour phase to the substrate surface, and subsequent condensation on the surface of a substrate to form a film. The application covers over a very wide range from decorative to superconducting films (Bushah 2001).

2-3-2 Thick film

2-3-2-1 Ink Jet Technique

This technique demands well dispersed ceramic inks which pass through a nozzle. In continuous form uniform sized droplets of ink are deflected from a recycled stream onto a substrate (Blazell and Evans 2000). The substrate may be deformable or uneven. The selective adhesion of compacted ceramic powder allows extremely complex refractory shapes to be produced. The process can be used to produce a wide range of coatings from organic semiconductors (Yuming et al 2004) to functionally graded materials (Mott and Evans 1999).

2-3-2-2 Thermal spray

Thermal spray is a general term used to describe all the techniques consisting of the melting of selected powders in a high temperature chamber, followed by accelerating and directing the droplets onto a substrate. The coating is formed by the immediate solidification of the molten droplet on the surface of the substrate, which is normally at a much lower temperature.

This technique covers a wide range of modifications (Wachtman and Haber 1993) from atmospheric plasma spraying (Guessasma et al 2005) to multi-layered ceramic coating prepared by combined laser and flame spraying (Li et al 2004). The variety of thermal spray applications is impressive. They have wide industrial applications to provide wear resistance (Psyllaki et al 2001), corrosion resistance

(Singh et al 2005) and thermal insulation (Sharafat et al 2002) on metallic substrates.

2-4 Coating Characterization Techniques

2-4-1 General

Ceramic coatings are being used effectively in various applications including optical, and at high temperatures for wear, abrasion and corrosion resistance. Adhesion in this case is defined by ASTM (D907-70) as “the state in which two surfaces are held together by interfacial forces which may consist of valence or interlock forces or both”. These bonding forces are effective at the coating-substrate interface. The coating adhesion is central to the functionality of the coating-substrate system.

In most applications, the minimum criterion for acceptable performance is that the adhesion of the coating to the substrate should be sufficient such that the coating remains in place for the lifetime of the component in its operating environment (Rickerby 1996). Attempts have been made to measure coating-substrate properties (Petrie 2000) alongside the bulk properties of adhesives (Dean and Duncan 1998). Surveys of the test methods for coating adhesion have been reported by Rickerby (1996) and Maxwell (2001). Table 2.4 shows some of the methods for measuring the adhesion properties of coatings. Indentation (Lawn 1998), scratch (Meneve et al 2001), and wear (Axen 2000) tests as well as pull-off, tensile (Maxwell 2001) and bend (Kadolkar and Dahotre 2003) tests are among the most widely used ones. Modelling of the coating response has also attracted intensive attention (Bull et al 2004, Christofides et al 2002).

More recently the soft impresser test has been developed to study the deformation and fracture of materials under either single or multiple point contact load application. This has primarily been developed by Guillou et al (1993) and Henshall et al (1995) with Brookes et al (1997), Waddington et al (1997) and Maerky (1997) having applied the method to assess the integrity of coatings.

Table 2.4 *Methods that can be used to determine coating-substrate properties (Rickerby 1996)*

Qualitative	Quantitative
<i>Mechanical methods</i>	
Scratch test	Direct pull-off test
Scotch tape test	Laser spallation test
Abrasion test	Indentation test
Bend test	Ultracentrifuge test
	Bend test
	Linear elastic fracture mechanics
<i>Nonmechanical methods</i>	
X-ray diffraction	Thermal method
	Nucleation test
	Capacity test

2-4-2 *Micro Hardness Test*

The hardness measurement of traditional (Kim 2002) and advanced ceramics (Ullner et al 2001, McColm 1990) has been of a great interest, since it is related to a number of other important properties or performance aspects of ceramics and its value helps to characterise resistance to deformation, densification and fracture (Quinn 1998).

The concept of hardness has no precise definition and several models being used to interpret hardness values such as “tensile strength” and “ease of plastic flow” (McColm 1990). An inverse square root relationship between hardness and grain size, similar to equation 2.1, has been observed in a number of ceramics over a range of grain sizes and indentation loads that is, hardness generally increases with decreasing grain size (Chinn 2002) as the dislocations generated by the indenter are blocked by the grain boundaries (McColm 1990).

$$\sigma_f = \sigma_o + K / \sqrt{D} \quad (2.1)$$

D = Equivalent Grain Diameter

σ_f = Fracture Stress

σ_o = Friction Stress

K= Constant

However, some authors have reported hardness decreasing with decreasing grain size (mainly at large grain diameters) (e.g. Rice et al 1994), probably, reflecting the relatively weak bonding in the grain boundary region (McColm 1990). For instance, for ceramics such as Al_2O_3 , the hardness has been reported to firstly decrease with increasing grain size up to the 10-50 μm range, and then to increase with further increase in grain size to the single crystal value (Rice et al 1994).

Furthermore, for a given material, the hardness number obtained generally increases with decreasing load. It has been proposed that the reasons for this are associated with the varying response of the material under the high localised pressure of the indenter, involving plastic flow and fracture (Morrell 1985), although there is no interpretation which is commonly accepted.

Microhardness, or more accurately microindentation hardness, is a measurement of the size of a microindentation made by a diamond pyramid-shaped indenter of specified size and shape pressed into a polished surface with a known load. It is usually measured using a Vickers or Knoop Diamond indenter.

The Vickers indenter has four-fold symmetry but makes a deeper indentation and is more inclined to cause fracture in brittle materials than the Knoop indenter.

Vickers microhardness uses a pyramid with 90° base angles and 136° face angles and loads up to ~ 1000 g. The Vickers indenter is not recommended for microhardness measurements of most sintered ceramics, because the indentations are very small and tend to crack the surrounding regions, and therefore the true size of the indentation is difficult to determine accurately. The hardness is calculated from the mean length of the two diagonals as shown in equation 2.2 (Chinn 2002).

$$HV \text{ (kgf/mm}^2\text{)} = 1.8544 P / \bar{d}^2 \quad (2.2)$$

HV = Vickers hardness number

P = Indenter load (kg)

\bar{d} = The mean of the two diagonals (mm)

The Knoop indenter has only two fold symmetry and is commonly used on ceramics, because the long axis of the indentation is typically 2.5 times the diagonal length of a Vickers impression at the same load, and thus should be more readily measurable (Morrell 1985). It uses a pyramid with two 136° base angles and loads up to approximately 1000 g. It often gives a higher value than the equivalent Vickers value at low loads and a lower value than the Vickers at high loads (Quinn 1998). The hardness is calculated from the length of the longer axis only of the indentation, and the applied force (Chinn 2002). It uses the projected area of the impression instead of the actual surface area (Morrell 1985).

$$HK \text{ (kgf/mm}^2\text{)} = 14.229 P/d^2 \quad (2.3)$$

HK = Knoop hardness number

P = Indenter load (kg)

d = Length of the longer diagonal of the Knoop indentation (mm)

The microhardness of a coating is best measured on a polished cross-section through it, which is thus independent of the flatness and smoothness of the surface of the coating and is less prone to influence by the substrate.

There is generally a fair scatter of results obtained on ceramics as a consequence of 1) their multiphase nature, 2) their general non-cubic crystal symmetry and, 3) their porosity, which may be unseen below the surface of the test piece (Morrell 1985). The effect varies with the size of the indentation and porosity and grain boundary phases (Morrell 1987). As a result, a coefficient of variation up to 15% (Chinn 2002) or 20% (Morrell 1985) for microhardness measurements on one specimen is considered acceptable.

2-4-3 *Scratch Test*

The adhesion between a coating and its substrate would generally be an important parameter affecting the performance under service conditions. The scratch test can be used to provide a measure of coating-substrate adhesion. In most cases, a diamond stylus is drawn across the coated surface under an increasing load. Each coating technique is intended to satisfy the specific needs of a given application (stepwise or continuous) until some well-defined failure occurs. The normal load corresponding to the failure is called the critical load (Meneve et al 2001). In the automatic scratch test the normal load is continually increased along the length of

the scratch track by a spring loaded mechanism. The alternative manual test procedure uses deadweight loading and hence requires the performance of many scratches to assess the critical load for coating detachment. The important factors affecting the critical load include, loading rate, scratching speed, machine factor, indenter tip radius, coating and substrate properties (Rickerby 1996). The failure could include coating detachment, plastic deformation and through-thickness cracking or cracking of the coating or substrate (Bull 2001).

The scratch test has also been used to determine both interfacial and cohesive failure strength for thick films. In this case the material to be tested is in the form of a polished cross section and scratches are performed across the coating by starting from the substrate using stepwise increasing loads. This can be used to qualitatively rank coating-substrate adhesion (Rickerby 1996).

2-4-4 Bend Test

In mechanical methods, adhesion is determined by the application of a force to the coating/substrate system. This force may be normal to the interface as in the pull-off test, or parallel to it as in shearing test or bend test (Bunshah 2001). Most of the methods used to evaluate adhesive properties of coatings give semi-quantitative or qualitative results only.

Three-point and four-point bending tests are widely used to assess adhesion between a coating and its substrate. These techniques involve inducing a tensile strain in the coating using three or four-point bending and detecting damage caused to the coating, for example by using acoustic emission monitoring (Maxwell 2001). The fracture stress (flexural strength) in the test piece is calculated from the force applied at the moment of fracture and the dimensions of the test-jig and the test piece. Flexural strength results depend on the span between supports, the specimen geometry, and the condition of the surface and surface defects. Three point bending has the advantages of being easier to undertake with a simpler test-jig arrangement, and also being less prone to errors of test jig geometry and alignment, which makes it favoured for QA purposes. Four-point bending, despite requiring more attention to detail, is preferred because a larger volume of the test sample is placed under a more uniform stress. Consequently, strengths determined in four-point tests are more representative of

the average surface material and are more appropriate for obtaining design data. For in-house quality assurance or materials development use, or for particular component or test-piece shape, testing can be performed in any appropriate manner, provided that the stressing geometry is consistent (Morrell 1997).

Since ceramics are brittle, it should also be noted that the larger a specimen is, the greater the volume under test, and the lower the average strength. In bending with three-point loading, rather than four-point loading with the same overall span, a higher mean strength will result because a smaller volume is being subjected to high stress.

2-4-5 *Friction and Wear Tests*

Friction and wear are caused by a set of microscopic interactions between surfaces that are in mechanical contact against each other. These interactions are the result of the topographical characteristics of the surface and the condition of the experiment such as temperature, atmosphere, type of contact, etc. Most common wear tests use either wearing surfaces with fixed (or loose) abrasives, or sliding (or rolling) wearing surfaces (Axen 2001).

2-5 *Ceramic Powder Manufacture*

Due to the nature of ceramics, the raw materials used in their production have a much greater impact on their final properties than in the cases of other groups of materials such as metals or polymers. Ceramics have traditionally been based on oxide minerals, or other minerals that can be decomposed to yield oxides, such as hydroxides, carbonates, sulphides, halides, phosphates etc.

2-5-1 *General*

Ceramic powder processing commonly uses ceramic materials, liquids and processing aids. The starting batches undergo different chemical or physical operations such as crushing, milling, washing, chemical dissolution, flotation, magnetic separation, dispersion, mixing, classification, filtering and dry spraying (Reed 1995). Drying is commonly used to remove residual processing liquid. Finally, application of a surface coating may be used, such as with electronic powders.

2-5-2 Alumina Powder

Alumina, the most versatile of ceramic oxides, has been reviewed in detail in Gitzen and Louis (1970) and Morrell (1987). Alumina is insoluble in water and very slightly soluble in strong acid and alkaline solutions. The interatomic bonding forces, which are partially ionic and partially covalent, are extremely strong and its structure is physically stable up to 1500-1700°C (Smallman and Bishop 1999).

Some useful properties of alumina are its high melting temperature (2050°C), chemical resistance, electrical resistance, compressive strength and hardness (Lee and Rainforth 1994), although the mechanical properties generally decrease above ~1100°C (Miyayama 1991). Alumina is brittle and should not be subjected to either impact or excessive tensile stresses during service. In addition, its sensitivity to thermal shock should be considered (Smallman and Bishop 1999). Table 2.5 shows some of the engineering properties of Alumina (Miyayama 1991).

Table 2.5 *Engineering properties of alumina, 99.9% (Miyayama 1991)*

Density	3.99 g/cm ³
Modulus of elasticity	393 GPa
Poisson's ratio	0.22
Hardness	85 R45N
Coefficient of thermal expansion	7.4 10 ⁻⁶ /K
Thermal Conductivity	0.39 W/cm.K

Alumina is produced in relatively large quantities using the Bayer process. The principal raw material for alumina production is bauxite (Al₂O(OH)₄). In this process, prepared bauxitic ore is digested under pressure in a hot aqueous solution of sodium hydroxide and then 'seeded' to induce precipitation of Al(OH)₃ crystals (Gibbsite). The Bayer process removes impurities such as SiO₂, Fe₂O₃, TiO₂ leaving a nominal 99.5% alumina product with time, temperature and agitation as the main process parameters. Gibbsite is chemically decomposed by heating (calcined) at a temperature of 1200-1400°C. Bayer calcine, which consists of α-Al₂O₃ (>99%) is graded according to the nature and amount of impurities. Sodium

oxide, Na₂O ranges up to 0.6% and is of some significance as a result of its affect on the sintering behaviour and electrical resistance. The Bayer process produces highly-aggregated powders in the range of 0.5 -100 µm and the chosen grade of alumina, together with any necessary additives, is ground in a wet ball-mill to a specific size range. This enables high packing densities and reduced porosities in the green state (Smallman and Bishop 1999). Eventually the powder is dried giving an alumina of up to 99.99% purity (Lee and Rainforth 1994).

Deliberate additions may be made to an alumina for a number of reasons, including lowering the sintering temperature, avoiding grain growth, improving the rheology in powder shaping, and modifying the properties of the final product (Morell 1987). Development of alumina to meet increasingly stringent demands has focused mainly on control of the chemical composition and grain structure. The high-alumina ceramics can be divided broadly into a number of groups based on composition, porosity, grain size and application. Consequently, there is a wide range of particle size, chemical compositions, purity levels and microstructures produced to meet the desired properties. A detailed review of alumina groups has been presented by Morrell (1987).

The term 'high-alumina ceramic' is normally used for alumina ceramics containing more than 80% Al₂O₃, depending on the application, usually with corundum as the principal crystalline phase with its hexagonal structure (Morrell 1987).

Alumina used for high temperature applications, such as thermocouple sheaths and boats, needs to have a minimum amount of glassy phase and large grain size (up to 200 µm). The alumina content for use at temperatures above 1200°C needs to be more than 99% Al₂O₃ (Morell 1985). Many parts for electrical and engineering application have 99-99.7% Al₂O₃. The electrical resistance is greatest, and dielectric loss factor is lowest, in materials of highest alumina content and lowest alkali content.

High purity alumina (>99.7%) powders are used to produce essentially single phase ceramics of fairly uniform grain size. A small amount of MgO (0.05%) may be added to suppress grain growth during solid state sintering. When MgO is added the grain size is considerably reduced and the product is stronger.

Materials with 94-99% alumina have a deliberately formulated glassy phase produced by the addition of amounts of SiO₂, MgO, and/or CaO. Depending on the amount of secondary phase, the microstructures show evidence of this glassy phase at the grain boundaries and in isolated pockets. Secondary crystalline phases may also be present depending on the added component(s), as well as the sintering temperature and cooling rate. Phases such as anorthite (CaO.Al₂O₃.2SiO₂), mullite (Al₂O₃.2SiO₂) and cordierite (2MgO.2 Al₂O₃.5SiO₂) may be present in lower alumina content ceramics (Morrell 1985).

2-5-3 *Zirconia Powder*

Zirconium oxide (ZrO₂) has a very high melting point (2680°C), chemical durability and is hard and strong. It has long been used for refractory purposes and as an abrasive medium. A major difficulty limiting the widespread applications of ceramics in engineering has been their low toughness. The discovery in 1970 by Garvie (1970) of a method of controlling the microstructure to produce relatively high toughness in zirconia led to development of a wide range of zirconia based ceramics. The preparation and properties of zirconia-based materials have been reviewed in detail by Steven (1986 and 1991).

Zirconia is polymorphic, existing in three crystalline forms, the monoclinic (m), tetragonal (t), and cubic(c) phases (Smallman and Bishop 1999). In pure zirconia the monoclinic phase is stable up to about 1170°C where it transforms to the tetragonal phase, which is stable up to 2370°C, when the cubic phase exists up to the melting point (2680°C).

The technique of transformation-toughening depends on stabilizing the high-temperature tetragonal(t) metastable phase at room temperature. Stabilization, partially or in whole, is achieved by adding certain oxides (Y₂O₃, MgO, CaO) to zirconia (Stevens 1986). In the metastable condition, the surrounding structure opposes the expansive phase transition from tetragonal to monoclinic. When a crack is propagating, in the stress concentration region around the crack tip the martensitic transformation of t-zirconia rich solid solution into the less dense (3-5%v) and stable m-phase occurs. This transformation mechanism is responsible

for the toughening effect resulting from the existing metastable phase in the microstructure.

Yttria is particularly effective as a stabilizer, although there is a significant problem associated with the degradation experienced in steam at 100-120°C. Generally three kinds of stabilized zirconia can be found. The relative stability can be expressed in terms of the phase diagram of the zirconia rich end of the ZrO_2 - Y_2O_3 system as shown in Fig. 2.2. The same principles apply in a general sense to the other stabilizing oxides.

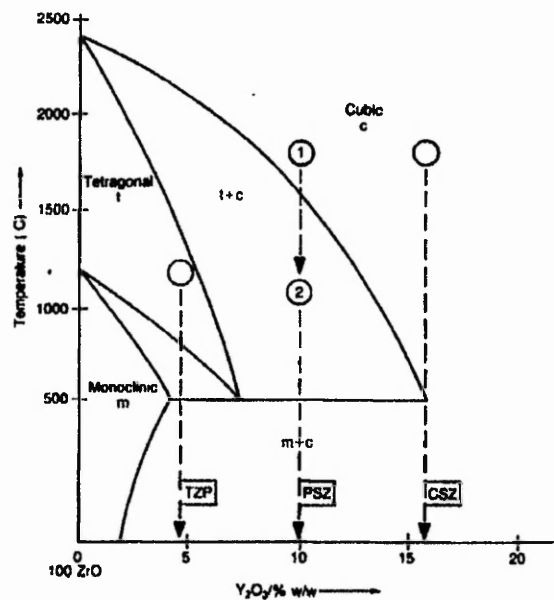


Fig. 2.2 Schematic phase diagram for the ZrO_2 - Y_2O_3 system (Smallman and Bishop 1999),

TZP= Tetragonal Zirconia Polycrystalline

PSZ=Partially-Stabilized Zirconia

CSZ=Fully-stabilized Cubic Zirconia

1- Tetragonal Zirconia Polycrystalline (TZP) contains the least amount of oxide additives. Up to 2.5 % mole Y_2O_3 can be taken into solid solution allowing a fully tetragonal ceramic to be obtained (Lee and Rainforth 1994). It is single phase and is produced by sintering ultra-fine powder in the temperature range of 1350-1500°C, well within the phase field for the tetragonal solid solution.

2- Partially-Stabilized Zirconia (PSZ) is generated in zirconias containing more than 3 mole% Y_2O_3 . Small t-crystals are dispersed as a precipitate throughout a matrix of coarse cubic grains. Zirconia is mixed with a higher percentage of additives (8-10% mole) and heat treated in two stages. Sintering in the temperature range of 1650-1850°C produces a parent solid solution with a cubic structure, which is then modified by heating in the range 1100-1450°C. This second treatment induces the precipitation of coherent t-crystals within the cubic grains (Smallman and Bishop 1999).

3- Fully-stabilized Cubic Zirconia (CSZ) refers to materials in which the crystal structure is completely cubic, and thus cannot take advantage of the toughening transformation. These materials are used as refractories or, in single crystal form, gemstones.

The ceramic toughness is controlled by the amount of transformation. A large number of factors control transformability such as composition, solute content, elastic modulus, grain size, particle shape and residual stress (Lee and Rainforth 1994, Stevens 1986, Smallman and Bishop 1999).

2-6 Cyanoacrylate

2-6-1 General

Solvent-free, one-part cyanoacrylate adhesive first appeared in the industrial market nearly 45 years ago when Eastman 910 was introduced. Since then it has become widely used in a range of industries including the automotive, beauty aid, electrical, electronic, machinery, medical, and plumbing (Scheenberg 1990). The lower members of the series are used for applications such as the assembly of delicate electronic components and household items. The higher homologues, i.e. butyl-, hexyl-, and heptyl- being wetted well by blood, are used in surgery, e.g. as tissue binder and fingerprinting (Negulescu et al 1987). Thus they can have different formulations, viscosities, cure times, strength properties, temperature resistance and low odour and non-blooming characteristics, which have been developed to satisfy particular application requirements (Loctite 2004).

In principle, cyanoacrylate monomers can be prepared simply. An alkyl cyanoacetate and formaldehyde are condensed in the presence of a basic catalyst. The resultant polymer is carefully dried and stripped of solvent. The dry polymer

is pyrolysed to generate the monomer which is redistilled in an atmosphere of sulphur dioxide to give the final product (Millet 1981). Although as a result of recent studies many new kinds of cyanoacrylates are being developed to improve their performance, they behave fundamentally in the same way. Since cyanoacrylates form polar molecules and most substrates are also polar, the adhesion is good because polar materials attract one another by bringing their polar charged areas as close together as possible.

Table 2.6 lists several commercially available cyanoacrylate esters and their properties (Scheenberg 1990).

Table 2.6 *Commercially available cyanoacrylate esters (Scheenberg 1990)*

Ester	Radical group, R	Properties
Methyl	—CH ₃	Strongest bonds on metals; good solvent and temperature resistance
Ethyl	—CH ₂ CH ₃	General purpose; forms strong bonds on metals, plastics, and rubbers
Allyl	—CH ₂ CH=CH ₂	Use temperatures above 100°C
Butyl	—CH ₂ CH ₂ CH ₂ CH ₃	Plastic and rubbers; improved flexibility; less irritating vapour than that of lower cyanoacrylates
2-methoxyethyl	—CH ₂ CH ₂ OCH ₃	Low odour; improved flexibility; Non-fogging
2-ethoxyethyl	—CH ₂ CH ₂ OCH ₂ CH ₃	Same as 2-methoxyethyl

The advantages of cyanoacrylates include:

- Extreme rapidity of cure under very light pressure
- High tensile and shear strengths of the bonds.
- Low fire and toxic hazards because no solvents are involved
- Ease of application: the adhesive is a one component system requiring no mixing, hence automation is facilitated
- Versatility: cyanoacrylates are capable of bonding most substrates. Polyethylene, polypropylene, and Teflon are exceptions.

- Solvent resistance: cyanoacrylates generally resist most solvents. The exceptions are acetone, nitro-methane, dimethyl sulphoxide and dimethylformamide.

Cyanoacrylates have many desirable properties, but they are not ideal adhesives.

The disadvantages of cyanoacrylates can be listed as follows:

- Inadequate performance under peeling and impact loading
- Susceptible to acidic or very dry substrate surface conditions
- Poor heat and moisture resistance
- Relatively expensive

2-6-2 *Cyanoacrylate Chemistry and Polymerization*

Cyanoacrylate adhesives are polar and linear molecules which are based on acrylic monomers and are characterised by their extremely fast cure to form a thermoset polymer. The cyanoacrylate monomers can be polymerized by both free radical and anionic mechanisms, but the latter hold much greater interest. This is mainly because for this mode of polymerization, they are among the most reactive monomers known and, as a consequence of this extreme reactivity, they are capable of initiation by relatively weak covalent bases (Szeto 1989). This occurs through anionic addition across the carbon-carbon bond, as illustrated in Fig. 2.3 (Cook and Allen 1993).

A carbon-carbon double bond exists in each molecule, and the glue remains fluid as long as these bonds exist. Changing the bond to a single one produces a free extra bond, which allows the molecules to form long chains of new single bonded molecules. The result is polymerized glue.

This anionic reaction is inhibited at $\text{pH} < 5.5$ (Cook and Allen 1993), hence monomers are kept in their liquid form by the addition of a weak acid during storage and prior to use. In order to be an effective stabilizer, the inhibitor must be soluble in the monomer. Lewis acids are appropriate inhibitors. These include sulphur dioxide, carboxylic acids (Cook and Allen 1993), trichloroacetic, picric, and para-toluene sulphonic acid (Birkinshaw et al 1996) and sulfones (Lee 1981). Oxygen, CO_2 and H_2O have virtually no effect on the development of polymerization due to the relatively high stability of the cyanoacrylate carbanions (Negulescu et al 1987).

Prior to polymerization, neutralization of the acids takes place. Any practical, weak electron donor base, such as moisture on the surface of a substrate, can trigger the polymerization reaction. Basic chemicals such as sodium carbonate, phosphates, amines, or pyridine can be used to neutralize the stabilizer and so accelerate polymerization. (Lee 1981, Birkinshaw et al 1996). However, if the speed of bonding is too fast, the bonds become weakened during formation (Lee 1981) due to inadequate substrate wetting or to the formation of an inert skin that can prevent full cure (Scheenberg 1990). Dombroski and Weemes (1976) have used caffeine to polymerize cyanoacrylate in a gap as thick as 15 mm.

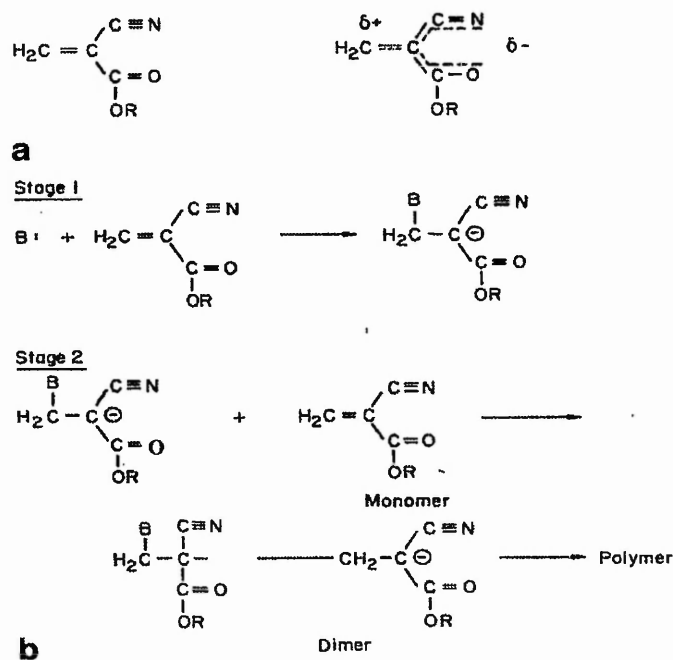


Fig. 2.3 (a) Simple structure of cyanoacrylate ester (left) and polarized form (right). (b) Stages of polymerization for cyanoacrylate (Cook and Allen 1993)

Generally, the final bonding properties depend on many factors. The most important ones are: chemical compatibility between the adhesive and the substrate, contaminants on the surface, humidity, ambient temperature and surface morphology (Cook and Allen 1993).

2-7 Liquid/solid mixing

2-7-1 General

A mixture of ceramic powder and liquid binder should have appropriate viscosity, morphology and composition to produce a suitable feedstock for subsequent processing. Two objectives of the mixing are to coat each particle with a thin layer of the polymer and to achieve a homogenous mixture. Wei et al (1998) have noted that the mixing sequence can also affect the viscosity and homogeneity of alumina-based formulations for injection moulding. Electrostatic and Van der Waals forces lead to the formation of small particle agglomerations, which in turn result in a high porosity in the mixture, low packing density, and non-uniform properties. As a result, additives are usually required to achieve adequate dispersion of the particles, and thereby obtain optimum flow and packing in the feedstock, by wetting the particles, breaking the agglomerates and lowering the viscosity (Mutsuddy 1991). Close packing reduces the amount of porosity, which must be removed during sintering, and also increases the sintering rate.

2-7-2 Powder

As for all ceramic forming techniques, the particle characteristics are of prime importance for a PIM technique. Although the most important parameters are powder size, shape distribution and packing characteristics, the chemical nature of the particles and/or binder can also play a major role.

As the particle size decreases, the surface area to volume ratio increases, and thus surface effects begin to have a greater influence on the particle behaviour in the mixture (Mutsuddy 1991). In general, the smaller the particle size, the higher is the viscosity of the moulding mix (Janney 1995). Round particles have been shown to yield the highest packing densities (Mutsuddy and Ford 1995).

Particle size distribution is also an important parameter affecting the packing density. Practically, the particle size distribution can generally be changed in two ways, i.e. mixing two or more particle sizes (coarse and fine powders), or using a wide continuous distribution of particle sizes (Mutsuddy and Ford 1995). This enables the finer particles to fill the holes between the large particles. Hence, broad (Yeh and Sacks 1988) or multimodal (Sato 1998) distributions are preferred

to a narrow distribution. The definition of an ideal PIM powder could be as follows (German and Bose 1997);

- Particle size between 0.5 and 20 micrometres, with D_{50} between 4 to 8 micrometres
- Either a very narrow or very wide particle size distribution
- Density over 50% of theoretical
- No agglomeration
- Nearly spherical, equiaxed powder,
- A compact angle of repose over 55°
- Dense particles free of internal voids
- Low explosion and toxicity hazards
- Clean particle surface
- Minimal segregation

The packing density of the mixture changes as the relative amounts of the coarse and fine fractions in the mixture changes. According to the Furnas model (1928) based on a simple space-filling argument, a size ratio of at least 7 is needed to get an optimum packing density in a binary mixture of spherical particles. In practice, as result of deviations from an 'ideal' powder, such as non-spherical shape and agglomeration, this ratio should be at least 10 (Mutsuddy and Ford 1995).

Increasing the number of particle sizes in the mixture can also increase the packing density. The effect of different size ratios on the specific volume for different weight fraction of fine particles is shown in Fig. 2.4. As can be seen, the minimum specific volume increases with an increase in the size ratio.

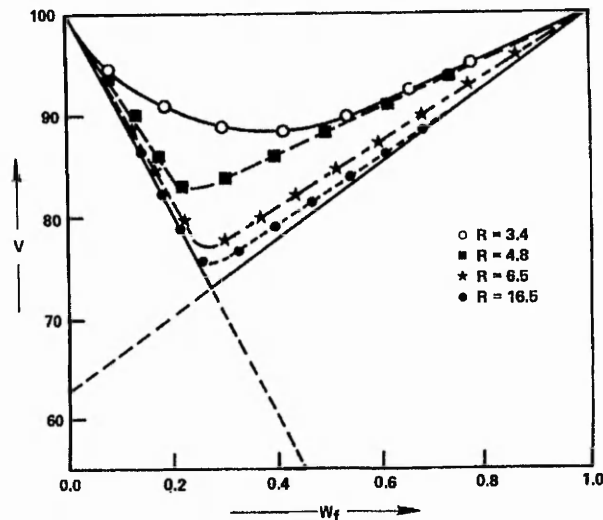


Fig. 2.4 Effect of particles with different size ratios on the specific packing volume (Mutsuddy and Ford 1995)

One of the standard ‘rules-of thumb’ for a bimodal system is that a ratio of approximately 70% ‘coarse’ particles and 30% ‘fine’ particles can result in the highest packing density (Smith 1984, Sato 1998, German 1996).

However, it must be borne in mind that for a particular application certain particle features may dominate. For instance, although small particle size would generally lead to faster sintering, which is usually commercially beneficial, it would also give rise to a higher viscosity in the mixture and also increase the time required for debinding. Also, a wide distribution size helps to give a higher packing density but may lead to an inhomogeneous microstructure, as well as a longer debinding time (German and Bose 1997). Another example is that spherical powders are frequently selected to improve the packing density and to lower the viscosity, but they would generally form a weaker compact after debinding (Goncalves 2001).

2-7-3 *Binder*

Although the binder is temporary and should not affect the final composition of the mixture, the selection of a binder formulation that gives the correct flow properties is of primary importance and has a major influence on the success of any PIM process. German and Bose (1997) have divided the characteristics of a binder for injection moulding into four types;

- 1) Flow characteristics: the binder should have viscosity below 10 Pa.s at the moulding temperature and little viscosity change during moulding. It should also be strong after moulding and consist of small molecules which can fit between particles.
- 2) Powder interaction: it should have low contact angle and good adhesion with the powder, be chemically passive with respect to the powder and thermally stable during mixing and moulding. For example, the mixing of silicon carbide powder with an acidic waxed based binder is difficult, but mixing alumina with the same binder is much easier (German and Hens 1991)
- 3) Debinding: it is desired that the binder be made of multiple components with different characteristics. The decomposition products should be non-corrosive, non toxic and have low ash content. The decomposition temperature should be above the moulding and mixing temperature, with complete removal before sintering.
- 4) Manufacturing: it is necessary for the binder to be inexpensive and readily available, safe, environmentally acceptable and re-usable, with a long shelf life and no volatile component. Beyond that, it should have high thermal conductivity, low coefficient of thermal expansion, and short chain length with no orientation.

Most of the binders in use fall into three categories; wax or oil based binders, water based binders and solid polymers (German and Hens 1991). Waxes such as polyethylene and polystyrene are widely used in ceramic forming and vary in their chemical and physical properties. The binder may be natural vegetable, animal or mineral in origin, or made by chemical reaction (Mutsuddy and Ford 1995). In most cases they are multi-component, with the mixture being developed to suit a particulate application, with the backbone polymer generally controlling the flow, viscosity, green strength and debinding behaviour.

2-7-4 Additives

Additives affect the performance of the feedstock during injection moulding by modifying the cohesive forces between the binder and the ceramic powders. The primary function of surfactants is to provide a modification of the powder surface in order to achieve some degree of steric stabilization between powders in a polymer matrix. They can provide either sufficient repulsion between particle surfaces or a reduction in the inter-particle attraction (Tseng 2000) which has the effect of reducing the mixture viscosity, without sacrificing the solid loading. Particle interactions in ceramic suspensions and the roles of processing additives have been reviewed by Horn (1995) and Reed (1995).

Additives may also be required for other reasons; they may act as lubricants to decrease friction, and/or they may be used as sintering aids to assist densification (Richardson 1992). They can also be used as wetting agents and deflocculants (Mutsuddy and Ford 1995). Among the most commonly used additives are oleic acid, stearic acid, fish oil, dibutyl phthalate and olefin sulonate.

2-7-5 Powder to Binder Ratio

Another important factor is a balanced and appropriately selected powder to binder ratio. Most PIM mixtures have a solid loading between 45% to 75% by volume, and many ceramic powders are in the range 50-55 vol.% depending on the particular powder and binder. The optimum amount of binder represents a compromise between maintaining the desired rheological conditions and minimizing the amount of binder. The relative proportions will depend on powder and binder compositions, and the powder particle size distribution (Mutsuddy and Ford 1995).

The term critical solid loading is defined as a composition where the particles are packed as closely as possible, and all the space between them is filled with binder. This provides the maximum mixture density, and varies with each powder-binder system. The critical solid loading can be measured by several approaches such as density measurement, melt flow, mixing torque and viscosity versus composition (German and Bose 1997). Above the critical solid loading, the viscosity is very high and voids form in the mixture. On the other hand, excess binder results in slumping during debinding and shape distortion. Most mixtures are made with

less powder than the critical powder loading, which gives a sufficiently low viscosity for moulding, and good particle-particle contact. It has been reported that the viscosity starts to increase rapidly at about 55 vol% solids for a uni-modal powder, and over 70 vol% solids for a bi-modal powder containing 25% fine powder (Richardson 1992).

The optimal concentration of the binder in a mixture depends on the particle packing parameters, such as particle size, distribution and shape. The optimum binder content is generally between 102 and 115% of the void volume (Richardson 1992) or 2-5% more than that corresponding to the critical solid loading (German and Bose 1997).

2-7-6 *Rheology of Liquid-Solid Mixtures*

Rheology is the science of deformation and flow. The rheology of an injection-moulding mixture is determined by the volume percentage of solids and the nature of the binder, plasticizer and other additives (Richardson 1992). Although there is considerable interest in employing formulations with the maximum volume fraction of powder in order to achieve high green density and reduce shrinkage on sintering, the viscosity increases with increase in filler loading, and therefore it is necessary to reduce the viscosity as far as possible (Edirisinghe and Evans 1987).

In general, the smaller the particle size, the higher the viscosity of the injection moulding mixes and the coarser the powder, the higher the viscosity of the binder needed to achieve a good mixture. Broad, or multimodal, distributions are preferred to reduce the viscosity of the mix (Janney 1995).

Systems containing ceramic particles and a binder are rather complex and depend strongly on the nature of the components. The effects of binder may be profound at low shear rates, but at high shear rates the viscosity behaviour becomes more dependent on other factors such as particle size, shape, distribution and particle loading (Reed 1995).

The flow behaviour of the mixture can also be time-dependent (thixotropic). If a thixotropic mixture is allowed to stand for a period of time and then sheared at a constant rate, its apparent viscosity decreases with time until a balance is reached between structure breakdown and re-formation.

Apart from the variable-speed rotating cylinder viscometer, which is the method most widely used for ceramic suspensions, the viscosity of very viscous liquids and pastes may be calculated by measuring the axial displacement of a cylinder in a tube filled with material. If carefully controlled, the coefficient of viscosity of a material can be determined for a controlled displacement rate (Reed 1995).

2-8 Debinding

2-8-1 General

Debinding means removal of the binder from a mixture prior to sintering of the remaining powders. The goal in debinding is to remove the binder in the shortest time with the least impact on the compact. Failure to properly remove the binder before sintering can result in component distortion, cracking, slumping and contamination.

When the binder is removed, the component becomes very fragile until sintered. Thus, final debinding occurs as part of the heating process before the sintering temperature is reached, since handling a fully debonded but unsintered structure is virtually impossible (German and Bose 1997).

In practice, binders are made up of multiple components (Trunec and Cihlar 2002, Mutsuddy and Ford 1995) which are removed in stages, which helps the gradual formation of passages within the part with increasing temperature and time. These passages allow the major binder ingredient to escape more easily at higher temperatures without causing the part to fail (Richerson 1992).

2-8-2 Debinding Processes

There are several debinding techniques, categorized as solvent or thermal processes (Mutsuddy and Ford 1995). Binder extraction generally involves fluid flow through the pores as either a liquid or a gas. Solvent debinding depends on liquid flow, while thermal debinding depends on vapour flow. Debinding techniques are normally combined in order to remove binders in controlled stages to affect the pore formation during the process and to reduce the overall debinding time (Hwang and Hsieh 1996). Different debinding methods have been reviewed by German and Bose (1997), and more technically by Robinson and Paul (2001).

2-8-2-1 Solvent Extraction

Solvent extraction involves immersing the compact in a fluid which dissolves at least one binder phase, leaving an open pore structure between the remaining particles of the powder for subsequent binder burnout (thermal evaporation at an elevated temperature). There are three methods for dissolving the binder in a solvent: simple immersion, high-pressure solvent, and a process that involves heating the component in the presence of a reactive vapour. The choice of method depends upon the type of binder and the solvent used, and also the geometry of the component.

2-8-2-2 Thermal Debinding

The alternative method to solvent debinding is to remove the binder by heating. This is a common method due to its simplicity, ease of operation and the low cost of investment in equipment (Hwang and Hsieh 1996; Trunec and Cihlar 1997). Although there are several modifications of the process, such as debinding under vacuum or high pressure, draining through a porous bed and pyrolysis, the mechanism for thermal debinding can best be described as follows (Mutsuddy and Ford 1995, German and Bose 1997).

Thermal degradation involves three basic stages. Assuming an initial condition in which the pores are fully saturated by binder, after the temperature of the green compact has been raised enough to melt the binder, thermal expansion of the liquid binder induces hydraulic pressure. Evaporation will occur initially from the component surface. At the beginning of the process, molten binder flows to the surface faster than it evaporates. As a result the debinding rate depends only on heat input for degradation and is controlled by the binder degradation rate. Hence, pores open up near the surface and the molten binder flows fast enough to feed the process. Accordingly, behaviour similar to that shown in Fig. 2.5 is expected.

Over time, the depth from which the binder needs to migrate to the surface increases to a point where liquid flow is slow, leading to a surface free of binder.

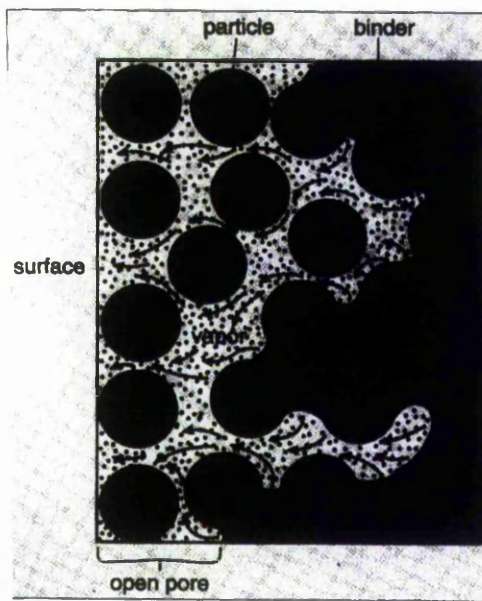


Fig. 2.5 A model showing a point in time where the binder is permeating to the surface through open pores during thermal debinding (German and Bose 1997)

When the saturation level of the binder is sufficiently reduced, the liquid remaining in the mix is driven to the surface by capillary pressure, where it can evaporate. Because of capillary forces, the small pores in the surface region have more attraction for the liquid binder than the larger pores. Thus, the largest pores at the component surface open, possibly leading to cracking. Plus, any regions with a low packing density are pulled apart by regions of higher packing density, which retain the binder for a longer period. This is the basic reason for ensuring a homogenous mixture, a high solid loading, and avoiding separation of the powder and binder. As the binder is removed, flow to the surface comes from greater depths and the liquid migration rate becomes the limiting factor.

In the final stage of debinding, gas pockets begin to coalesce, forming a network of interconnected pores and internal structure burnout occurs from within the compact, thereby allowing diffusion to play an important role in binder removal. Flow through the pore structure depends on the porosity, pore size, and permeability of the mixture. Higher temperature and an agitated atmosphere can lead to a rapid evaporation.

In all forms of debinding, faster rates are achieved at higher temperatures, (German and Bose 1997) but high temperatures increase the probability of forming defects or distorting the component. Thus, the selection of a suitable

temperature and heating rate are fundamental to a successful debinding process. The most obvious effect of temperature is an increase in the partial pressure of the binder components.

There are other parameters such as the effect of critical thickness (Li et al 2003), atmosphere (Lii 1998, Edirisinghe 1991), solid content and surface to volume ratio (Liu 1999), which also affect the debinding process. For instance, where the critical thickness is large, the temperature can be increased relatively rapidly during the initial stage of debinding and the debinding time can be shorter. On the other hand, the critical thickness is proportional to the particle size and inversely proportional to the holding time (Li et al 2003). The particle size determines the size of the available channels for binder diffusion between the powders. The larger the particle size, the larger the space between the powders and the easier binder removal is. This emphasises the effect of the binder diffusion/migration stage (from the interior to the surface of the sample), which can restrict the overall binder removal kinetics. Atmosphere can influence the degradation behaviour, such as the softening point of the binder(s) and consequently affects the bonding structure and flowability.

Modelling of the debinding process has been studied by many authors (Calvert and Cima 1990, Lewis and Galer 1996) with an emphasis on the capability of the binder being transported due to capillary forces acting in the compact, but most of these models are simplistic when compared with actual events.

Optimization of the debinding parameters to avoid defects has been an interesting and extremely challenging subject. Cracking and distortion are the most common defects and can be produced in the part as a result of various sources, such as uneven extraction of the binder (German and Bose 1997) and density variations within the part as a result of uneven packing (Mutsuddy and Ford 1995). The other sources for cracks could be too high a heating rate and/or high volumetric binder ratio in the mixture (Tseng and Hsu 1999).

2-8-3 *Thermal Degradation of Cyanoacrylate*

The thermal degradation behaviour of cyanoacrylate has been shown to be a chain end-initiated unzipping reaction (Birkinshaw et al 1996). The thermal degradation of lower alkyl cyanoacrylate oligomers at temperatures of 140°C to 180°C is a

chemically simple process (Rooney 1981) and the shape of the DTG and DTA curves of ethyl cyanoacrylate polymers are composed of only one sharp peak (Fig. 2.6).

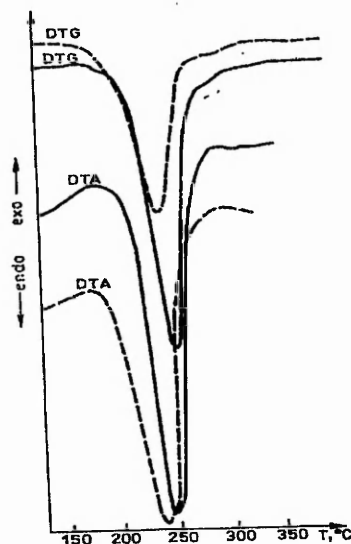


Fig. 2.6 Thermal degradation of poly ethyl α -cyanoacrylate in air (---) and nitrogen (___) (Negulescu et al 1987)

Fig. 2.7 shows no appreciable effect of the nature of the atmosphere on the rate of thermal degradation, although it is strongly dependent upon the chemical composition of the polymers.

It seems that one way to improve the temperature resistance of the polymers is connected with the formation of a temperature-initiated crosslinking, thus yielding a three-dimensional structure (Kotzev 1981) in the adhesive layer in order to reduce its depolymerization tendency (Denchev and Kabaivanov 1993).

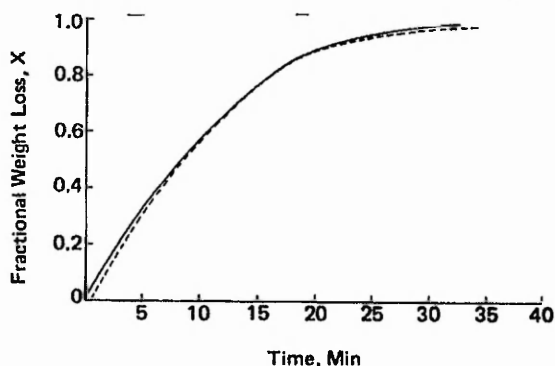


Fig2.7 Thermal degradation of ethyl cyanoacrylate polymers at 163°C and atmospheric pressure in air (---) and nitrogen (___), (Rooney 1981)

Fig. 2.8(a) shows the thermal degradation curves of cured cyanoacrylate adhesives for a linear increase in temperature in an inert atmosphere (Denchev and Kabaivanov 1993). The poly-ethyl cyanoacrylate sample started losing weight at about 170°C, with the maximum rate of weight loss being in the 200°C-210°C range. With regard to poly-allyl cyanoacrylate and polyallyloxyethyl cyanoacrylate, their depolymerization is relatively markedly reduced at the corresponding temperatures. Fig 2.8(b) shows the curves of the thermal degradation of cured samples in an inert atmosphere under isothermal conditions. It shows a 45% weight loss after 3hr at 140°C for a poly-ethyl cyanoacrylate sample (Denchev and Kabaivanov 1993).

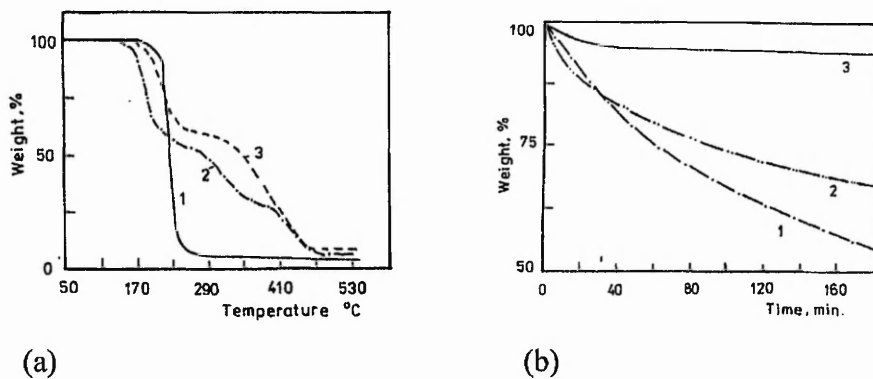


Fig.2.8 TG curves of poly (2-Cyanoacrylate).
a) Scanning mode (10 °C/min) b) Isothermal mode (3h/140°C)
 1- poly-ethyl; 2- poly-allyl ; 3- poly-allyloxyethyl cyanoacrylates
 (Denchev and Kabaivanov 1993)

2-9 Sintering

2-9-1 General

Success in sintering is due to reaching to an acceptable density, with controlled and repeatable dimensions and properties. The chemistry, microstructure, processing and properties each influence the others, and are also influenced by the atmosphere and furnace type (German and Bose 1997). Debinding can leave some binder in the compacts for shape retention up to the sintering temperature, or it can be taken to total binder elimination by including a pre-sintering step.

After sintering, the final density would generally approach 95-100% of the theoretical value. As a result of pore elimination, the final dimensions are smaller

than the starting ones. The extent of such shrinkage depends on the green density. Maintaining a high, and uniform, powder packing density in the mixture lowers shrinkage and eliminates one source of distortion. In general, an ideal powder should have the attributes of small particle size, equiaxed particle shapes, narrow size distribution and high purity or controlled dopant content and not be agglomerated. Furthermore, these parameters which control the sintered microstructure also control the final properties.

The bond between the particles grows by the motion of individual atoms via either solid state or liquid phase events. This particle bonding during sintering gives a significant increase in hardness, strength and other engineering properties.

2-9-2 *Solid State Sintering*

In Solid State Sintering (SSS), solid bonds form between the particles during heating. At the microscopic level, sintering occurs by the motion of atoms to fill the pores between particles. The atoms may take many paths to form the bond (Fig. 2.9) including, mass flow along the particle surfaces (surface diffusion), across the pore space (evaporation-condensation), along grain boundaries (grain boundary diffusion) and through the lattice interior (volume diffusion). The rate of neck growth, shrinkage and densification all depend on the cumulative rates of transport by these various paths (German 1996).

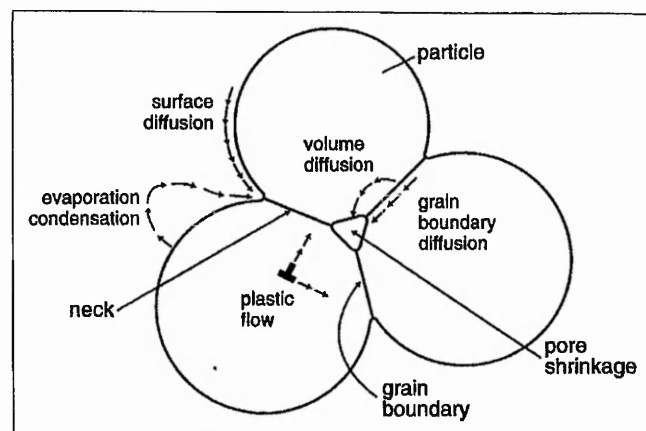


Fig. 2.9 *Various mechanisms of sinter bonding (German and Bose 1997)*

For most materials the vapour phase transport contributions are small and can be ignored. Surface diffusion produces a loss of surface area during neck growth and

is involved in pore smoothing, particle joining and migration during the later stage of sintering but fails to result in shrinkage or densification. Volume or bulk diffusion along grain boundaries (grain boundary diffusion) or through lattice dislocations does give densification, since atomic transport is faster along these regions and creates a continual flow of mass into the pores. In other words, in solid state sintering, pore shrinkage occurs by the diffusion of vacancies to the grain boundaries, dislocations, phase boundaries or other microstructural interfaces and their annihilation there (Reed 1995, German 1996, German and Bose 1997).

Factors affecting the sintering rate are: particle size (fine particles can be sintered more rapidly and at a lower temperature), particle shape and particle size distribution, uniformity of particle packing (which may be affected by agglomeration), atmosphere and the time-temperature cycle (higher temperatures and longer times generally give more densification). The heating and cooling rate can also affect the mechanical integrity of the part (Richerson 1992).

Solid State Sintering can be divided into three overlapping stages;

initial stage:

The initial stage of solid state sintering involves rearrangement, slight movement or rotation of loose powders and initial neck formation at the contact point between each particle (Richerson 1992). In this stage, the neck size is sufficiently small that neighbouring necks grow independently of each other. Various theoretical analyses have been developed to link the neck size ratio to other sintering parameters such as shrinkage, surface area or density. A simplified two-sphere model for sintering (Fig. 2.10) is used to introduce the neck growth concepts. This consists of two spheres of diameter D joined at a circular cross-section neck of diameter X . Equation 2.4 shows a simple initial stage model for the neck size ratio X/D as a function of sintering time under isothermal conditions, which can reproduce some key processing factors (German 1991);

$$\left(\frac{X}{D}\right)^n = \frac{Bt}{D^m} \quad (2.4)$$

X = Neck diameter

D = particle diameter

B = combination of material and geometric constants

t = isothermal sintering time

m and n depend on the mechanism of mass transport during sintering.

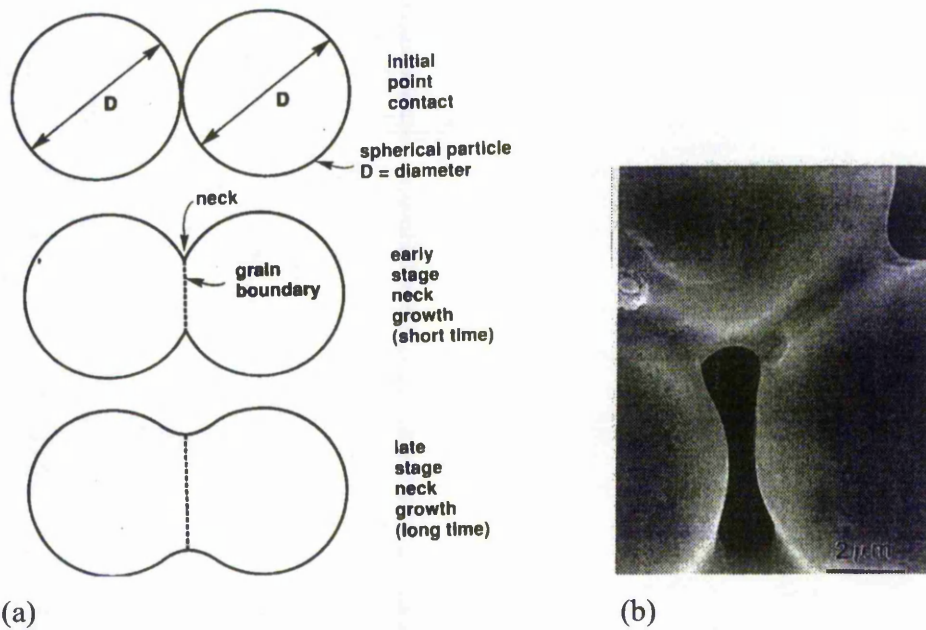


Fig. 2.10 (a) Two-sphere model for sintering with the development of the interparticle boundary where two grains of diameter D are bonding with a neck of diameter X . (b) SEM of neck formation due to sintering of nickel spheres (German 1996)

- A high sensitivity to the inverse particle size means that smaller particles give more rapid sintering.
- The temperature dependent material constants contained within the parameter B have an exponential form, which means that small changes in temperature can have a large effect on the sintering rate.
- Finally, time has a relatively small effect on sintering in comparison to temperature and particle size.

There are similar laws for the initial neck growth stage for non-spherical particles (German 1996).

intermediate stage:

Initial stage sintering is active for the early portion of neck growth i.e. $X/D < 0.3$ (German 1991), but there is only a minor degree of densification in this stage. The intermediate stage is most important for densification and determining the properties of the sintered compact. In this stage, the size of the neck between the particles grows, the grain boundary begins to move, porosity decreases, the centres of the original particles move closer together, with the degree of shrinkage dependent on the amount of porosity decrease (Richerson 1992). This stage is characterized by simultaneous pore rounding, densification, and grain growth. Grain boundary energy is low in comparison to surface energy, thus the pores typically remain attached to the grain boundaries through most of this stage and the rate of pore elimination (densification) depends on the diffusion of vacancies away from the pore, which occurs mainly by volume diffusion and/or grain boundary diffusion. Pores located on the grain boundaries disappear more rapidly than isolated pores. With smoothing of the grain boundary during sintering, its effectiveness as a vacancy sink reduces, but it is still a good path for mass transport. Sintering depends on the size, shape and packing of the particles and chemical dopants (which increase the vacancy flow) as well as time and temperature. Smaller grains increase the rate of pore elimination as a result of the strong role of grain boundary diffusion control, and diffusion enhancing materials enhance densification. On the other hand, particle agglomeration is a common source of inhomogeneous sintering (Reed 1995).

There are several models for this stage, but these are generally not very accurate since more than one mass transport mechanisms may be contributing to the change in the microstructure. Typically the practical sintering rate is higher than that proposed by the models, possibly as a result of the non-uniform microstructure (German 1996).

final stage:

The final stage is a slow process involving the removal of the final porosity by vacancy diffusion along the grain boundaries (Richerson 1992). Unfortunately grain growth is also a natural process associated with high temperature sintering. The reason for this is that the grain boundary regions are high in energy; consequently, the elimination of surface area will be accompanied by the

elimination of grain boundary area as well (German and Bose 1997). Usually the grain boundary mobility is much greater than the pore mobility and at a critical point it breaks away from the pore. As the grain continues to grow the pore becomes further separated from the grain boundary and finally, the pore becomes trapped within the grain. These pores are harder to eliminate, resulting in low densification by long-range volume diffusion. Rapid grain growth is observed once the grain boundaries break away from the pores (German 1996). With increasing sintering time, the number of pores decreases, while their size increases. Therefore grain growth must be controlled to improve the removal of the final porosity.

The need is to sustain small pore attachment to the grain boundaries by increasing pore mobility or decreasing boundary mobility and retention of small grain sizes (German and Bose 1997). The atmosphere is also important as gas trapped in closed pores will limit pore shrinkage unless the gas is soluble in the grain boundary and can diffuse from the pore (Reed 1995).

2-9-3 *Liquid Phase Sintering*

Liquid phase sintering (LPS) is a widely used process for the fabrication of both ceramic and metallic materials intended for high technology applications. This includes technically important ceramics such as alumina substrates, plugs and mechanical seals.

The main advantages of liquid phase sintering are fast sintering rate and tailoring of the properties. The liquid phase provides for faster atomic diffusion than solid state processes. In addition the formation of a wetting liquid during sintering provides sufficient capillary force to eliminate the need for an external force to reach full density. The disadvantages are susceptibility to shape distortion which occurs when too much liquid is formed during sintering, and complication of the sintering parameters because of the presence of the liquid phase which imposes wetting, solubility, diffusivity and segregation effects (German et al 1988, Kwon 1991).

There are three general requirements for liquid phase sintering (Kwon 1991):

- Formation of liquid phase at the sintering temperature
- Good wetting of liquid on solid

- Solubility of solid in liquid

During sintering, the wetting liquid acts on the solid particles to reduce the interfacial energy and thus eliminate porosity in the powder compact (German 1985). In general, the density increases due to a rapid dissolution-transport-precipitation phenomenon. Particle size, viscosity and surface tension control the rate of LPS. The viscosity and surface tension are affected strongly by composition and temperature. For most compositions, a small increase in temperature could result in substantial increases in the amount of liquid phase, which would increase the rate of sintering. Major factors which affect the sintered microstructure include particle size, amount of liquid present at the sintering temperature, and the cooling cycle. Smaller particles result in higher capillary pressure and have a higher surface energy, and as a result more driving energy for densification than coarse particles (Richerson 1992). LP sintering is sensitive to temperature; too low a temperature results in residual porosity and too high a temperature leads to extensive grain growth (German and Bose 1997).

The classic theory of LPS assumes densification occurs in three overlapping rate controlling stages (German 1985). Fig. 2.11 illustrates the classic sequence of these three steps. Based on this theory no densification takes place prior to liquid formation. These three stages of classic LPS are summarized in Fig. 2.11 in terms of the key microstructural changes.

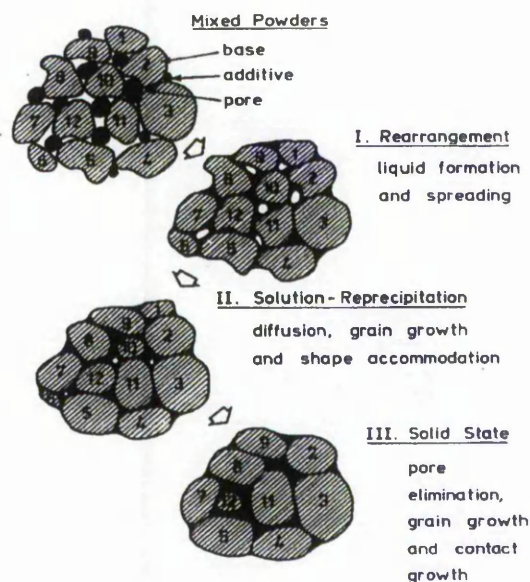


Fig. 2.11 Classic sequence of LP sintering (German 1985)

rearrangement:

During this stage, both solid and liquid are subject to rearrangement to achieve better packing. Initially, the mixed powders are heated to a temperature at which liquid forms and a rapid densification occurs because of the capillary forces as a result of wetting effects on the solid particles. Accordingly, minimising the surface energy in the system leads to the elimination of porosity. Since the viscosity of the system decreases with the elimination of porosity, the densification rate continually decreases during sintering. The liquid also reduces the inter-particle friction and dissolves sharp particle edges, thereby aiding rearrangement of the solid particle (German et al 1988).

The amount of densification in the sample by rearrangement depends on many factors; the most important ones are the amount of liquid, particle size of the solids and its/their solubility in the liquid. Usually finer powders give better rearrangements. On the other hand, rearrangement can be hindered by irregular particle shapes. The driving force for rearrangement arises because of the imbalance in capillary pressure as a result of the particle size distribution and irregular particle shapes, as well as anisotropic material properties (Kwon 1991).

solution-precipitation:

As densification by rearrangement slows, solubility and diffusivity effects become dominant. This second stage is termed solution-precipitation. The solubility of a grain in the liquid varies inversely with the grain size. The smaller the grain size, the higher is the solubility. As a result of the differences in the solubilities of different grain sizes, a concentration gradient in the liquid is established and material is transported from small grains to the larger ones by diffusion. This process is termed Ostwald ripening. The result is a progressive growth of larger grains and densification. The grain shape is changed as a result of diffusion to allow tighter packing of the grains, and as a result leads to pore elimination. The grain shape is determined by the relative solid-solid and solid-liquid interfacial energies and the amount of liquid. The amount of liquid affects the process in term of the diffusion distance. This mass transfer results in contact-point flattening and corresponding linear shrinkage. The densification rate decreases as the density of the powder increases (Kwon 1991).

pore removal:

The last stage of classic LPS is solid-state controlled sintering with a slow densification rate because of the solid skeleton. The rigidity of the solid skeleton inhibits further rearrangement, but microstructural coarsening continues by diffusion. The residual pores will enlarge if they contain entrapped gas.

Several processes can occur simultaneously, including growth and coalescence of grains and pores, dissolution of the solid into liquid and phase transformation(s). There are many variants of these stages affecting the rate of sintering and microstructural evolution (German et al 1988). In real powder compacts, there exists a range of particle sizes and shapes. As a result, the process is more complicated than the simple processes described herein. This includes factors such as the limitation of densification due to the penetration of liquid into agglomerates of particles, as well as the formation of liquid pools because of heterogeneous liquid redistribution (Kwon 1991).

2-9-4 *Sintering of Alumina*

Alumina is a frequently used advanced ceramic material because of its superior mechanical, thermal, chemical and electrical properties, and its relatively low cost. Solid state sintering of alumina is usually done using high purity powders in air at a peak sintering temperature of 1600°C with holding times of 1 to 4 hours (German 1997).

The initial sintering of alumina (to ~0.77 theoretical density) powders is controlled by grain boundary diffusion, with the coarsening kinetics dominant during further densification (Zeng et al 1999). In the first part of sintering the densification rate is a function of the homogeneity of the green compact (Lance et al 2004). Once agglomerations are eliminated, the most important criterion for lower the sintering temperature is the use of smaller particle sizes and more uniform green density (Zeng et al 1999). In the final stage of sintering, a plateau of densification is observed for heterogeneous green compact samples.

Bi-modal powder mixtures improve packing density because the smaller particles fit into the pores between the larger particles. The maximum packing density depends on the ratio of the particle sizes and inherent packing density of the two powders. The sintering behaviour is intermediate between that for each powder; shrinkage declines as the larger particle content increases, reflecting the role of a

larger average particle size (German 1996). Using various fine to coarse particle size ratios Smith and Messing (1984) concluded that grain growth occurred for fine particles whether they were isolated between coarse powders or formed a continuous structure.

Many studies on the role of additives in the sintering of Al_2O_3 have been reported. Small additions of various oxides such as MgO , TiO_2 , MnO_2 , Li_2O_3 and ZrO_2 to alumina have been shown to influence the densification processes by reducing the sintering temperature, suppressing or promoting grain growth and allowing sintering to theoretical density, which can affect the microstructure and/or mechanical properties of the sintered parts. In general, an additive can function either in solid solution or as a second phase or both by various mechanisms (Erkaifa et al 1998, Sathiyakumar and Gnanam 2003). In contrast, some impurities, such as carbon, retard densification. As a result complete burn out of carbon containing binders is necessary prior to sintering (German 1997). Among the beneficial additives MgO has been most studied. It has a solid solution drag effect and tends to inhibit grain growth in pure alumina powders and provides resistance against abnormal grain growth due to inhomogeneous densification (Zhao and Harmer 1987). MgO can restrain grain growth in the more densely packed regions until the less densely packed regions have the opportunity to densify, thus smoothing out the consequences of inhomogeneity (Shaw and Brook 1986).

Atmosphere may have two possible effects on the sintering of ceramics: modifying the densification rate (due to change in the number of vacancies with changing oxygen pressure) and affecting density (due to diffusivity of trapped gas in the solid) (Miranzo et al 1990). Alumina doped with MgO can be sintered to zero porosity in an atmosphere of H_2 or O_2 , which are soluble, but not in air that contains insoluble N_2 . The density of the oxides sintered in air is often 92-98% (Reed 1995). Finally, the consolidation technique (Roosen and Bowen 1988) can affect the green compact structure, and consequently sintering behaviour, of alumina powders.

Liquid phase sintering of alumina is a widely used process. It is much more frequently utilised than solid state sintering of this material (Kosmos 1996). These LPS aluminas, which have up to 15 wt% liquid forming additives, facilitate easy

and economical processing by allowing sintering at lower temperatures, as well as the use of less pure aluminas and sintering aid component(s) (Latella and O'Connor 1999).

The densification rate increases significantly with increasing liquid volume as a result of the decreased fractional grain contact area. Many different additives are used to produce the liquid phase with the aim of promoting liquid phase sintering and develop the desired microstructure. For example, 95% relative density was observed in less than 3 minutes with 20% vol liquid forming glass (V_l) and almost 300 minutes was needed to reach the same density with 3%vol. As with the particle size, with $V_l = 10\%$ and using $0.9 \mu\text{m}$ alumina particles, it takes 10 times longer to reach 95% density compared to $2.1 \mu\text{m}$ particles (Kwon and Messing 1990).

Aluminosilicate glasses of various compositions are well documented as effective additives for the liquid phase sintering of alumina (Kwon and Messing 1990). The microstructures in aluminas where the glass is used simply as a densification aid show a uniform distribution of alumina crystals completely separated by glass. The pores are usually located at the grain boundaries within the glass. Phases such as anorthite ($\text{CaAl}_2\text{Si}_2\text{O}_8$), gehlenite ($\text{CaAl}_2\text{SiO}_6$), spinel (MgAl_2O_4), mullite ($\text{Al}_6\text{Si}_2\text{O}_{13}$), or cordierite ($\text{Mg}_2\text{Al}_4\text{Si}_5\text{O}_{18}$) may form on cooling or be crystallized from the glass after prolonged heating above 900°C . SiO_2 has low solubility in alumina and segregates to the grain boundaries. If enough SiO_2 is present a liquid phase forms at high temperatures, which on cooling usually forms a glass, although some crystallisation may occur depending on composition.

Different ratios of calcia and silica have an effect on the microstructures and mechanical properties of sintered parts (Svancarek et al 2004). Using 5%w additives, Galusek (2002) studied the effect of different SiO_2/MgO and SiO_2/CaO ratios on the hardness and elastic modulus. In all cases, the additive containing aluminas were found to be softer and less stiff than pure alumina with the same grain size ($0.4 \mu\text{m}$). Using talc as the liquid former, Kim et al. (2000) studied the effect of different levels of the additive and sintering temperature on the densification behaviour of coarse and fine alumina powders. They observed an acceleration in the densification rate in coarse powder with added talc, due to its role in particle arrangement. In the case of fine alumina, appreciable densification

occurred below the temperature where liquid forms. As a result of the formation of a rigid skeleton of fine alumina, the rearrangement process was inhibited and the densification process slowed. The sintered density of fine alumina samples decreased as the talc content increased.

The viscosity of the liquid phase is also an important characteristic, which can influence densification in these stages. The viscosity depends on the temperature and chemical composition of the liquid, and increases by formation of the reaction products between alumina and the liquid phase which can be avoided by adjusting the CaO/MgO ratio (Kosmos 1996).

The LP sintering behaviour of bi-modal alumina powders has been studied. Taruta et al (1996) reported a higher density in liquid phase containing samples compared to non additive ones at 1500°C, with the open pore size changes depending on the packing structure.

The fabrication route (Goswami and Das 2000), and level of porosity (Latella and O'Conner 1999), are also important in determining the mechanical response of the LPS alumina ceramics and their susceptibility to degradation such as wear.

2-9-5 Sintering of Zirconia

Zirconia ceramics are regarded as strong candidates for engineering applications due to their excellent mechanical properties combined with high chemical and corrosion resistance. Various types of additives, such as yttria, ceria and magnesia are used to control the microstructure and transformation toughening behaviour. Because of its high melting point, small particle sizes are preferred to promote rapid sintering. Although small zirconia particles can be sintered to full density by sintering for one hour at 1100°C, agglomeration can result in only sintering to 95% density at a temperature of 1500°C and holding time of four hours (German 1997). A normal sintering schedule for ZrO₂ is heating the compact at a controlled rate, followed by holding at the highest temperature, such as 1500-1550°C. The grain size of the samples increases continuously with density, and abnormal grain growth probably occurs in the final stage of sintering (Lee 2004). Fast heating rates are preferred and the final mechanical properties depend on grain size, additives and final density. The achievement of high toughness is only possible by

growing t-ZrO₂ grains via optimization of the sintering parameters or by post-sintering treatment at high temperature.

The sintering of yttria stabilized zirconia (YSZ) is usually carried out using a small amount of SiO₂, which becomes liquid at the sintering temperature. The ionic conductivity of YSZ is sensitive to the intergranular liquid (Jung et al 2003) and the grain size (Laberty-Robert et al 2003).

3

Materials Processing & Mixing

Introduction

The aim of this first phase of the present investigation was to be able to prepare a mixture of fine powder in a cyanoacrylate binder which would be suitable for deposition as a coating, and which would have the following attributes:

1. A uniform distribution of particles in the mixture. The particles may be either ceramic, metallic or a combination, with mean particle sizes in the range 0.1 - 10 μm , which would be expected to give sintered coatings with reasonable hardness and toughness.
2. The volume fraction of particles should be as high as possible, subject to the above constraints and the requirements imposed by the debinding process.
3. Reproducibility of the mixing process in terms of uniformity and effective viscosity.

To achieve these, it was necessary that the following processing parameters should be investigated and determined at an early stage:

- Types of appropriate cyanoacrylates and powders for developing coating mixtures with the desired characteristics.

- Prevent polymerization of the cyanoacrylate during mixing with the powders, probably through use of an appropriate inhibitor.
- Ensure that the viscosity of the mixture is such that it can be handled manually.
- The highest volume fraction of powder that can be incorporated into the mixture.

This chapter discusses the selection and properties of the chemicals to be used in the preparation of the coating mixture, as well as the procedures for mixing the chemicals, and the effect of additives on the comparative viscosities of the mixtures.

The first section describes the characteristics of the ingredients investigated to prepare the coating mixtures and has seven parts: binder, powder, stabilizer, initiator and substrate, which are the essential ingredients in this process, as well as the use of an indicator or surfactant.

The second section describes the development of the basic methods and procedures used to prepare a mixture of ceramic powder and binder suitable for coating. These include sequence of mixing and methods of adding each component to the mixture, and their comparative advantages and disadvantages. The third and fourth sections outline the results of various investigations into variations in the basic procedure, such as increasing the powder concentration, and possible methods for comparing the viscosities of the mixtures and monitoring the pH prior to polymerization.

3-1 Materials Specification

3-1-1 Binders

The starting point for the process was to investigate a selection of suitable cyanoacrylate binders, which would be most appropriate to meet the requirements of the process. Previous work using butyl cyanoacrylate as a binder to make feed stock for the CIM process (Ridgeway 2000) shows that such a binder has a good match with the characteristics required to meet the stipulations proposed by German and Hens (1991) for an ideal binder including: little viscosity variation with change in temperature, strong and rigid after cooling, adherence to the powder, and exhibiting a decomposition temperature well above the mixing

temperature, whilst depolymerizing at a low temperature prior to sintering. However, the companies which manufacture cyanoacrylates have chosen to withdraw this grade at present. Consequently, a comparative study was conducted to select an appropriate cyanoacrylate for the purpose of producing a mixture suitable for coating. The result of binder effect could be discussed in section 3-3-3 and the details of composition influence on viscosity of coating mixtures would be shown in sections 3-4. Table 3.1 lists the binders that have been investigated, and their relevant properties. The binders used cover a wide range of viscosities for the most common cyanoacrylates used in industry.

Table 3.1 *Properties of the cyanoacrylates used in the present study*

[Note: This table is based on data taken from the manufacturers' literature]

Designation	Chemical type	Density (g/cm ³)	Viscosity at 25 °C (cP)
Loctite 406	Ethyl cyanoacrylate	1.05	20 (10-30)
Loctite 408	Alkoxyethyl cyanoacrylate	1.1	7 (4-10)
Loctite 420	Ethyl cyanoacrylate	1.05	2
Loctite 454	Ethyl cyanoacrylate	1.1	Gel
Loctite 460	Alkoxyethyl cyanoacrylate	1.1	45 (30-60)
3M 2000	Methyl cyanoacrylate	1.1	2000

Although many different kinds of cyanoacrylates have been formulated in recent years, they basically act the same in terms of reacting with the powder and polymerization; thus the focus was on using a type of cyanoacrylate with the lowest possible viscosity and best technical compatibility with the coating aims.

3-1-2 Ceramic Powders

Five different kinds of powders were examined to find the most suitable powders to be used for the present study. Table 3.2 summarizes the properties of the powders based on data available from their respective manufacturer. The estimation of the mean particle size generally depends on the assumption that the particles are spherical. In general, commercially available powders are not spherical and would be predominantly either cuboidal, angular, platelet, or acicular in shape. The scanning electron microscope provides a useful method for

visualizing the actual powder shapes. Fig. 3.1 is a series of SEM micrographs of the powders showing the range of particle shapes. It was noticed that the fused alumina powder (Fig. 3.1 (a)), which is suitable for flame spray applications, has a very large particle size ($\sim 30 \mu\text{m}$) together with an angular particle shape.

The shapes of the particles in the coarser Alcan alumina powder, Fig. 3.1(b), are a mixture of angular, acicular and platelets. The finer Alcan alumina powder, Fig. 3.1(c), consists of small cuboidal particles, which are strongly agglomerated. Both ALCAN aluminas are low-soda, high purity alpha powders. The MA2LS powder (No.2) does not contain a grain growth inhibitor but the RC45B powder (No.3) contains MgO additive as grain growth inhibitor.

The zirconia powder, Fig. 3.1(d), also appears to be mixture of larger ($> 5 \mu\text{m}$) and smaller ($< 1 \mu\text{m}$) particles, with there being some degree of attachment/agglomeration apparent in the micrograph. This could possibly occur as a consequence of the method of preparing the samples for examination in the SEM.

Fig. 3.1 (e) shows that the aluminium powder has a wide apparently non-uniform particle size distribution, with larger ($> 10 \mu\text{m}$) angular/acicular particles and smaller ($\sim 1 \mu\text{m}$) cuboidal/spherical particles.

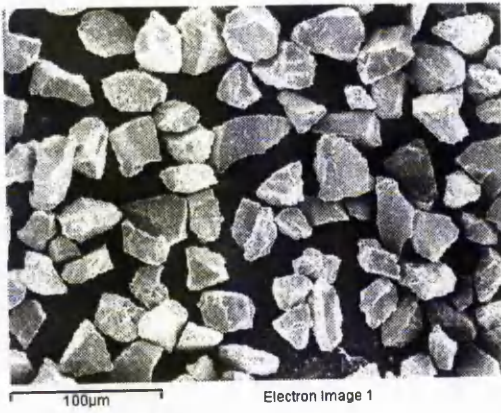
The main particle size and surface areas of the stabilized zirconia and two alumina powders, i.e. numbers 2-4, were measured. A laser scattering technique was used for measuring the main particle sizes of the fine alumina powder (No.3) and an electrical sensing technique for the coarser alumina (No.2) and stabilized zirconia (No.4) powders. A gas adsorption technique was used for measuring the surface areas of all three powders. Table 3.3 presents the relevant results and provides a comparison of the experimental and manufacturers' technical data on the particle sizes and surface areas.

Assuming a spherical particle shape for the powders, the mean particle size of the powders was also calculated using the experimental data for the surface area of the powders. Equation 3.1 (German and Bose 1997) has been used for the calculation and the results are also included in Table 3.3.

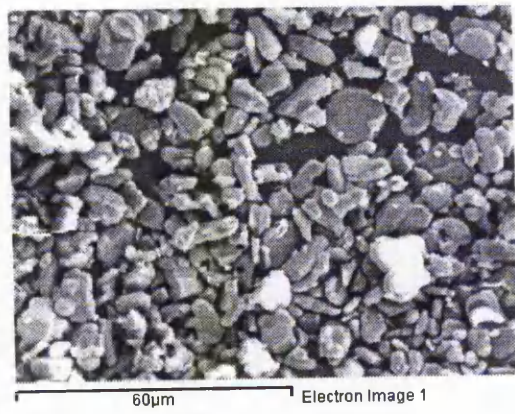
Table 3.2 Technical data for ceramic powders (taken from manufacturers' literature/specifications)

Powder No.	No. 1 Alumina	No. 2 Alumina	No.3 Alumina	No.4 5% Yttria stabilized Zirconia	No. 5 Aluminium
Manufacturer and Designation	H.C.Stark AMPERIT 740.355	Alcan MA2LS	Alcan RAC45B	Unitec Ceramics PYT05.0-010H	ALPOCO
Chemical Composition (weight %)	<0.02 SiO ₂ <0.05 Fe ₂ O ₃ <0.3 Na ₂ O Al ₂ O ₃ balance	99.7 Al ₂ O ₃ 0.05 Na ₂ O 0.05 SiO ₂ 0.02 Fe ₂ O ₃ 0.02 CaO	>99.8 Al ₂ O ₃ 0.04 Na ₂ O 0.01 SiO ₂ 0.01 Fe ₂ O ₃ 0.01 CaO 0.05 MgO	94.30 ZrO ₂ +HfO ₂ 5.30 Y ₂ O ₃ 0.12 TiO ₂ 0.03 SiO ₂ 0.25 Al ₂ O ₃ 0.03 Fe ₂ O ₃ <0.10 Na ₂ O	commercial purity Aluminium powder
Surface area (m ² /g)	n/a	0.4	8.0	n/a	n/a
Density (g/cm ³)	n/a	3.97	3.94	6.2 (*)	n/a
Mean Particle Size (µm)	n/a	8.0	0.45	10	10

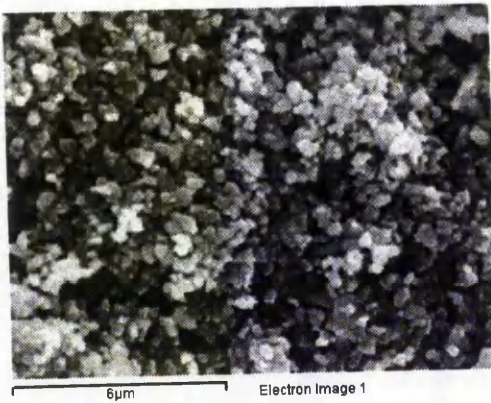
(*) Value not specified by suppliers, but assumed from data on other similar material



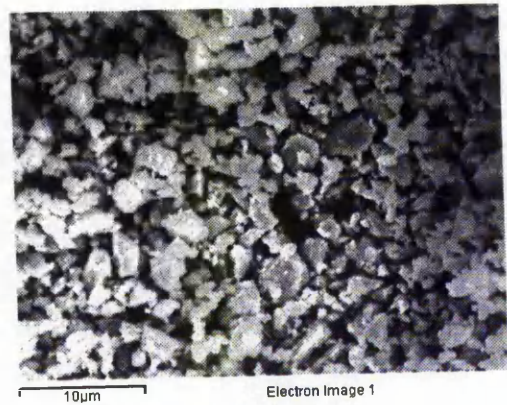
(a) Fused alumina powder (No.1)
Angular - X350



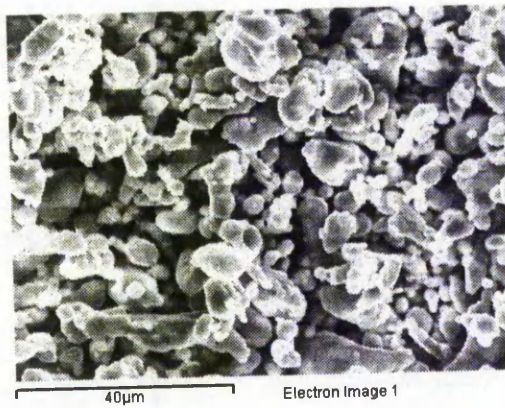
(b) Alumina Powder (No.2)
Irregular - X950



(c) Alumina powder (No.3)
Agglomerated - X8500



(d) Zirconia powder (No.4)
Spongy or irregular/angular - X3000



(e) Aluminium powder (No.5)
Ligamental - X1200

Fig. 3.1 SEM micrographs of powders

$$S = \frac{6}{\rho D} \quad (3.1)$$

S = surface area of powder

ρ = Density

D = Mean particle size

As can be seen there is reasonably good agreement between the data provided by the manufacturers and the experimental measurements, except for the mean particle size of powder number 2. The sources for this discrepancy are mainly the non-uniform particle size and agglomeration in the powder system.

Fig. 3.2 shows an example of the data particle size distribution of alumina powder No.3 provided by the laser scattering method. The maximum intensity is very close to the average particle size claimed in manufacturers' data sheet for the powders, which suggests that the specifications are practically accurate. A higher packing density of particles can be achieved by using binary powder mixtures (Richerson 1992). It has been suggested that an ideal PIM powder should have a particle size between 0.5 and 20 μm with D_{50} between 4 and 8 μm (German 1997) and that for bi-modal powders the size ratios must be greater than 7 (Reed 1995). Based on these recommendations, and the observations in the SEM studies, two different particle sizes of alumina powders (8.0 and 0.45 μm) have been combined to make a bi-modal powder.

Table 3.3 Comparison of mean particle sizes and surface areas

Powder	Mean Particle Size (μm)		Surface Area (m^2/g)	
	Manufacturer's Data	Experimental and calculated data	Manufacturer's Data	Experimental data
Alumina, Alcan MA2LS (No.2)	8.0	3.5 (3.8*)	0.4	0.5
Alumina, Alcan RAC45B (No.3)	0.45	0.46 (0.19*)	8.0	8.2
Zirconia, Unitec Ceramics (No.4) PYT05.0-010H	n/a	1.1 (3.0*)	n/a	3.25

(*) = Mean particle size calculated from the measured surface area.

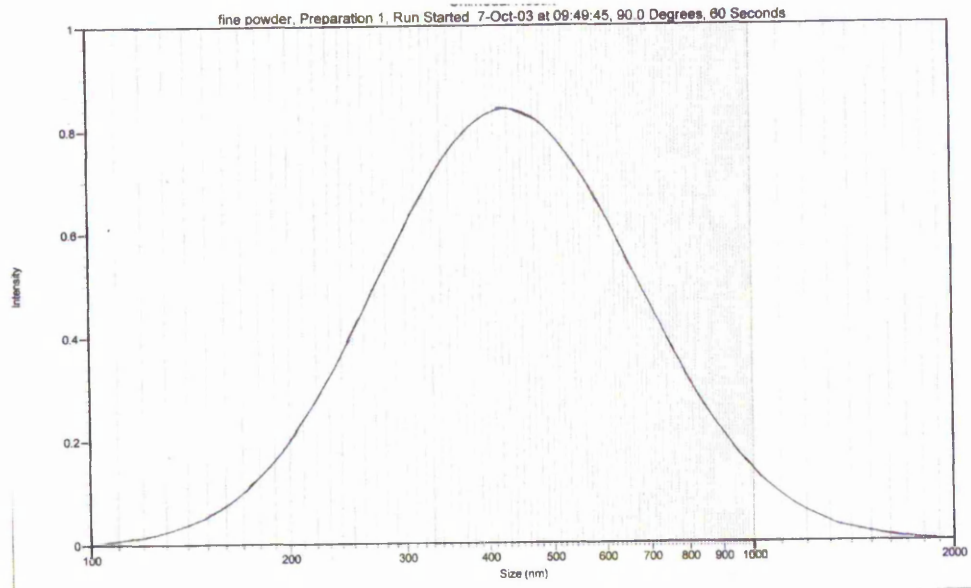


Fig. 3.2 Laser scattering result for the particle size distribution of Powder No.3

A simple paddle type mixer (Fig. 3.3) was made for blending 70%w coarse ($8\ \mu\text{m}$) and 30%w fine ($0.45\ \mu\text{m}$) alumina powders (Table 3.2 nos. 2 & 3, respectively), which is consistent with the recommendation of many authors (e.g. Mutsuddy and Ford 1995, Reed and Bose 1997). The rotational speed was fixed at 100 rpm and the mixing time was three hours.

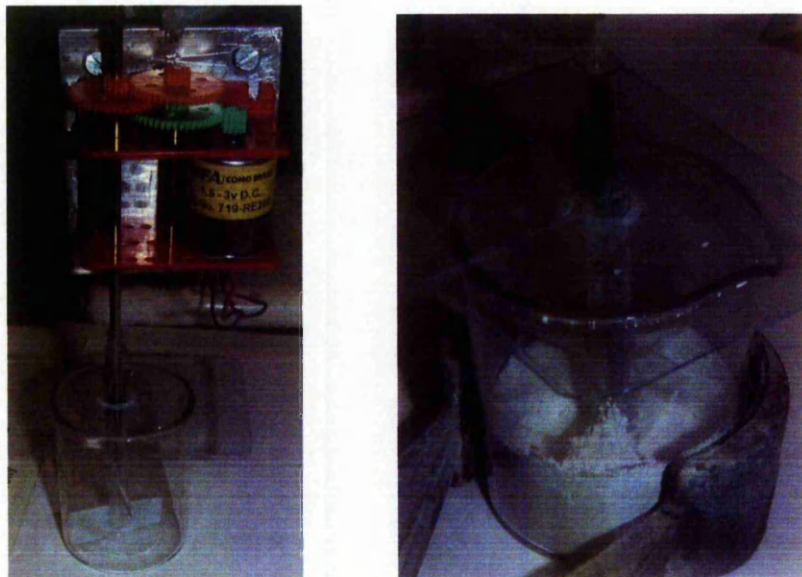


Fig. 3.3 Device used to prepare bi-modal powder

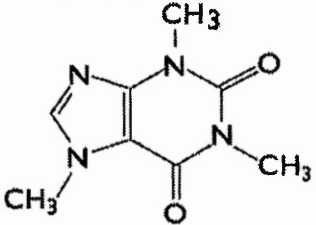
3-1-3 Inhibitor

As noted in Chapter 2, an inhibitor needs to be added to the cyanoacrylate to maintain the pH below ~ 5.5 (Cook and Allen 1993) to ensure that it does not polymerize during the mixing stage. Lewis acids have previously been used to prevent polymerization. These include sulphur dioxide, carboxylic acids (Cook and Allen 1993), trichloroacetic, picric, and sulfones (Lee 1981). Birkinshaw et al (1996) and Ridgway (2000) have previously successfully used Para-Toluene Sulphonic acid ($\text{CH}_3\text{C}_6\text{H}_4\text{SO}_3\text{H}\cdot\text{H}_2\text{O}$) to inhibit the cyanoacrylate polymerization. Therefore it was decided to use this acid in the present investigation. The actual powder used was ALDRICH Monohydrate, 98% with a density equal to 1.24 g/cm^3 .

3-1-4 Initiator

After mixing the powder and cyanoacrylate, it is very desirable for the polymerization of the binder to start and be completed within a reasonable time interval. Different methods to initiate polymerization of the cyanoacrylate have been investigated in this study. Briefly these are: oven heating, water vapour, application of vacuum, surface activation, or addition of a chemical to the cyanoacrylate or the coating mixture. A detailed description of the methods is presented and discussed in chapter 4. Finally, caffeine, in the form of a white powder (ALDRICH, 99%), was selected and successfully used as an initiator to cure the applied coating layers. Table 3.4 summarizes the relevant data for caffeine.

Table 3.4 Properties of caffeine

Caffeine, $\text{C}_8\text{H}_{10}\text{N}_4\text{O}_2$		
Specific gravity (g/cm^3)	1.23	
pH (1% aqueous solution)	6.9	
Melting point ($^\circ\text{C}$)	238	

Note: some carbon and hydrogen atoms are omitted for clarity.

3-1-5 Indicator

To study the pH changes during the curing of the mixture, normal pH measuring papers, and bromocresol green ($C_{21}H_{14}Br_4O_5S$) have been used as indicators. The latter has a change in colour from yellow to blue in the pH range 3.6-5.2, with the upper range being very close to the critical pH for that corresponding to the start of polymerization for cyanoacrylate (i.e. $pH > 5.5$). 0.2%w bromocresol green was dissolved in cyanoacrylate at 40°C for this purpose.

3-1-6 Surfactant

Surfactants are used to improve processing parameters such as viscosity, dispersion and dispersion stability. Two types of surfactants (anionic and non-anionic) were examined, DISPEX (Bath Potters' Suppliers), which is a polycarboxylic acid, and alkyl ethoxylate (EMPLIAN KA590, Albright & Wilson Ltd).

3-1-7 Sintering aid

Liquid phase sintering is a common process for the sintering of alumina powders. Fumed silica (CAB-O-SIL, BDH) with a surface area of 200 m^2/g was examined as a sintering aid additive.

3-1-8 Substrate

Commercially pure aluminium plate and stainless steel (AISI 304) plate were used as substrates for coating mixtures which were not to be debonded and sintered. To study the effect of coating the mixture onto an irregular shape, a plain carbon steel screw (M12) was used. The substrates used to make sintered coated layers were standard alumina plates (96% Al_2O_3 [Ceramic Substrates & Components Ltd]), pure alumina tiles (99.99% Al_2O_3 [Dynamic Ceramic Dynalox A100]), and commercially pure molybdenum plate (99.95% [Johnson Matthey]). The flat substrate thicknesses varied between 2.0 mm and 2.5 mm. Fig. 3.4 shows a micrograph of the 96% Al_2O_3 substrate, which was ground and polished using a final finish of 1 μm diamond paste and etched in fused caustic soda for 110 seconds. The microstructure consists mainly of equiaxed alumina grains plus a few larger angular alumina grains, and another phase, presumably glassy, which is present both as small islands at triple points and

as thin films between most of the alumina grains. The average hardness of the substrate was measured as 1535 HK_{0.3}.

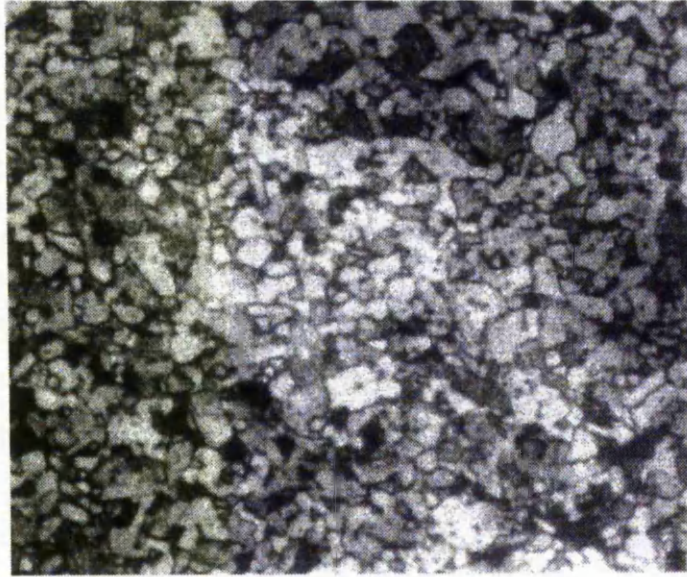


Fig. 3.4 *Microstructure of the 96% Al₂O₃ substrate (X 640)*

3-2 Coating Mixture Preparation

Preparation of the coating mixture is an important step in the process since any deficiencies in its quality can affect the final quality of the coating. Hence, it is important that the mixture be homogenous and free from agglomeration, or powder-binder separation. These could result in coating defects such as cracks or voids, which could in turn result in non-uniform shrinkage or improper debinding and/or sintering (German and Bose 1997).

The main objectives of the preparation and mixing procedures that were investigated, were to ensure the cleanliness and reproducibility of the processes. It was decided that all mixing should be undertaken manually, although it would clearly be necessary to implement a mechanised automated system for larger scale applications.

3-2-1 Pre-Processing Treatments

In an effort to reduce the possibility of free surface moisture acting as an initiator, conventional drying in an oven at 220°C was performed for all powders for at least 2 hours immediately prior to use.

Mechanical polishing using 120-grit SiC paper and acid cleaning by immersion in chromic acid at 40 °C were both investigated as a means of removing the oxide layer from the surface of the aluminium plate.

In all cases, the surfaces of the substrates were cleaned with acetone prior to coating.

3-2-2 *Mixing Procedures*

Mixing the powder with the binder is the initial stage of making a coating by this method. The particle size distribution, shapes, and level of agglomeration affect the formation of a uniformly dispersed mixture. Although there are several mathematical models available (Barriere et al. 2003), in practice, real powders are far from the ideal assumed in these models. As a result, the suitability of a particular powder to be mixed well in a particular binder is normally determined by experimental investigation.

The sequence of adding ingredients can affect the mixture properties. Consequently, several methods were investigated to ensure the production of a uniform dispersion of powder in the cyanoacrylate matrix. The two mixing procedures which were found to be the most successful are described below:

1. In the first mixing method, measured quantities of para-toluene-sulphonic acid and cyanoacrylate binder were dispensed into a small plastic cup.
2. The solution was heated at 45°C in a water bath for 30 minutes, whilst the acid dissolved in the cyanoacrylate monomer.
3. The cup was removed from the bath and a measured quantity of caffeine was added to the solution.
4. The solution was returned to the water bath and was heated at 45°C for another 30 minutes.
5. The cup was removed from the heat, and a measured quantity of ceramic powder was added (in small amounts) into the solution, whilst continually mixing by hand.

The second method involved introducing the caffeine into the mixture at the end of the process, i.e. after the addition of the appropriate amount of powder to the solution of binder and acid.

Considerable care was taken to avoid the formation of agglomeration or air entrainment in the mixture during mixing to ensure uniform properties throughout the coating.

3-3 Mixing Component Composition and Concentration Effects

The mixing process depends on numerous parameters such as: time, temperature, sequence of materials addition, powder characteristics, property and formulation of the binder and powder loading (Supati et al. 2000).

However in this study, only three parameters were selected in order to establish a suitable mixing condition, while keeping the remaining parameters constant. The parameters chosen were the three parameters commonly considered to be the most important in the CIM process i.e. type of powder and binder, and powder volume fraction. In addition, the effects of other process additives, e.g. inhibitor and initiator concentration, have been studied.

The next objective was to establish a suitable mixture composition which, together with an optimized and reproducible mixing sequence, would lead to successful application of the mixtures onto the substrates.

3-3-1 Inhibition of the Cyanoacrylate Polymerization

On adding the ceramic powders to the stabilized cyanoacrylate, acid-base equilibrium will be established between the surface of the powder as an initiator and the acid. For polymerization to start, the acidity of the binder must be reduced to below a critical value, which is typically pH 5.5.

It was noted that different levels of stabilizer were needed to inhibit polymerization during mixing. This was dependent on the kind of the powder (in particular its surface chemistry) and surface area available. For a specific powder, the inhibition period reduced as the powder concentration increased, confirming the importance of the powder surface area. As a consequence of localized polymerization starting, presumably at the surface of the powders, the viscosity of a mixture would rapidly increase. This would lead to the volume fraction of powder in the mixture being much lower than expected/required. It was found that a higher powder volume fraction could be obtained only by using a higher level of inhibitor. On the other hand, once a sufficient concentration of acid had been added to inhibit the

polymerization, there was no further improvement observed on increasing the acid concentration above this level. Thereafter the viscosity increased only due to increasing the solid particle content. To keep the level of acid in the cyanoacrylate at the minimum level, the dissolved acid concentration was increased in steps of 0.5%w each time, till no further increase in particle loading could be achieved by further increase in the amount of dissolved acid without increasing the viscosity.

Although different aspects of the polymerization of the mixture will be discussed in chapter 4, it is worth mentioning that the amount of caffeine, and the method of adding it (dissolving or direct mixing), could also affect this optimum level of acid. The combined effect of acid to caffeine ratio on the rheological behaviour of the mixtures has been studied as discussed below, section 3-4.

3-3-2 *Effect of Powder*

The five powders described in Table 3.2 have all been investigated. It was found that a specific concentration of acid was needed to stabilize the cyanoacrylate during mixing with the different powders. The concentration of acid required for a specific powder depended on its particle size and the volume fraction. This is presumably as a result of the different surface chemistry and/or surface area of the various powders. It was noted that the powders with the smaller particle sizes needed more acid to prevent premature polymerization, and also to prevent increasing viscosity and agglomeration during mixing. Table 3.5 summarizes the minimum required acid concentrations for the different powders used in this study.

As has been observed previously for other CIM techniques (German 1997), the higher surface area powders often cause more difficulties (in terms of agglomeration and sharp increase in viscosity) while mixing with the binder. Furthermore, it was observed that mixing the very fine alumina powder, i.e. powder No. 3 with an average particle size of 0.45 μm , with the cyanoacrylate resulted in agglomerated mixtures, no matter how much inhibitor was added to the mixture. This is mainly due to the very high surface area available to the cyanoacrylate during mixing, which presumably results in localised polymerization and agglomeration.

3-3-3 *Effect of Binder*

Alumina powder No.2 was used to make mixtures containing different cyanoacrylates as binders. It was found that the cyanoacrylates with the lower viscosity values were able to form a workable mixture with a greater volume fraction of powder. Thus, the best candidates were considered to be Loctite grades 420, 408 and 406 with viscosities of 2, 7 and 20 cP respectively. Ethyl cyanoacrylate releases an obnoxious gas during mixing. This gas also produces voids during the final stages of curing. The Loctite Company were contacted (Redway 2002) regarding this outgassing, whence it transpired that it is an inevitable feature of cyanoacrylates, and is inherent in its technology. Alkoxyethyl cyanoacrylates behave in a similar manner, but on a reduced scale. Hence, Loctite 408 was selected as the primary binder to be used in this study. The reasons for this are that it has a very low viscosity combined with a low odour and non-blooming characteristics

3-3-4 *Solid Loading*

A preliminary study showed that, as expected, as increasing amounts of a given powder were added to the cyanoacrylates, the viscosity of the mixture increased to a point where it was not possible to be able to stir the mixture at the strain rates achievable with manual mixing. As noted above, in the present study the powder volume fraction should be as high as possible, but should result in a mixture, which has a viscosity that enables it to be applied to the substrate in a controlled and reproducible manner. Also, the cured mixture should be able to be debonded without slumping or cracks once the binder has been removed.

To calculate the weight fraction (% W_p) and volume fraction (% V_p) of the powder only the main ingredients e.g. powder and binder were taken into account. The reason for this is that the weight percentage of additives is so small that their effect on the resultant concentrations is negligible.

The following formulas were used for the calculations;

$$\%W_p = \frac{W_p}{W_p + W_B} \times 100 \quad (3.2)$$

$$\%V_p = \frac{\frac{W_p}{\rho_p}}{\frac{W_p}{\rho_p} + \frac{W_B}{\rho_B}} \times 100 \quad (3.3)$$

where W_p and W_B are the weight of powders and binder, V_p and V_B are the volume of powder and binder in the mixture, and ρ_p and ρ_B are the density of powder and binder, respectively. As discussed above, too high a concentration of powder results in very high viscosity. Also, too low a powder concentration results in inhomogeneities and separation. Thus, a balanced mixture of powder and binder is necessary.

To study the effect of solid loading, Loctite 408 was used as the binder and PTS acid and caffeine used as inhibitor and initiator, respectively. These were dissolved in the binder in a manner described in section 3-2-2. Finally, the powder was added into the solution, whilst continually mixing by hand. The quantity of powder that was added at any one time decreased as the concentration increased. It was observed that initially the proportion of powder that was added could be as high as 25% of the total amount. This was mixed uniformly into the liquid within approximately one minute. In the final stages, the powder was added in relatively small increments, ~10% of the total, with mixing taking approximately one minutes. Typically, the powder was added in 7 batches and the total mixing time was 7 minutes.

The critical solid loading in the mixture depends on many factors, including the viscosity of the binder and the powder characteristics. The viscosity of the mixture increased rapidly with increasing solids concentration near the critical point, thus rendering it more difficult to ensure a uniform distribution of powder in the binder. The optimal volume fraction for the powders was chosen to be less than the critical value to ensure that a uniform mixture was obtained.

This tolerance was selected to allow for variations in powder and binder characteristics and inhomogeneities as well as mixing attributes. For example, a mixture containing 46.5%v alumina powder No.2, could be made before the viscosity became too high, but a mixture concentration of 45%v powder was chosen to be standard in this study. An additional reason for doing this was that it was very difficult to apply the mixture as a coating when the solid loading was very close to the critical point. The effect of powder volume fraction on viscosity would be discussed in more detail in section 3-4. Table 3.5 summarizes the selected mixture compositions used to make coating mixtures from the different uni-modal and bi-modal powders. The actual concentrations were determined by weighing the components, with densities of 2.7 g/cm³ and 3.97 g/cm³ being assumed for the

Table 3.5 *Composition of the mixtures used to make coating layers. In all cases Loctite 408 was used as the binder*

Powder system	Maximum %w Powder	Maximum Vol% powder	%w P-T-S Acid*
Alumina (No.1)	78.5	50	2
Alumina (No.2)	75	45	2
Zirconia powder (No.4)	81	43	4
Aluminium powder (No.5)	76	56.5	2
70%w Alumina (No.2)- 30%w Alumina (No.3)	85	58	4

* The acid concentration is weight % of the cyanoacrylate, not total weight.

aluminium powder (No.5) and fused alumina powder (No.1), respectively, to calculate the volume fractions.

3-3-5 *Effect of Surfactant*

A surfactant is a substance added to a mixture to reduce the surface tension of the binder or the interfacial force between the surface of the powder and the binder to increase wetting, viscosity and/or dispersion. Commonly, surfactants have one end that is polar whilst the other end is non-polar.

Both anionic (DISPEX) and non-ionic (Alkyl ethoxylate) surfactants were examined. Anionic surfactants have a relatively large lyophobic (non-polar) group and a negatively charged lyophilic (polar) group, which is the surface active portion of the molecule (Reed 1995). The cyanoacrylate containing the dissolved acid started to cure locally as soon as the DISPEX was added. A possible reason for this is that even though DISPEX is acidic, its lyophilic end will be absorbed into the cyanoacrylate and the anions thus act as initiators and consequently start the polymerization.

Non-ionic surfactants do not ionize when dissolved in liquid. Alkyl ethoxylate, was added in small amounts ranging from 0.17 to 0.38%w. Although it was found to lower the viscosity of a cyanoacrylate-45%v alumina mixture, the cured coated layers were brittle and contained cracks, and there was also an apparent lack of adhesion to the substrate after curing.

Considerable further development would be required to enable an appropriate surfactant, and the required concentration in the mixture, to be identified. The coatings produced with no surfactant addition were found to be satisfactory. Therefore, it was decided not to use a surfactant in the mixture for the remainder of the present study.

3-4 Influence of Coating Mixture Composition on Viscosity

As in any CIM processes, the optimum binder content for a ceramic-binder system is a function of the compromise between maintaining the desired viscosity and maximizing the amount of powder. This depends on the binder characteristics (such as viscosity, wetting ability and chemical compatibility) as well as the powder particle size, shape and its distribution for any ceramic-binder system. The processing viscosity of highly filled mixtures is influenced mainly by the selection of the binder and the powder characteristics such as particle size distribution, particle shape and density of the powder (Reed 1995).

By fixing the kind of powder and cyanoacrylate used, the maximum feasible percentage of powder in the mixture can be obtained by focusing on the rheological behaviour and coatability of the mixtures. The most important rheological property in CIM is viscosity. It is well known that a high viscosity of a feedstock makes moulding difficult (German and Bose 1997).

The nature of the material being investigated, i.e. very adhesive binder and abrasive particles, meant that the author was not permitted to use any of standard techniques for viscosity measurement which are available within the university. Thus, in an attempt to provide an assessment of the rheological behaviour of mixtures, a device was designed and made to compare the viscosity of the mixtures by measuring the amount of mixture that was extruded from a syringe under a constant weight for a fixed period of time (Fig. 3.5). In all cases, the syringes were initially filled with the same volume of mixture.

It is well known that the mixture viscosity increases as the solid fraction in the mixture increases (German and Bose 1997). The present experiments showed that dissolving very small amounts of acid in cyanoacrylate cannot produce enough inhibition to enable a sufficiently fluid mixture to be obtained after adding a high volume fraction of powder. Thus, different weight percentages of acid, starting

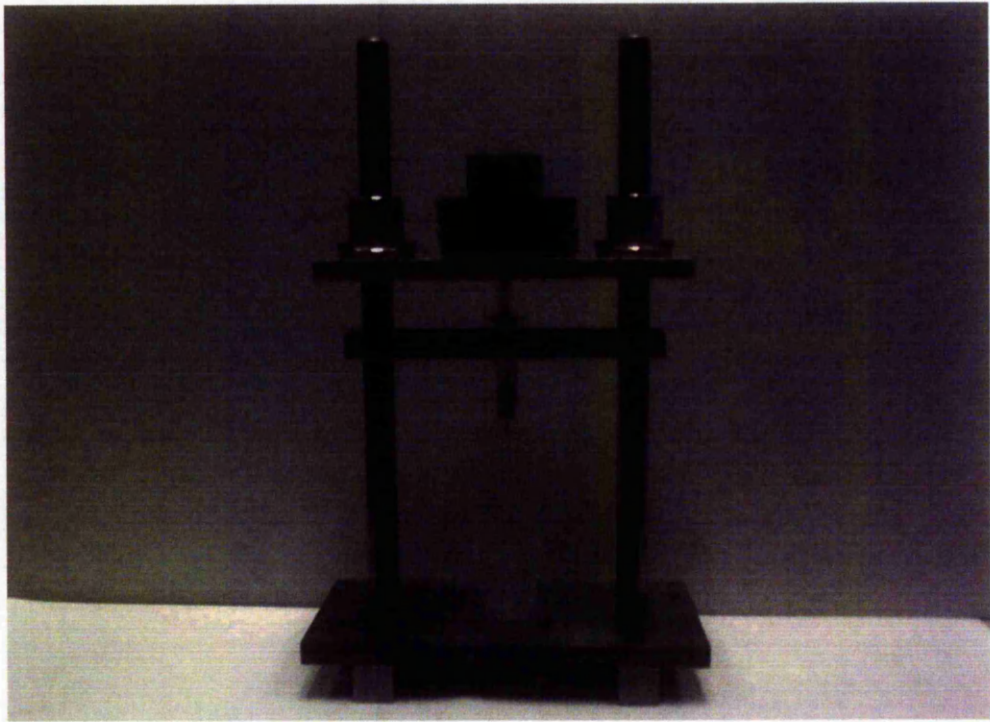


Fig. 3.5 Apparatus designed and made for comparing the viscosity of the mixtures

from 0.5%w (the weight percentage of the additives to the mixture, e.g. inhibitor and initiator, are given as a percentage of the cyanoacrylate weight only), were selected for this study.

In order to investigate the combined effect of amount of acid and caffeine dissolved, three different caffeine to acid ratios, i.e. 0.8, 1.0 and 1.2, were used. The compositions of the samples used in this study and the results obtained are presented in Table 3.6. Fig. 3.6 demonstrates the effect of caffeine-acid ratio, C/A, on the viscosity of the coating mixtures using alumina powder No.2 with Loctite 408 as the binder.

As can be seen, for all the acid concentrations used, increasing the caffeine effectively increases the viscosity. Adding 2% acid to the cyanoacrylate, results in a relatively low viscosity with a lower sensitivity to caffeine concentration.

Table 3.6 Samples created with cyanoacrylate and alumina powder No.2

Sample No	Acid level %w	Binder	Caffeine/Acid Ratio C/A (by weight)	Powder %v	Amount of material discharged in one minute (g)
R1	0.5	408	0.8	45	1.38
R2	0.5	408	1.0	45	0.3
R3	0.5	408	1.2	45	0.24
R4	1.0	408	0.8	45	2.54
R5	1.0	408	1.0	45	0.41
R6	1.0	408	1.2	45	0.33
R7	2.0	408	0.8	45	2.25
R8	2.0	408	1.0	45	2.12
R9	2.0	408	1.2	45	1.54
R10	1.0	408	0.8	46.2	0.89
R11	2.0	408	0.8	46.2	1.15
R12	1.0	420	0.8	45	1.58
R13	1.0	420	1.0	45	0.57
R14	1.0	420	1.2	45	1.04
R15	1.0	406	0.8	45	0.17
R16	1.0	406	1.0	45	0.10
R17	1.0	406	1.2	45	0.54

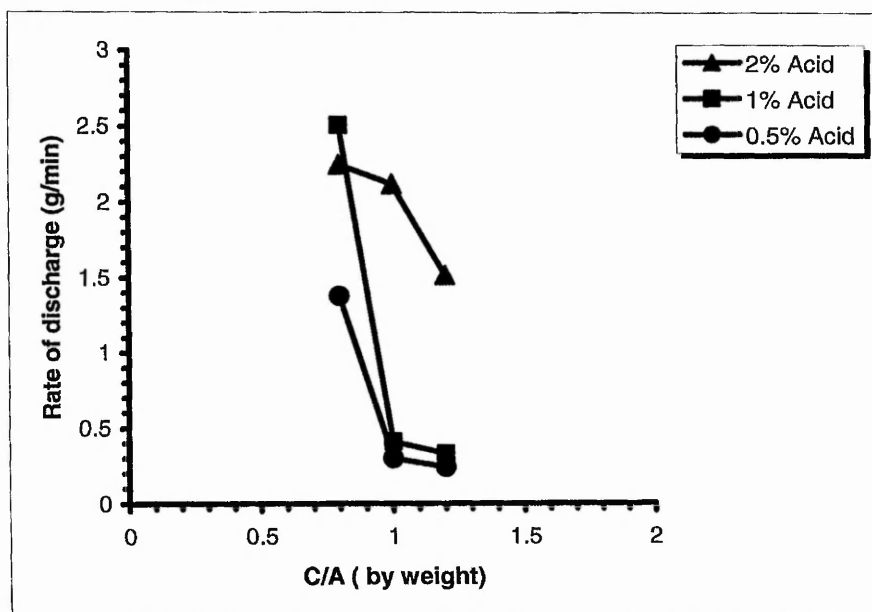


Fig. 3.6 Effect of caffeine to acid ratio, C/A , on the amount of material discharged in one minute for a mixture of Loctite 408 plus 45%v alumina (powder No. 2)

In order to compare the effect of the binder composition on the viscosity of the mixtures containing 45%v alumina powder No. 2, three different cyanoacrylates (Loctite 420, 408 and 406), with one percent pre-dissolved acid were investigated (Fig. 3.7). These results indicate that the lower the original viscosity of the cyanoacrylate, the lower is the viscosity of mixture with the same amount of powder and C/A ratio. The effect of volume fraction of loaded powder was also investigated, as shown in Fig. 3.8. Increasing the powder volume fraction increases the effective viscosity of the mixtures.

There were some discrepancies from the general observations noted above, especially for Loctite 406. This has such a high viscosity that it is difficult for the effective viscosity to be compared with the other cyanoacrylate/powder combinations using this method. The effects of such factors as the mixture sticking to the inner surface of the polypropylene syringe and plugs, renders reproducibility even more difficult. Attempts were made to reduce these effects by, for example, lubricating and spraying with PTFE the inner surfaces of syringes, but with limited success.

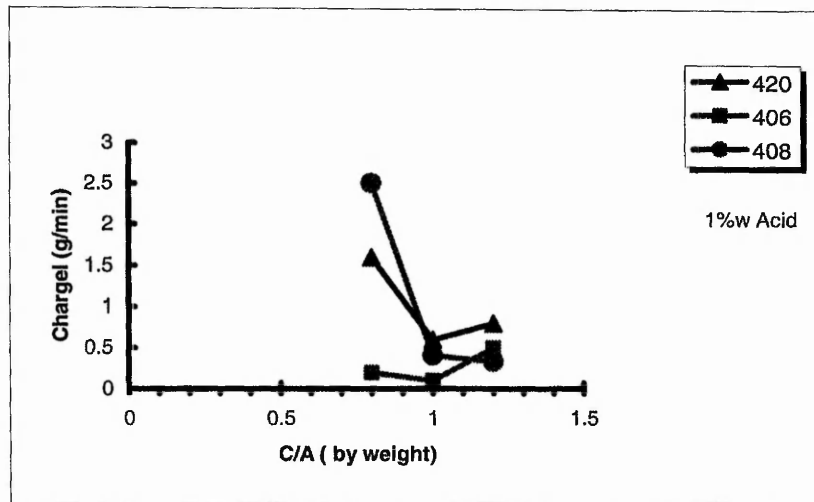


Fig. 3.7 Effect of cyanoacrylate type and caffeine to acid ratio, C/A , on the amount discharged in one minute for mixtures containing 45%v alumina powder No.2

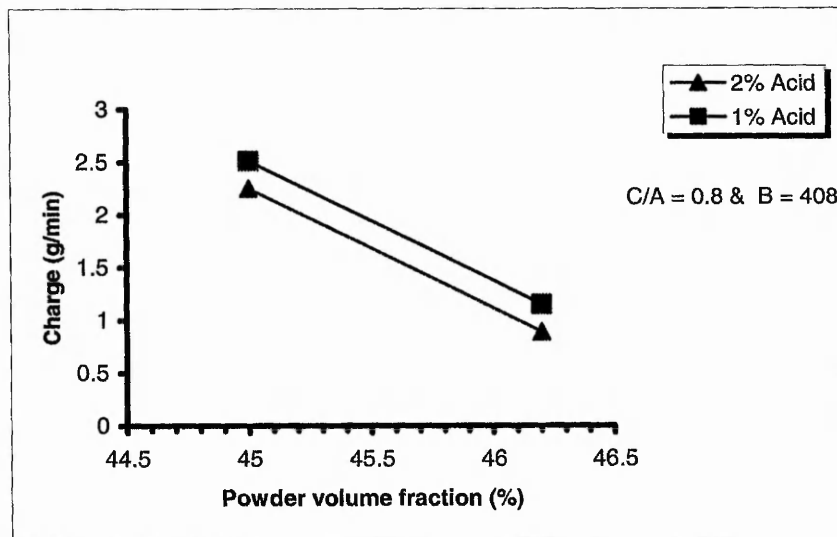


Fig. 3.8 Effect of powder volume fraction for two different acid concentrations on the amount discharged for mixtures of Loctite 408 and alumina powder No. 2. The caffeine to acid ratio, C/A , was 0.8 in all cases

3-5 pH Measurements

The ceramic powders used in this study have relatively small sizes, and hence have high surface areas, and also negligible solubility. Thus surface chemistry tends to control their charging behaviour. Many oxide surfaces have surface groups, which are hydroxylated. The surface is positively charged at low pH and becomes negatively charged at high pH, and a suspension is stable only if the pH is kept sufficiently far from the Point of Zero Charge (PZC) or IsoElectric Point (IEP).

Although the PZC values for alumina and zirconia are 7-9.5 and 4-5 respectively, a binder may change the pH range for flocculation (Reed 1995). Consequently, attempts were made to measure the pH of some of the mixtures. Cyanoacrylate containing 1%w dissolved acid has pH \approx 1. Mixing in the powder results in a change in pH to 3-4, (as measured using pH paper). To investigate if it would be possible to monitor individual mixes to control the proportions required to effect curing in a fixed time, an attempt was made to measure the pH of a mixture, using bromocresol green as an indicator, since, when the pH reaches 5.5, curing should occur. 0.2%w bromocresol green was dissolved into a solution of acid and caffeine in cyanoacrylate. No change in colour was seen during the curing process. This is probably because of lack of diffusion and atomic mobility in the mixture, especially at the final stage of curing. This approach was therefore not used subsequently.

3-6 Summary

- Rapidly polymerized cyanoacrylate can be used as a carrier to make homogenous coating mixtures contain ceramic powders,
- A uniform, stable mixture of powder and cyanoacrylate can be made using para-toluene sulphonic acid as an inhibitor,
- The concentration of the acid that is effective in inhibiting polymerization, depends on the powder concentration, composition and surface area,
- A comparison of two alumina powders, one having a relatively coarse mean particle size (8 μ m), whilst the other had a much smaller mean particle size (0.4 μ m), showed that more acid was needed in the latter case to stabilize the cyanoacrylate during mixing,
- Increasing the solid loading in the mixture required a higher concentration of dissolved acid to prevent premature polymerization of the cyanoacrylate during mixing,
- A bi-modal alumina powder used in this study with a solid loading of 58%v, needed 4%w acid to stabilize the cyanoacrylate, while an alumina uni-modal powder (8 μ m) with a solid loading of 45% needed only 2%w acid to stabilize the binder,

- The viscosity of the coating mixture is affected by the concentrations of dissolved acid and caffeine,
- For all the acid concentrations used in the study (0.5, 1 and 2%w), increasing the caffeine concentration increased the effective viscosity of the coating mixtures containing 45%v alumina powder.
- Mixtures comprising Loctite 408 with powder volume fractions ~45%v (uni-modal alumina), or ~58%v (bi-modal alumina), with acid concentrations 2%w and 4%w (of the binder) and caffeine-to-acid, C/A, ratio of ~1 have been identified as suitable for the next stages of this research

4

Coating Application & Properties

Introduction

The previous chapter has described the results of the investigation into the determination of the appropriate composition and mixing procedure to be used. The next stage in the present study was to develop a successful procedure for the application of the mixture onto a substrate, which would lead to a homogenous coating with a uniform thickness after curing. To achieve these goals, the following criteria have to be met:

1. The curing process should occur over a period of time such that handling and deposition could be satisfactorily performed, but would not be too long. An interval of between 30 and 180 minutes after mixing was considered to be appropriate.
2. Any porosity in the cured coating to be limited in extent, e.g. less than 1%, and less than the particle size. This would mean that after debinding such porosity would only be of similar size to the voids left by loss of the matrix.
3. Reproducibility of the curing process.
4. The thickness of the deposited coating to be controllable between 0.2 and 2 mm.

5. The coating should be able to be applied to a variety of substrates, with there being a reasonable degree of adhesion between the coating and the substrate.
6. The coating should be able to be deposited with uniform thickness on shaped, as well as flat, surfaces.

The key activities in this stage are:

- Application of uniform coatings
- Investigating the methods of curing the cyanoacrylate
- Study the effect of initiator on curing time and polymerization behaviour of the coating
- Microstructural study of the cured coating and its interface with the substrate
- Measuring the bond adhesion between the coating and substrate, as well as the strength of the coatings
- Minimising the porosity due to gas evolution (blooming) in the coating mixture after application
- Establish a consistent procedure to apply and cure mixtures containing ceramic powders.

In this chapter, the application of the coating mixture is described. In addition, the curing techniques are discussed in detail regarding processing parameters such as time to cure, effect of initiator, effectiveness, and consistency. Furthermore, the compatibility between the coating and substrate, as well as the microstructures and mechanical properties of the manufactured coatings, are investigated using optical and scanning electron microscopy (SEM), and tensile and hardness tests.

4-1 Application of the Coating

Application of the coating was performed after mixing the ingredients including powder, binder, P-T-S acid and caffeine as described in Chapter 3. A PTFE mould equipped with ejection pins was designed and made to enable uniform thickness coatings to be prepared. The coating was manually applied to all the samples. The coatings were uniform in appearance, aside from some voids resulting from gas release during the curing, i.e. polymerization, of the cyanoacrylate.

Fig. 4.1 shows a sample cross-section of a cured layer as well as a SEM micrograph of the same layer, which contains 45%v alumina powder. The substrate is pure aluminium plate with a thickness of 2mm. Although application was performed by hand, a uniform coating thickness could be produced. In addition, there are no signs of cracks or crack-like defects in the cured layers. A more detailed study of the presence of pore shaped defects in the coating will be discussed later in this chapter. It can also be seen how the alumina particles in the mixture are surrounded by a thin layer of cyanoacrylate (Fig. 4.1(c)).

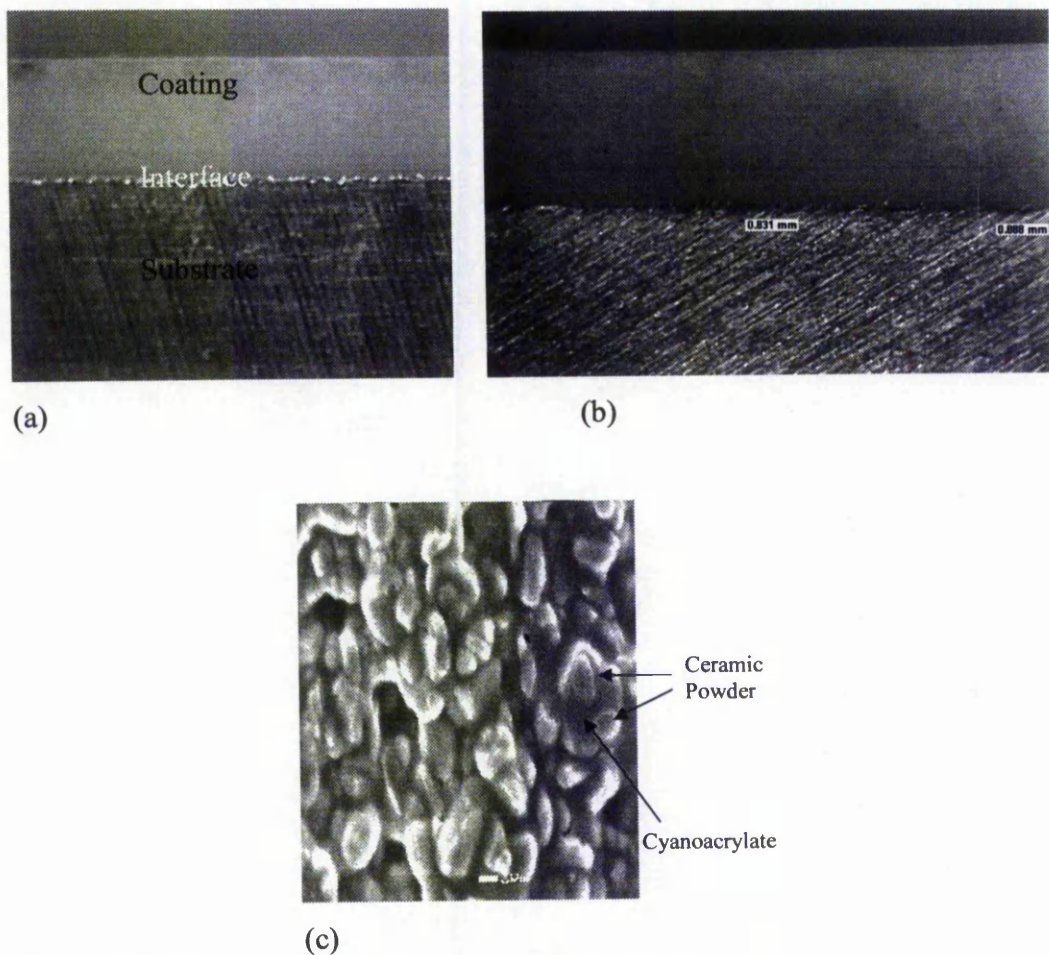


Fig. 4.1 (a) optical micrograph of cross section, (b) typical thickness of coating and (c) SEM micrograph of a cured layer, containing 45%v alumina powder on an aluminium substrate.

4-2 Curing of the Mixture

4-2-1 Curing Methods

It was necessary to ensure that curing would only take place after successful application of a homogenous coating mixture onto the substrate. Increasing the pH of the mixture to more than approximately 5.5 (Cook and Allen 1993) should initiate the polymerization process in the cyanoacrylate. Any practical, weak electron donor base can be used to effect curing.

In this study three different types of curing methods were investigated. These include curing by water vapour, surface activation and caffeine treatment.

4-2-1-1 Water Vapour

The initial trials to cure the coating mixture were undertaken on the basis of the information presented in Ridgway (2000). In his studies elevated temperature water vapour was used as the initiator to ensure the curing of ceramic parts formed using the PRIME method. In the present investigation several methods of effecting an elevated temperature saturated water vapour environment were tried. It was found that a commercial steam cooker (Fig. 4.2) was the most repeatable and appropriate method of producing a suitable atmosphere for curing.



Fig. 4.2 Steam cooker used for curing by water vapour

The samples were placed on a PTFE block, of approximate dimensions 100mm x 100 mm x 20 mm thick, which was positioned centrally on the perforated plastic plate in the steam cooker. Although the coatings were cured after three hours in this water vapour saturated environment, they became swollen and had a very porous surface, which is not suitable.

An attempt was made to eliminate this surface porosity by covering the surface with aluminium foil or teflon tape and applying pressure onto the surface. However, this procedure resulted in a substantial increase in the curing time and caused internal porosity by trapping the gases formed during curing within the coating. Thus, this approach was clearly not suitable.

4-2-1-2 *Substrate Surface Activation*

In the second group, curing by surface activation of the substrate was tried as a means of ensuring that any gas evolution did not become trapped beneath a cured surface 'skin'. The surface was activated by brushing solutions including water, sodium hydroxide and between three to five weight percent dissolved caffeine onto the surface. Methanol, water and chloroform were used as solvents for the caffeine at 45°C.

The experiments using water, sodium hydroxide and caffeine solution coating of the surface of the substrate to initiate polymerization from this surface proved to be unsuccessful. The reason for this is that there is too much acid in the coating mixture to be neutralized by substrate surface activation alone.

4-2-1-3 *Caffeine Treatment*

In the third group, it was decided to investigate the use of caffeine as an initiator. The caffeine powder was dissolved in the cyanoacrylate, after the acid inhibitor had been added, at 45°C for 30 minutes. For equal weight fractions of acid and caffeine dissolved in cyanoacrylate only, it was observed that the solution cured nearly in 3 days, gradually increasing in viscosity over this period. When the ceramic powder was added to the mixture it cured in 2 to 6 hours, depending on the type and amount of powder, and the amount of acid and caffeine in the

mixture. The details of caffeine effect on curing rate of the coating mixtures can be found in section 4-2-2.

An alternative procedure involved adding the caffeine to the mixture at the end of the process, i.e. after the addition of the appropriate amount of powder to the binder. Fig. 4.3 shows a flow diagram for the mixing procedure, which has been developed to produce satisfactory green coatings.

It was found that although this method required more caffeine, it has several advantages over dissolving caffeine prior to adding the powder, namely:

1. more consistent control of the curing time was achieved by adding the appropriate amount of caffeine without the risk of interfering with the mixing stage,
2. the cyanoacrylate binder with only acid inhibitor in it could be stored for a much longer period of time, and
3. the processing had fewer experimental difficulties, and greater consistency.

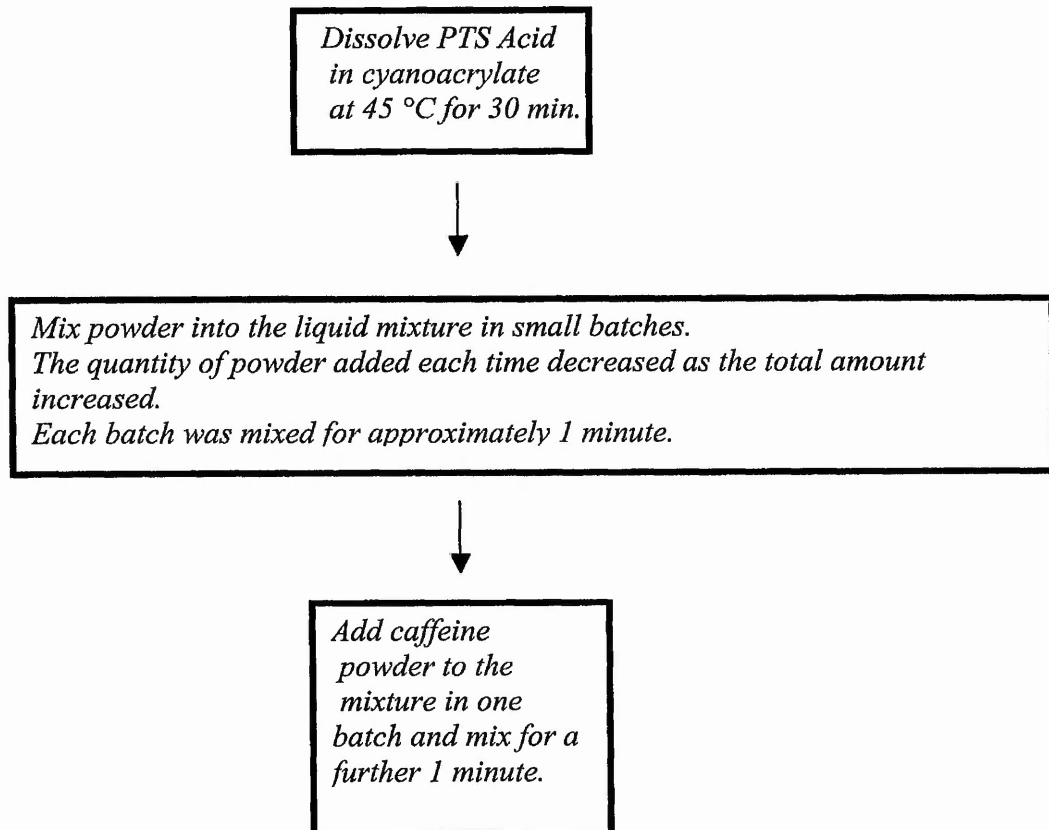


Fig. 4.3 flow diagram for the finalised mixing procedure

4-2-2 Effect of Caffeine on Curing

Since polymerization of cyanoacrylate is exothermic, curing can be accompanied by a sharp increase in temperature (Ridgway 1998). The procedure developed to follow the curing behaviour involved using a type K thermocouple embedded in a one gram specimen, either 'pure' cyanoacrylate or a mixture consisting of 75%w (45%v) alumina powder in cyanoacrylate, and measuring the temperature using a PC and A/D card (PICO-TC8) with associated software. For both samples 2%w acid and 2%w caffeine were dissolved in the cyanoacrylate, Loctite 408. Fig. 4.4 compares the temperature vs. time profiles after mixing for the present formulations excluding and including ceramic powder. There was a rapid, significant increase in temperature to 69°C approximately 8 hours after mixing for the 'pure' cyanoacrylate. This is very similar to the behaviour described in the literature (Ridgway et al 1998). In contrast, the temperature rise for the mixture with the alumina powder was much lower, occurred sooner after mixing, and was spread out over a longer period of time. This change in the timing of the temperature rise indicates that the decrease in maximum temperature cannot be due only to the increased thermal capacity associated with the alumina, but that there must be an effect on the chemistry of the curing process.

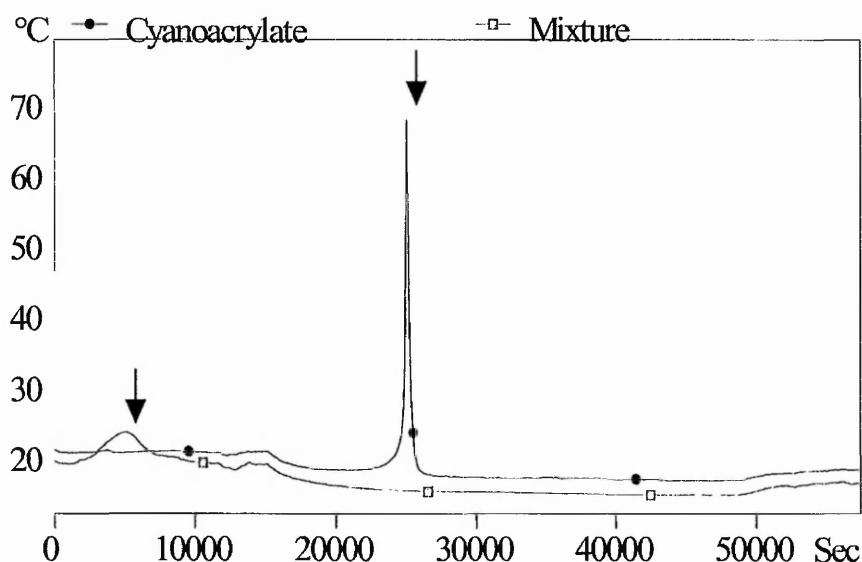


Fig. 4.4 Reaction time vs temperature curves for (a) Cyanoacrylate: Loctite 408 plus 2 w% PTS and 2 w% caffeine and (b) as (a) but with the addition of 75 w% alumina powder (MA2LS)

[Note the symbols are present from the software graph drawing package and do not represent specific data points]

To study the effect of caffeine percentage in the mixture on the curing behaviour, four samples were made with the same amount of cyanoacrylate, powder and acid and different amounts of caffeine. Fig. 4.5 shows the comparative curing behaviour of samples with four different concentrations of caffeine (1, 2, 3 or 4%w) incorporated at the end of the mixing stage. As can be seen, as the concentration of caffeine increases, the curing starts earlier and takes place over a shorter period of time. Furthermore, it shows that with the addition of more than 3% caffeine, curing starts while mixing, which can affect the viscosity, and thus 'coatability', of the mixture.

These results show that the concentration of caffeine can be optimised (1-2 %w in this experiment) to prevent premature curing during mixing and application of the coating on one hand, and avoiding long curing times to meet manufacturing requirements on the other hand.

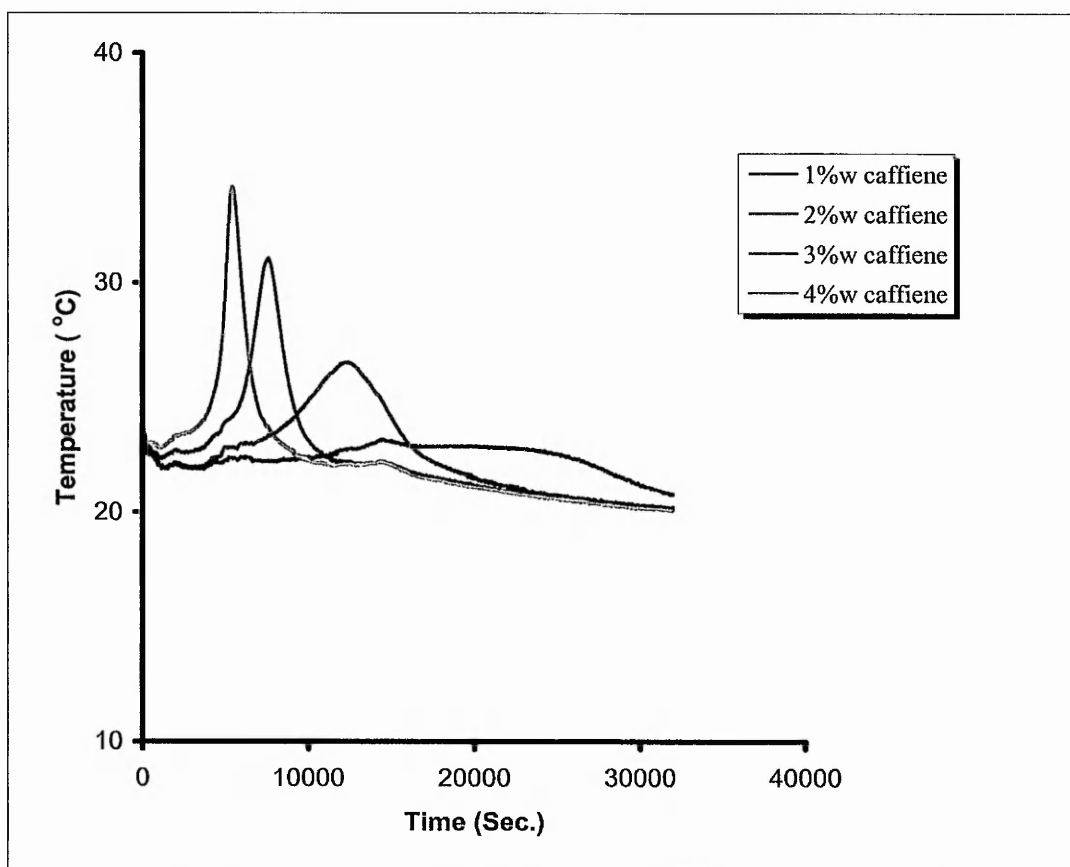


Fig. 4.5 Reaction time vs temperature curves for mixtures containing the indicated amount of caffeine plus 45 w% Alumina (MA2LS), 2 w% PTS, balance Loctite 408 cyanoacrylate.

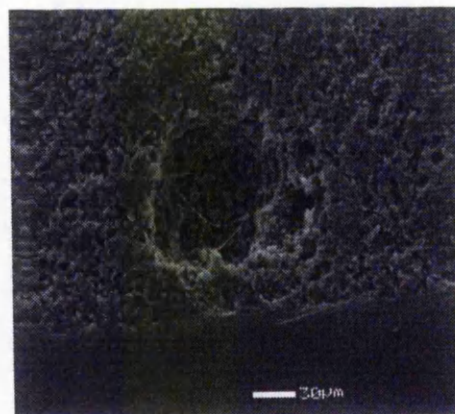
4-2-3 Gas release During Curing

The coatings were generally uniform in appearance, apart from some voids from gas release during the cyanoacrylate curing. These gas pores are produced at a late stage of curing. The Loctite Company were contacted (Redway 2002) regarding this outgassing, whence it transpired that it is an inevitable feature of cyanoacrylate, and is inherent in its technology. Fig. 4.6 demonstrates some micrographs of the typical voids produced in the coating mixture during the curing stage.

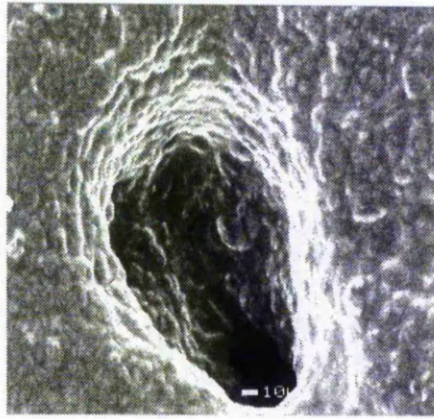
These voids are clearly undesirable and would almost certainly result in strength limiting defects after debinding and sintering. Several methods were considered to overcome this problem, e.g. cold isostatic pressing after curing. However it was noted that the gas voids appeared in the mixture at a very late stage in the curing, when the viscosity was very high. As a result it was decided that a small amount of caffeine (1.0%w) or even less (depending on required time to cure) could be incorporated into the mixture to provide a relatively slow curing rate. The key



(a)



(b)



(c)

Fig. 4.6 Examples of the range of voids observed in cured coatings: (a) optical micrograph, X40, top surface, Loctite 420, (b) SEM micrograph, transverse section, Loctite 408, (c) SEM micrograph, transverse section, Loctite 420

element though was to commence the debinding of the coating while the viscosity of the coating was high enough for handling, but before curing had been completed. This procedure was found to be very successful, and it was possible to eliminate virtually all the voids resulting from gas release during curing. This will be discussed in more detail in section 5-4, where the effect of this method on the amount of voids formed at the surface of debonded layer is illustrated in Fig. 5.9.

4-3 Powder-Substrate- Cyanoacrylate Chemical Compatibility

The interface between the deposited coating and the substrate is obviously important in determining the adhesion between the two. Therefore cross-sections of cured coated samples were prepared by sectioning perpendicular to the interface. The structure of the interface was studied using both optical and scanning electron microscopy. It was found that the SEM method was better suited to examination of the interfaces.

4-3-1 Sample Preparation

Cold mounting (room temperature epoxy) was used to prepare the sectioned samples for SEM study. It was noted that the coating materials required protection so that there was no reaction with the cold mounting constituents. Different methods to protect the coating material were examined, including spraying with

PTFE and covering with Teflon tape. The latter showed good results and was performed for all samples prior to cold mounting (Fig 4.7). The region labelled 'Affected Zone' in Fig. 4.7(a) shows the effect of the reaction between the coating and the cold mounting epoxy.

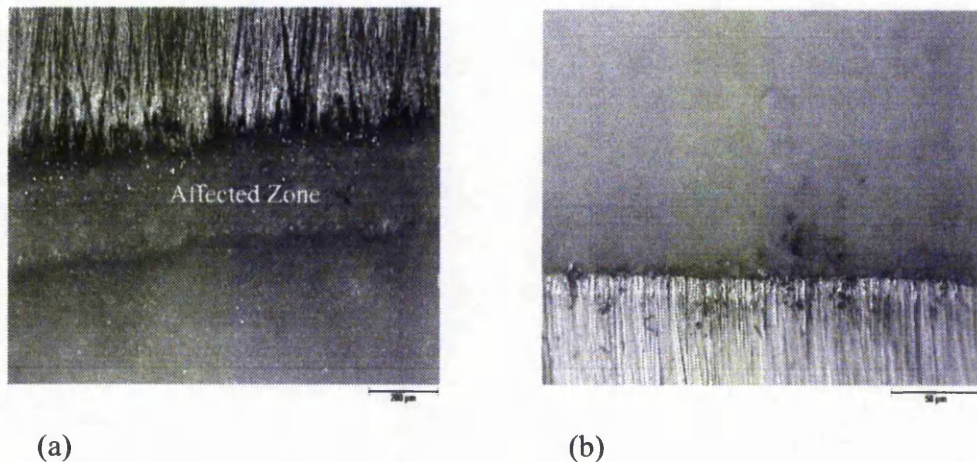


Fig. 4.7 interfaces (a) without and (b) with covering with PTFE tape prior to cold mounting

After sectioning, all samples were ground and polished to 1200 grit using SiC papers, prior to examination by optical and/or SEM.

4-3-2 *Surface Treatment of Aluminium Substrate*

As Fig. 4.8 shows, when an alumina-cyanoacrylate mixture (45%v alumina, 1%w acid, 2%w caffeine, balance Loctite 408) was coated onto a cleaned and degreased flat aluminium substrate (approximate dimensions 25 mm x 25 mm), it was found that a thin (2-3 µm) cyanoacrylate-only layer was formed at the interface. This layer could be a serious problem during debinding, as depolymerization of the layer would possibly result in weak adhesion at the interface. Several methods were investigated to overcome this problem. These included: caffeine treatment, mechanical polishing, acid cleaning and mechanical polishing followed by caffeine treatment.

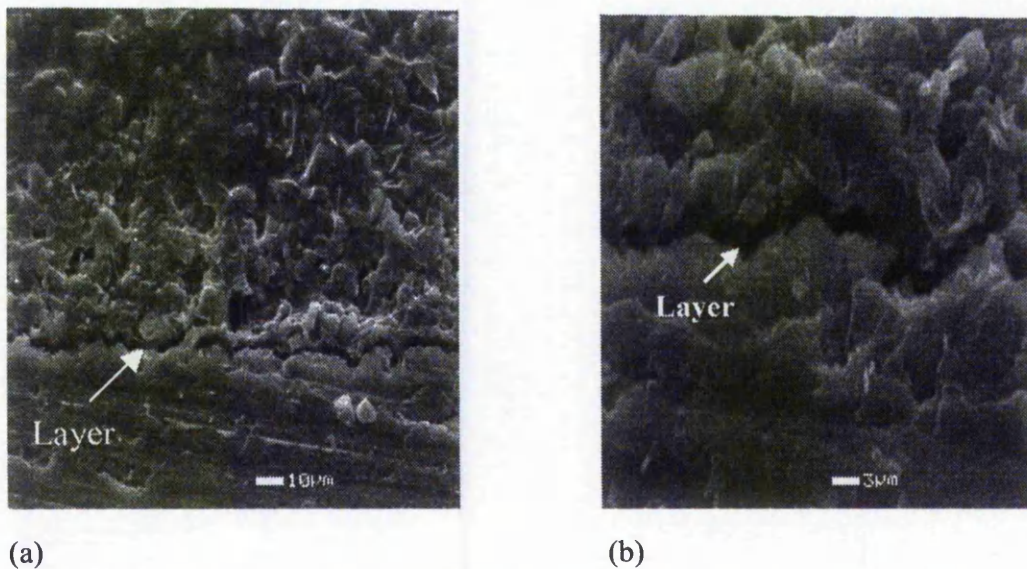


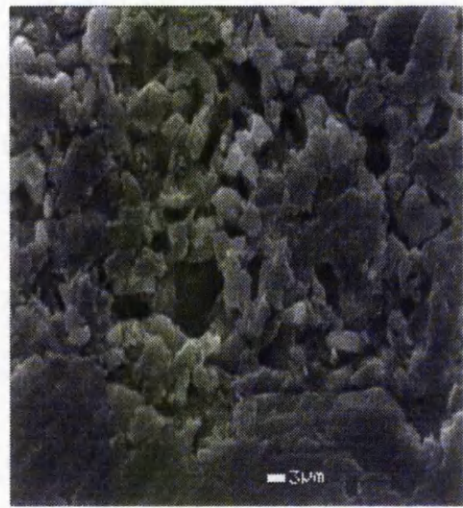
Fig. 4.8 SEM images of a transverse section of alumina-cyanoacrylate mixture applied onto an untreated aluminium substrate surface

Different solvents were used to dissolve the caffeine. Chloroform evaporated rapidly, rendering it impracticable for usage. Water only dissolved a relatively modest concentration, which meant that a thick layer of deposited caffeine was formed at the end. Caffeine dissolved in methanol provided the best results and the surface was ready after ~3 minutes. 2%w caffeine dissolved in methanol (5 minutes at 40°C) was used for the caffeine surface activation. The solution was brushed onto the surfaces of substrates.

Figures 4.9 to 4.11 show that the effect of mechanically polishing the aluminium substrate surface, acid cleaning, (which was used to remove the surface oxide layer from the Al substrate), and caffeine treatment of the mechanically polished surfaces (using SiC paper) prior to coating can effectively eliminate the cyanoacrylate only layer at the interface. Caffeine treatment alone has no obvious effect (Fig. 4.12) and caffeine treatment of an acid cleaned surface makes the problem even worse, possibly as a result of interaction between the acidic surface and caffeine pre-dissolved methanol (Fig. 4.13).



(a)

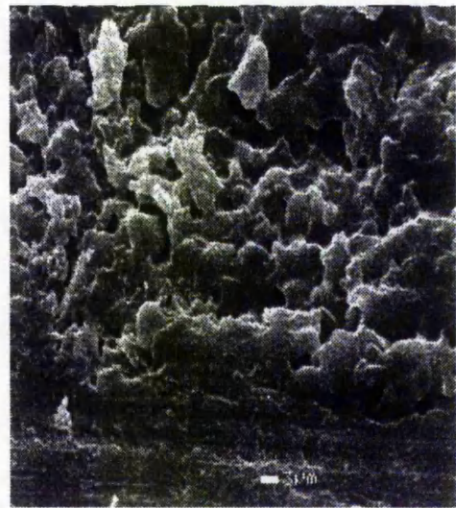


(b)

Fig 4.9 SEM images of polished cross section showing the interface between the coating and aluminium substrate with mechanically polished surface prior to coating: transverse section

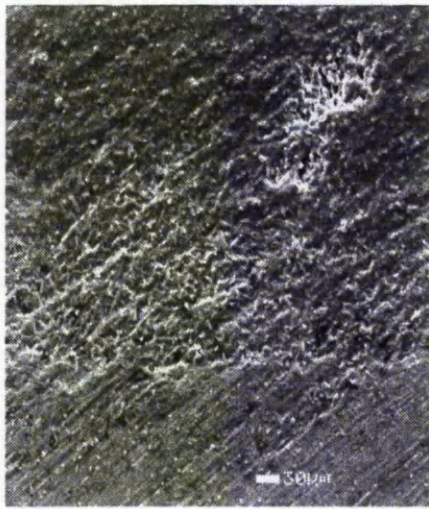


(a)

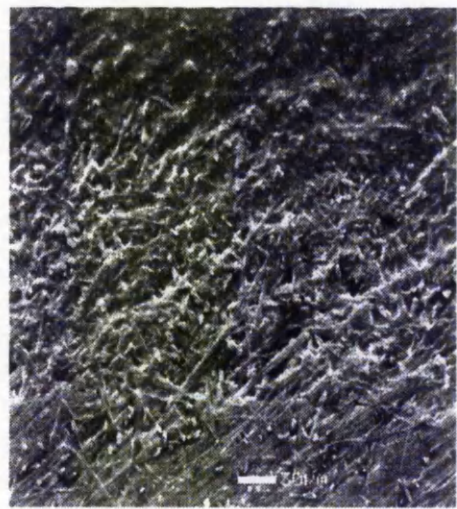


(b)

Fig 4.10 SEM images of coating deposited onto an aluminium substrate surface which had been acid cleaned prior to deposition: transverse section



(a)

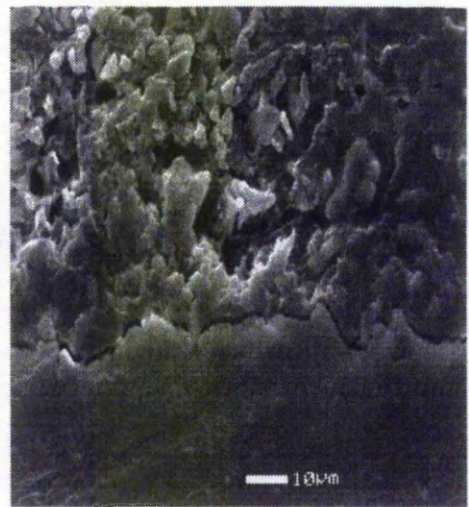


(b)

Fig 4.11 SEM images of coating deposited onto an aluminium substrate surface which had been polished and caffeine treated prior to deposition: transverse section



(a)



(b)

Fig. 4.12 SEM images of coating deposited onto an aluminium substrate surface which had been caffeine treated prior to deposition: transverse section

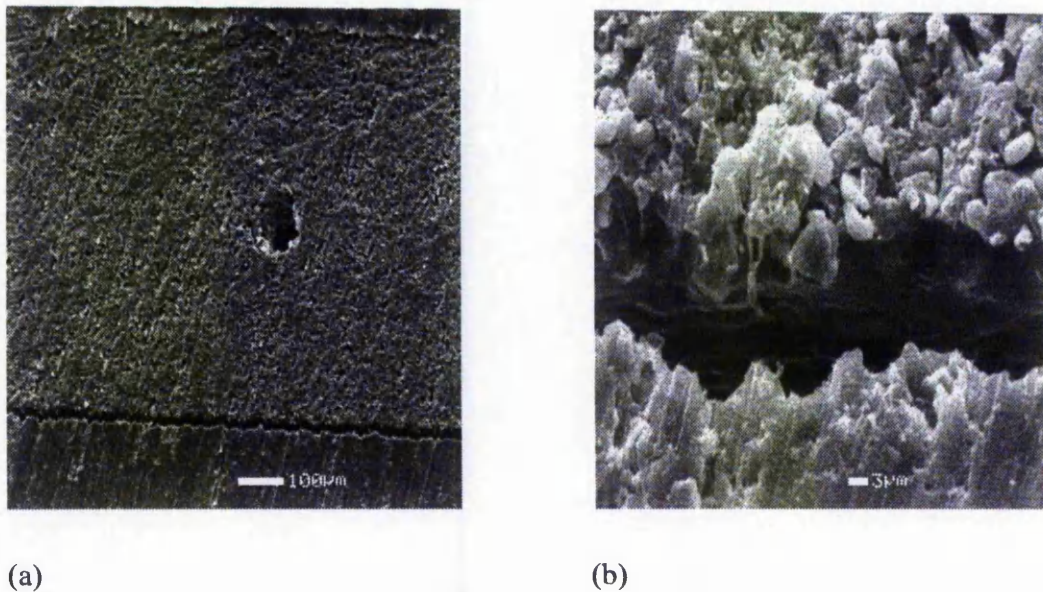


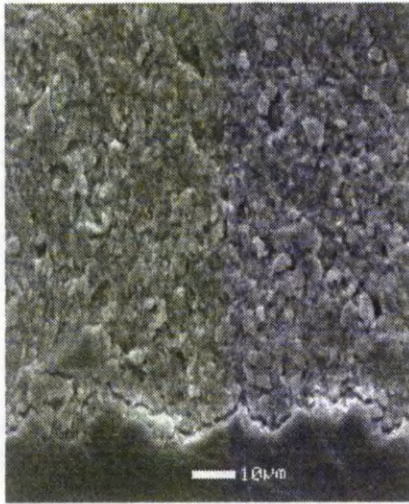
Fig. 4.13 SEM images of coating deposited onto an aluminium substrate surface which had been acid cleaned and caffeine treated prior to deposition: transverse section

4-3-3 Effect of Powder Chemistry

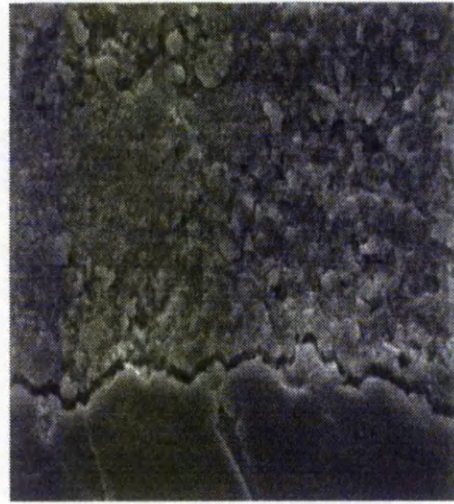
To investigate the effect of powder and substrate composition, alumina (No.2), or zirconia containing 5%w yttria, powders were used to make mixtures for coatings. Loctite 408 was used as the binder. The substrate was stainless steel and the weight fractions of alumina (No.2) and stabilized zirconia selected were 75% and 81% respectively. These correspond to volume fractions of 45% and 43%, respectively. It can be seen, by comparing figures 4.14 and 4.15, that the coating which consists of stabilized zirconia, has a cyanoacrylate only layer at the interface; however, in contrast, the interface of the equivalent alumina containing coating is sound.

These results again emphasise the effect of compatibility being required between the chemistry of the coating mixture and the substrate surface to ensure a layer free interface, which is most likely to have an effect on the coating properties after debinding.

Fig. 4.16 shows how surface treatment of an aluminium substrate, or substitution by a stainless steel substrate, can eliminate the formation of a pure cyanoacrylate layer between the coating mixture and the substrate surface.

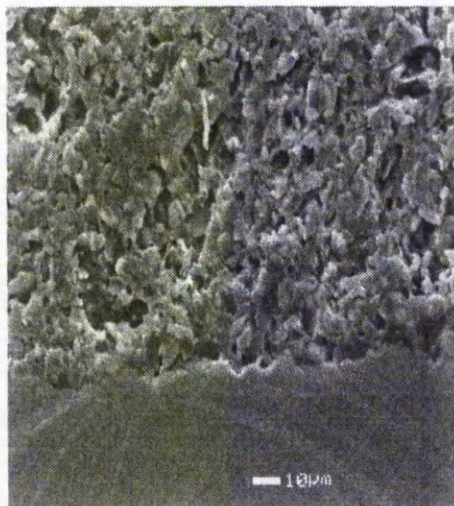


(a) X2700

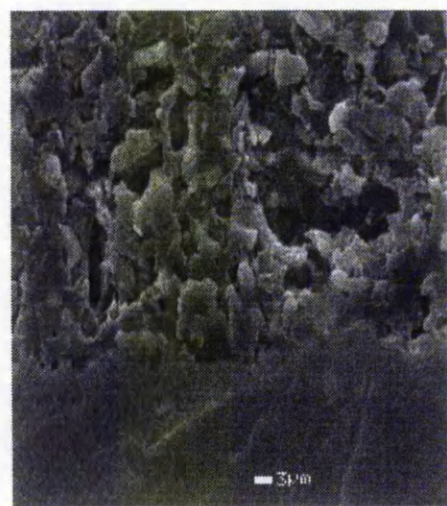


(b) X4480

Fig. 4.14 SEM images of coatings containing zirconia powder: transverse section



(a)



(b)

Fig. 4.15 SEM images of coatings containing alumina powder (No.2): transverse section

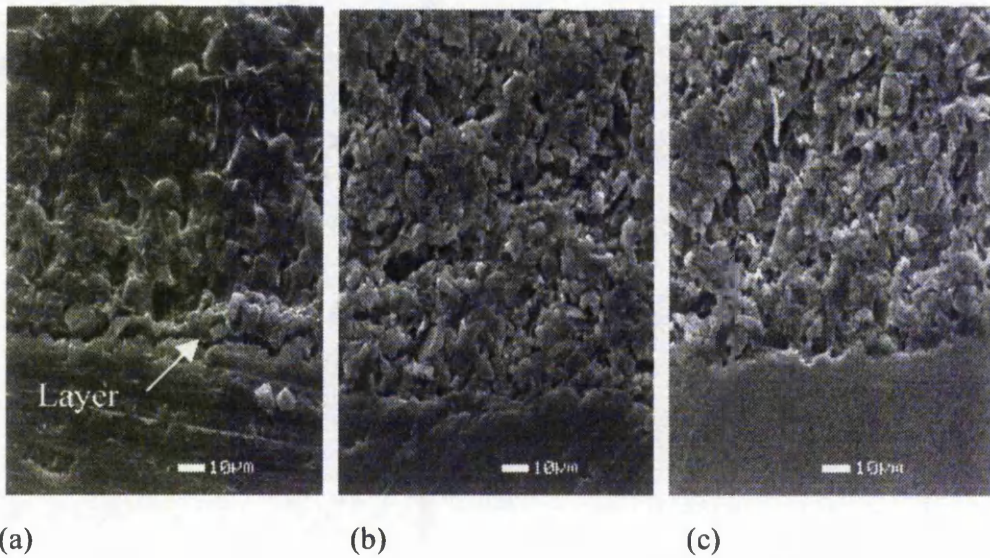


Fig 4.16 SEM images coating containing 45%V alumina powder (No.2)

- (a) Untreated aluminium substrate
- (b) Polished aluminium substrate
- (c) Stainless steel substrate

Attempts to make a uniform mixture of aluminium powder and cyanoacrylate were not successful. 2 %w acid and 1%w caffeine dissolved in cyanoacrylate (Loctite 408), as described in section 3-3-2, and 56.5%v of aluminium powder (No.5) was incorporated into the final coating mixture. As can be seen from Fig. 4.16, the coating consisted of a large number of voids. This is considered to be due to the lack of wettability of the cyanoacrylate with the surface of the aluminium powder. In addition, Fig. 4.17 shows the presence of an undesirable pure cyanoacrylate layer at the interface.

As a result of these observations, coatings containing aluminium powder were just used for preliminary studies on mixing, coating and debinding procedures and for comparison with the primary investigations concerning ceramic powders.

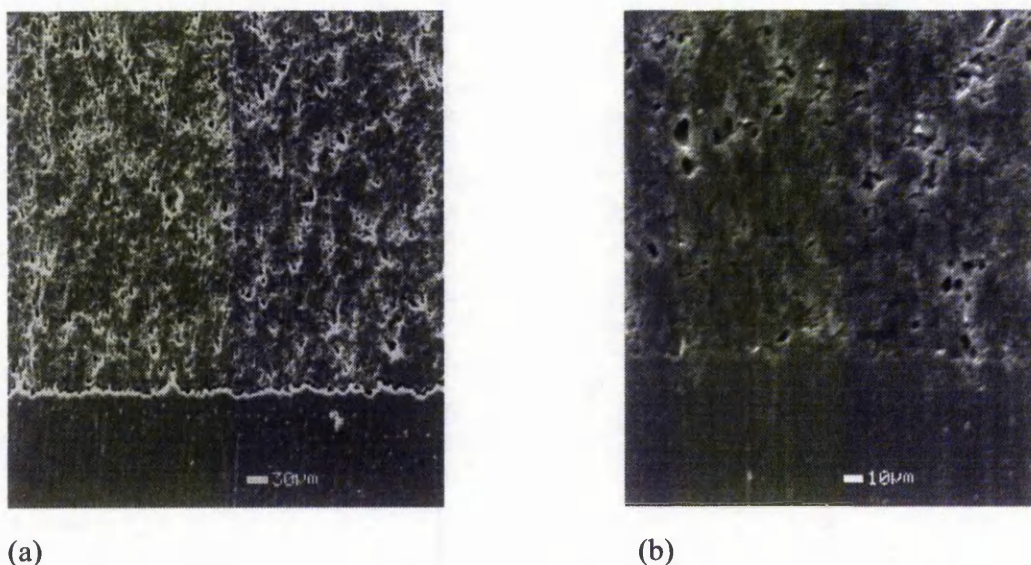


Fig. 4.17 SEM images of coatings containing 55%v aluminium powder on an aluminium substrate: transverse section

4-4 Property Testing Procedures

To study the influence of additives on the strengths of the interfacial bonding, the lap shear strengths of coatings with different levels of acid and caffeine were measured. The hardness of selected cured layers was studied as well.

4-4-1 Shear Strength Test

One method of measuring adhesion is to study its resistance to removal from the surface to which it is applied. The lap shear, or tensile shear, test measures the strength of the adhesion of the coating in shear. Shear stresses result when forces acting in the plane of the adhesive try to separate the adherent layer.

Shear strength tests on coated surfaces were carried out in accordance with ASTM standard D 1002-99 (2001). This is the most common adhesive test because of its relative ease of fabrication, simplicity of test apparatus and procedure, and the fact that it is inexpensive (Petrie 1996). Figures 4.18 and 4.19 show the geometry of the standard test specimen and a sample, which was made for the shear strength test, respectively. The specimen was loaded using a tensile test machine, causing the coating to be stressed in shear until failure occurred. A coating thickness of $1\text{mm} \pm 15\%$ and a displacement rate of 0.05 in/min were used for the tests.

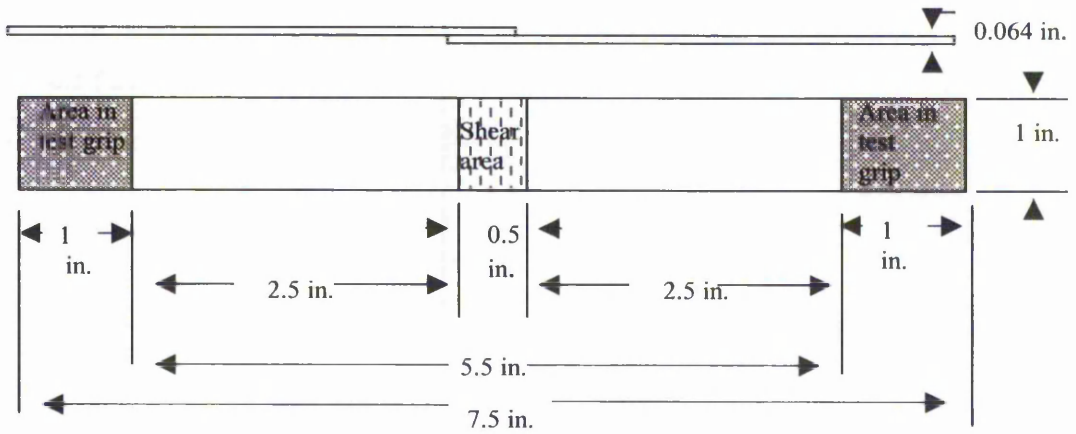


Fig. 4.18 Standard lap shear test specification design

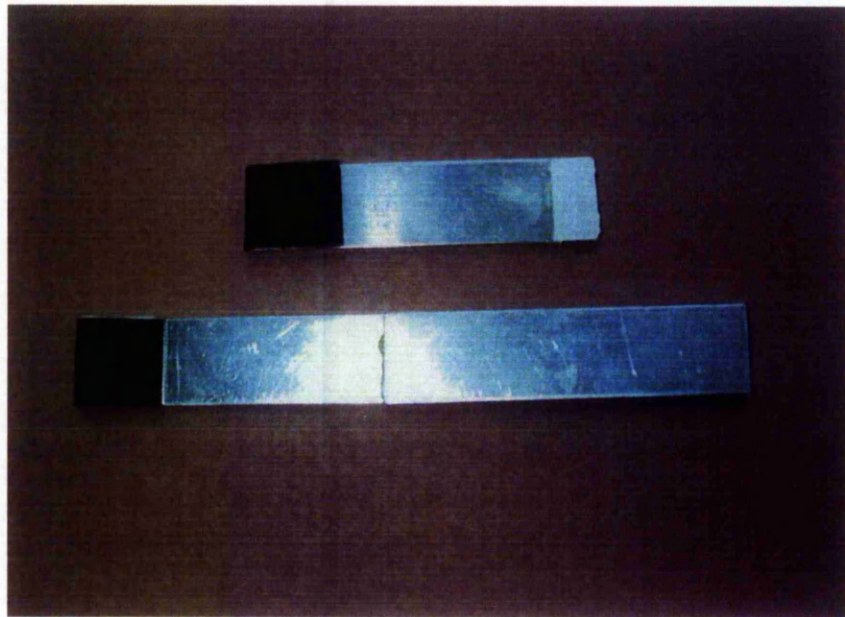


Fig. 4.19 shear strength test sample

The lap shear strengths of coated layers with different surface preparations/treatments that were evaluated are summarized in Table 4.1. All the coatings consisted of Loctite 408 into which 1% of para-toluene sulphonic acid and 2% of caffeine were dissolved, and 45%v of alumina powder was

incorporated to give a uniform suspension with the exception of Ad.1, which was pure cyanoacrylate. Aluminium plates were used as the substrate in all cases.

As can be seen, the lap shear strengths of pure cyanoacrylate adhesive and a coating containing 45%v alumina on non-treated aluminium substrates were measured as 8.3 and 4.32 MPa, respectively. These results reinforce the observations made above, section 4-3-2, that the alumina particles are adjacent to the aluminium substrate, with effectively no cyanoacrylate between the two surfaces, since the measured value is close to that expected for an area fraction of 55% cyanoacrylate, i.e. $0.55 \times 8.3 = 4.57$ MPa. Surface treatment marginally increases the adhesion of the coating to the substrate, but as discussed above, section 4-3-2, the most significant aspect of the surface treatment is to produce compatibility in the powder-cyanoacrylate-substrate system, which eliminates the layer of pure cyanoacrylate at the interface.

To investigate the combined effect of the additives, the effect of different caffeine to acid ratios (C/A) on the strength of the adhesion was studied. 0.5, 1 and 2 wt% acid were selected to make coatings on aluminium substrates. Alumina powder No.2 was used for making the coatings. One sample was used for each test.

Table 4.1 *Shear tensile strength data*

Sample No.	Substrate Surface Treatment/Adhesive	Shear Strength (MPa)
Ad.1	Pure cyanoacrylate/No treatment	8.3
Ad.2	No treatment	4.32
Ad.3	Caffeine treatment	4.32
Ad.4	Mechanical polishing	>5.12 (*)
Ad.5	Mechanical polishing and caffeine treatment	>4.64 (*)
Ad.6	Chromic acid cleaning	4.96
Ad.7	Chromic acid cleaning and caffeine treatment	>4.48 (*)

(*) Fracture of the sample did not occur at the interface between the coating and substrate

Table 4.2 is a summary of the results of lap shear tests on coatings containing 45%v alumina powder No.2 with different C/A ratios. An example of a lap shear

strength test graph is shown in Fig. 4.20. The displacement recorded is mostly as a result of sliding against the grips.

Fig. 4.21 shows the results for the alumina-cyanoacrylate coatings, which demonstrates that the lap shear strength decreases as the C/A ratio increases. This emphasises the importance of levels of additives not only on the viscosity, but also on properties of the cured layers.

Table 4.2 *Samples created with cyanoacrylate and alumina*

No	Acid %w	Cyanoacrylate Type	C/A (by weight)	Powder %v	Shear strength (MPa)
T1	0.5	408	0.8	45	5.1
T2	0.5	408	1.2	45	2.0
T3	1.0	408	0.8	45	4.6
T4	1.0	408	1.0	45	4.0
T5	1.0	408	1.2	45	2.1
T6	2.0	408	0.8	45	3.6
T7	2.0	408	1.0	45	3.6
T8	2.0	408	1.2	45	3.3
T9	0.0	408	----	0.0	8.3

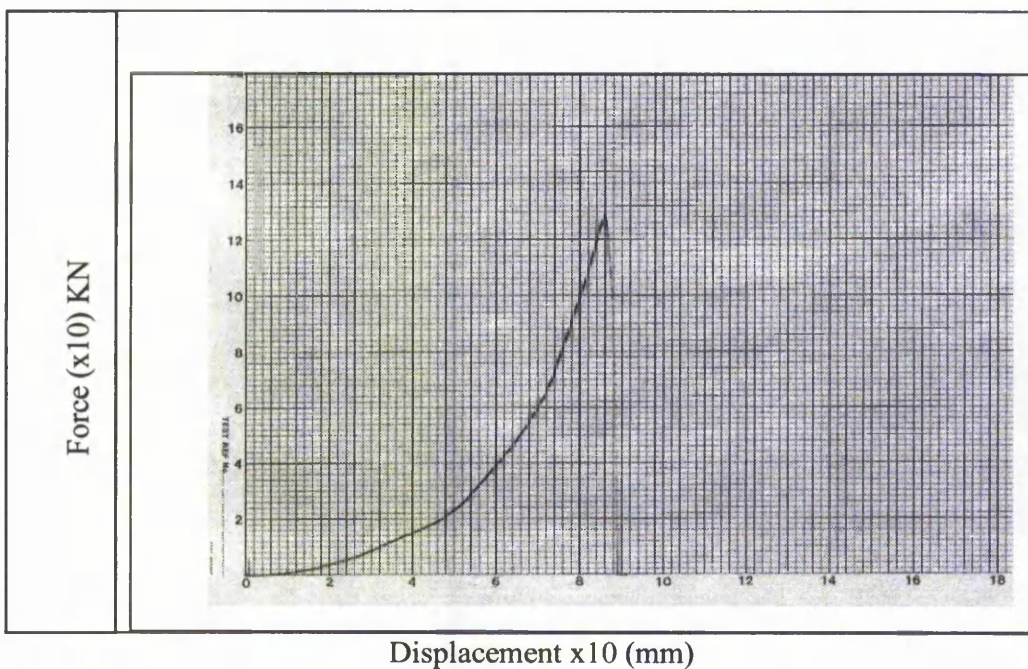


Fig. 4.20 An example of a lap shear strength test graph

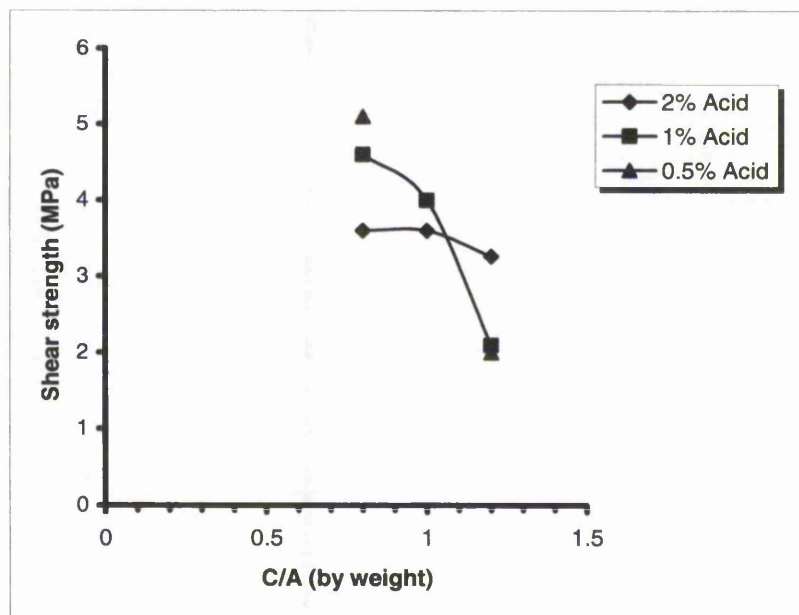


Fig. 4.21 Effect of C/A ratio on lap shear strength

4-4-2 Hardness Test

Macrohardness testing was also performed on selected samples using a standard Vickers hardness testing machine. The microhardnesses of cured coatings containing uni-modal alumina or bi-modal alumina powder were measured using a MINILOAD Leitz microhardness tester.

All samples were sectioned transversely, cold mounted and polished to 1200 grit, before testing. Fig. 4.22 shows examples of indentations on two coating mixtures, one consisting of a uni-modal alumina powder, and the other is a bi-modal alumina powder.

The hardnesses of the coatings were measured to be in the range 26.4 to 30.1 $HV_{0.2}$ for uni-modal alumina powder (No.2) and 33.0 to 37.1 $HV_{0.2}$ for bi-modal alumina (70%w powder No.2 and 30%w powder No.3) mixtures.

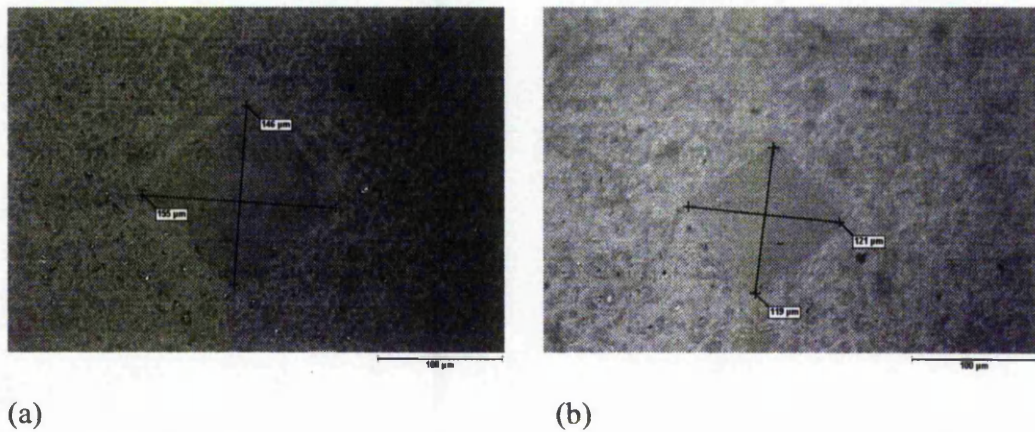


Fig. 4.22 Examples of microhardness indentations incurred coatings containing (a) uni-modal and (b) bi-modal alumina powder mixtures

The hardness of the cured cyanoacrylate (Loctite 408) was measured as 6.1 Kg/mm^2 ($HK_{0.025}$) and the hardness of Sapphire has been determined as 3419 Kg/mm^2 ($HK_{0.025}$) (Burnett and Page 1987). Using the rule of mixtures (Kim 2000);

$$\bar{H}_{up} = f_A H_A + f_C H_C \quad (4.1)$$

$$\bar{H}_{low} = (f_A / H_A + f_C / H_C)^{-1} \quad (4.2)$$

where H_A and H_C are the hardness of the alumina and cured cyanoacrylate respectively, and f_A and f_C are the volume fractions of alumina powder and

cyanoacrylate, respectively. \bar{H}_{up} and \bar{H}_{low} represent the upper and lower bound estimates of the hardness based on iso-stress and iso-strain models of composite deformation, respectively.

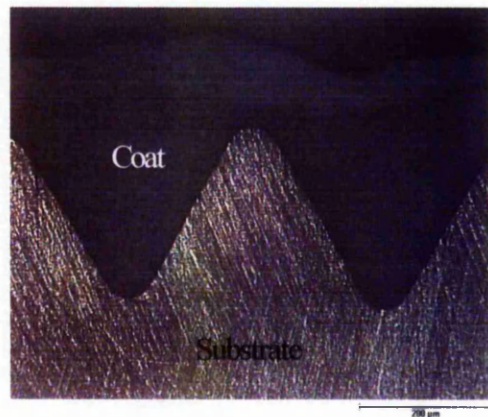
The calculated upper and lower bound estimates for the hardnesses are 1542 and 10 for uni-modal alumina, and 1986 and 14.3 for the bi-modal powder mixture, respectively. The measured hardness values are closer to the lower bound estimates. This would be expected since with the cyanoacrylate being the continuous phase, it will undergo most of the deformation, with the alumina powders acting as hard, non-deforming particles.

4-5 Irregular shape

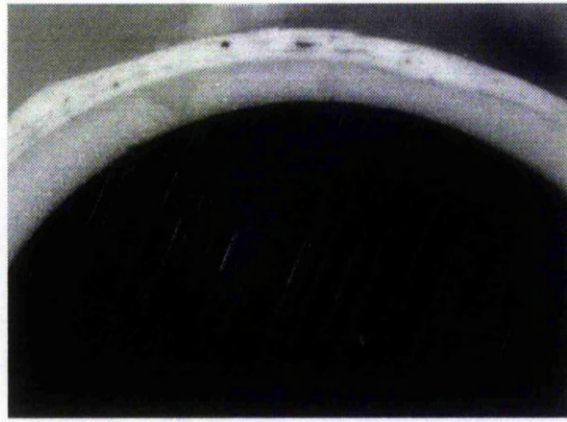
A standard M10 bolt, manufactured from plain carbon steel and a 6 millimetre diameter steel rod were used to study the effect of an irregularly shaped substrate on the formation of defects, which could occur during the curing stage. A mixture of 45%v alumina powder No. 2 in a matrix of Loctite 408 cyanoacrylate containing 2%w PTS acid and 2%w caffeine was prepared and applied using a small plastic spatula to completely cover several threads. No cracking was observed arising from the uneven surface or sharp corners (Fig. 4.23). Some voids were observed which were caused by gas release during curing.



(a)



(b)



(c)

Fig. 4.23 *Optical micrographs of an oblique transverse section of a coating applied to an irregularly shaped object, (a) and (b) bolt and, (c) rod*

4-6 Summary

- A method for application of uniform thickness coating was developed using a PTFE mould equipped with ejection pins. The coating was manually applied to all the samples using a small plastic spatula.
- An appropriate and suitable curing method was established using caffeine powder as an initiator. The caffeine was either be pre-dissolved (at 40°C for 30 minutes) in the cyanoacrylate or mixed directly into the coating mixture,
- The amount of caffeine could be varied between 1 to 2 %w of cyanoacrylate used, depending on the solid loading and type of powder.
- The curing time of the coating can be controlled by selecting an appropriate ratio of acid and caffeine in the mixture. For a fixed amount of acid, adding more caffeine results in a faster initiation of curing and shorter curing time,
- Mixing caffeine with the coating mixture has some advantages over pre-dissolving, including, better control of viscosity and cure time of the mixture and reproducibility of the process,
- The C/A ratio can affect the viscosity of the mixtures, as well as the strength of the adhesive bond between the substrate and the cured layers,
- Chemical compatibility between the coating mixture and the substrate surface (cyanoacrylate-powder-substrate system) is needed to produce a

layer free interface, which would generally be expected to affect the coating properties after subsequent thermal treating,

- The hardnesses of the coatings were measured to be in the range 26.4 to 30.1 HV_{0.2} and 33.0 to 37.1 HV_{0.2} for uni-modal alumina powder (No.2) and bi-modal alumina (70%w powder No.2 and 30%w powder No.3) mixtures, respectively.
- An irregular substrate geometry containing sharp corners does not cause defects during the curing stage.

5

Debinding

Introduction

The role of the binder in the coating mixture is to keep the particles attached firmly to each other, and to the substrate, during handling and other manufacturing process steps. It is temporary and has to be removed from the coating layer prior to densification at the sintering stage. This latter process step is termed debinding. The binder removal is a key step in the present method of applying a ceramic coating, since binder removal may lead to the creation of macro defects such as blistering, surface cracking and large internal voids, as a result of thermal expansion and vapour pressure attributable to the polymer rapidly decomposing.

Thermal binder removal involves several physical or chemical processes; these include polymer decomposition, monomer diffusion to the core, gaseous transport of monomer in the porous layer, and removal of the monomer from the surface (Shi and Guo 2004). These ingredients must be removed slowly, in a process that requires the gradual formation of passages within the layer with increasing temperature and time. These passages allow the major binder ingredient(s) to escape, generally by heating to a temperature in the range 150°C to 600°C, without causing the part to suffer significant degradation.

The main objectives in this stage were:

- 1- Study the thermal degradation of the cyanoacrylate, and coating mixtures containing cyanoacrylate as a binder.
- 2- Determine the depolymerization temperature range and rate.
- 3- Investigate methods to ensure that the debonded layer will retain its integrity after debinding.
- 4- Determine if sufficient adhesion remains at the interface of the coating and substrate after debinding.
- 5- Establish a thermal debinding cycle which leads to a macro-defect free debonded layer.

This chapter describes the various methods investigated for the thermal debinding of the cyanoacrylate used to give a coating of the desired structure and properties.

The key activities were:

- Thermal analysis of the binder using TGA and DSC techniques,
- Practical thermal debinding of cured coatings,
- Determining the most effective thermal debinding cycle for the cured coating using step and/or ramp heating of the samples,
- Debinding partially cured coatings to minimise the resultant macro-porosity in the coating mixture as a result of gas evolution during the polymerization of the cyanoacrylate.

5-1 'Pure' Cyanoacrylate Debinding Characterisation

A major drawback to the use of cyanoacrylates as an industrial thermoplastic adhesive is that they exhibit a low temperature resistance and decreased performance at raised temperatures compared to thermosetting adhesives such as epoxies. This is because of the quaternary carbon atoms in the main chain. This polymer type is known to have a low resistance to temperature due to its inclination to depolymerize rapidly at relatively low temperatures (Denchev and Kabaivanov 1993). In their study, Denchev and Kabaivanov (1993), noted temperature of 170°C for the start of depolymerization of ethyl cyanoacrylate,. The upper temperature limit for the sustained use of most cyanoacrylates is about 70°C (Millet 1981, Schoenberg 1990). This disadvantage of cyanoacrylate

polymers is actually a considerable *advantage* in the debinding stage of the coating layers. The fact that it is a one part adhesive which fairly rapidly debinds with *simplicity* at a low temperature, compared to the normal debinding temperatures and times for conventional binders, is a significant benefit.

The thermal degradation behaviour of cyanoacrylates has been studied in some detail (Rooney 1981, Negulescu et al 1987, Denchev and Kabaivanov 1993). It has been shown that cyanoacrylate polymers can be depolymerized thermally at low temperatures, and the product of the degradation is monomers, or oligomers with relatively small molecules. Furthermore, it has been shown that it is a chemically simple process with a chain end-initiated unzipping reaction (Birkinshaw and Pepper 1986).

It has been noted that for pure ethyl cyanoacrylates, thermal degradation of the binder is practically complete at temperatures around 250°C (Negulescu et al 1987) or 230°C (Denchev and Kabaivanov 1993) at a heating rate of 10°C/min. A lower degradation temperature was observed using a holding period at 140°C (Denchev and Kabaivanov 1993) or 163°C (Rooney 1981).

It has been noted that, although the shape of the thermal analysis curves (DSC) consists of a single sharp peak, the thermal behaviour of the cyanoacrylates is strongly dependent upon the chemical composition of the polymers (Neglect et al 1987, Denchev and Kabaivanov 1993). A slower depolymerization rate and higher heat resistance can be achieved by incorporating into the unsaturated esters of 2-cyanoacrylic acid such groups as allyl or allyloxyethyl 2-cyanoacrylates. It has been proposed that the reason for this is connected with formation of crosslinks in the adhesive (Denchev and Kabaivanov 1993). With regard to the effect of atmosphere on the thermal degradation of cyanoacrylates, Rooney (1981) and Negulescu (1987) found no appreciable effect of the nature of the atmosphere on the rate of depolymerization. Consequently, in this study all the debinding experiments were conducted in air at normal atmospheric pressure.

5-2 Binder Thermal Analysis

There are several analytical tools and models which are available that can provide information about decomposition products, rates, and mechanisms (Shi and Guo 2004, Shengjie et al 2004). However, these do not always provide *a priori*

accurate descriptions for practical cases. Thus, in this study it was decided to concentrate on an experimental investigation of the debinding characteristics of the present systems. In this case, it is appropriate that the thermal behaviour of the cyanoacrylate should be assessed as a prelude to performing debinding trials on the mixtures.

Although the thermal degradation of cyanoacrylates has been studied, a significant difference exists between the debinding characteristics of a pure binder and a powder mixture (German and Bose 1997). Therefore it was decided that an assessment of the general characteristics of the debinding process could be obtained by performing Thermal Gravimetric Analysis (TGA) and Differential Scanning Calorimetry (DSC) on a selected alumina – cyanoacrylate mixture. The main purpose of these analyses was to establish some initial guidelines on the nature of the degradation reaction, as well as its rate and the threshold temperature of cyanoacrylate curing in the coating mixture. These analyses were kindly performed at the University of Limerick (Birkinshaw

5-2-1 Thermal Gravimetric Analysis

Thermal Gravimetric Analysis (TGA) is the most frequently used method for measuring the rates of thermal decomposition of organic binders. The method records the percentage weight loss, in this case of binder material, as a function of

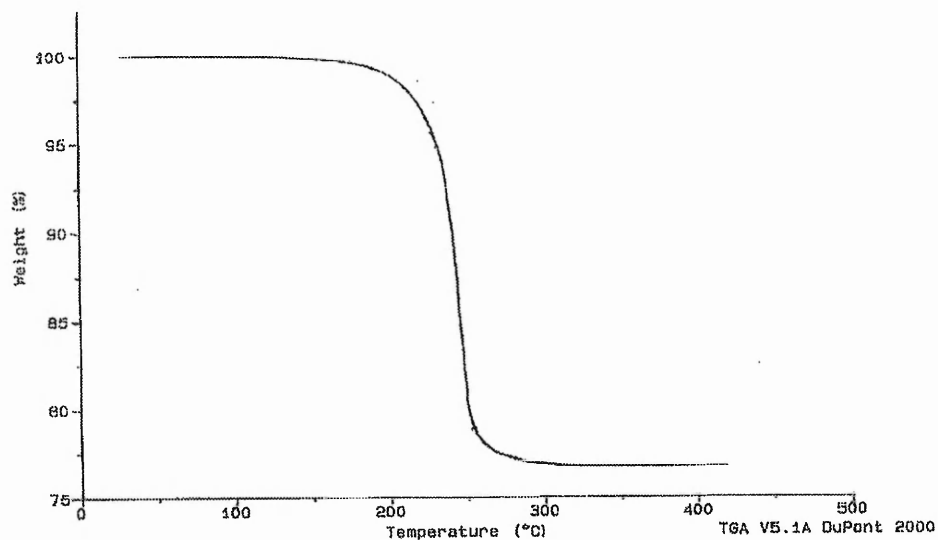


Fig. 5.1 Weight loss vs temperature for a mixture 45%v Al_2O_3 in Loctite 408 (Birkinshaw 2003)

time using a constant heating rate and can also be used to determine decomposition temperature and reaction kinetics. In this case a sample with 45%v alumina powder (No.2) and Loctite 408 binder was analysed using a DuPont 2000 instrument, in the presence of nitrogen, up to 400°C at a heating rate of 20°C/min. (Birkinshaw 2003).

5-2-2 Differential Scanning Calorimetry

Differential Scanning Calorimetry (DSC) is used most frequently to gather information about thermal characteristics and the rate of debinding. Fig. 5.2 shows the Differential Scanning Calorimetry result for a mixture of 45% Al_2O_3 (Powder No.2) in Loctite 408 (Birkinshaw 2003). The thermal decomposition exhibits only a single exothermic peak with the main heat output occurring at $\sim 230^\circ\text{C}$, although it can be noticed that the decomposition actually commences at a much lower temperature, i.e. between 100°C and 150°C . This result means that care is needed during the debinding process to ensure that localised regions do not experience rapid depolymerization, and thus increase in temperature.

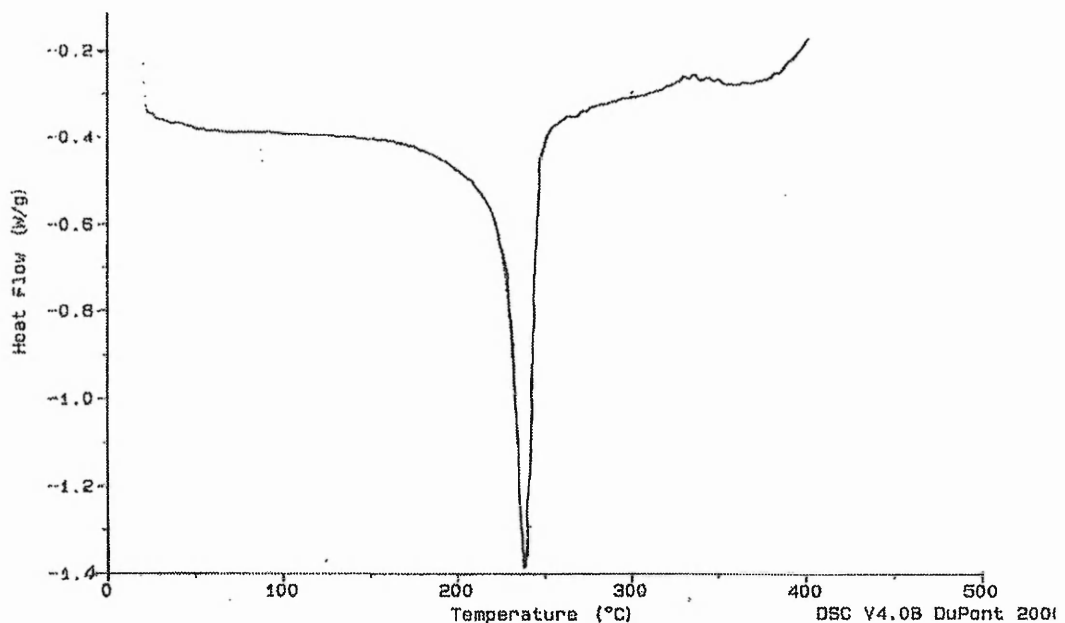


Fig. 5.2 DSC output for a mixture 45% Al_2O_3 in Loctite 408 (Birkinshaw 2003)

5-3 Heating Methods

Thermal debinding of actual coating layers was investigated using two methods; surface heating and oven heating. The reason for trying surface heating was to determine if the initiation of debinding from the surface of the layer would promote a debinding 'front' to gradually transit through the thickness of the coating.

A flat ceramic heating bracket of approximate dimensions 60 mm x 120 mm, with embedded thermocouple to control the temperature and to enable a fixed temperature to be set, was used for the surface heating. The heating element was placed parallel to the flat-coated specimens at various distances between 20 mm and 50 mm from the top surfaces.

The coated specimens were 25 mm x 25 mm with a coating thickness of 1 mm. Although the heating rate was not well controlled, the temperature of the heater could be set using a Eurotherm model temperature control. It increased quickly to the set temperatures (200°C, and 220°C), where it remained constant within ± 5 deg C.

It was noted that this method caused the coating to swell and the surface became porous after debinding. The main reason for that could be lack of precise temperature control at the surface and through the thickness of the coating.

As a consequence, attempts focused on the bulk (oven) thermal debinding of the layers, where better control of temperature can be achieved, accompanied by less potential environmental problems from the released cyanoacrylate monomer.

5-3-1 *Debinding Procedure*

The evolved products of the debinding process consist mainly of cyanoacrylate vapour, with some CO₂, NO₂ and H₂O. In order to avoid introducing cyanoacrylate vapour into the laboratory atmosphere, it was necessary to perform all the debinding experiments in a sealed oven (BINDER FED-50) with its exhaust vented externally. The oven was already available, but a suitable method of venting had to be designed and installed. This ensured that the monomer cyanoacrylate and any other obnoxious gases were sufficiently well dispersed. After debinding, the powder particles in the coating mixture were held together by

the weak attraction forces of the cyanoacrylate binder. These forces also provide the adhesion to the substrate interface after debinding.

It has been previously noted (Ridgway 2001) that the debonded monomers can be condensed and collected for re-use as polymers on an industrial scale. For the present research purposes, in which only a small amount of binder is used, it was considered to be more practical to release the gas into the atmosphere.

5-3-2 *Influence of Fast Heating Rate*

The thermal debinding of the coating mixtures was initially investigated using oven heating in air. This simply involved heating from room temperature to 250°C at an uncontrolled rate determined by the power input, and effective thermal mass, of the oven. The oven took 45 minutes to reach 250°C. As anticipated, it was found that this relatively rapid heating caused the coating to swell and the surface to become porous after debinding. Furthermore, there was no adhesion at the interface after debinding. Fig. 5.3 shows the swelling and the porosity resulting from this relatively rapid heating of the coating mixture. By visual inspection of the coatings at 10 degree intervals, it was found that the swelling mostly occurred at around 180°C.

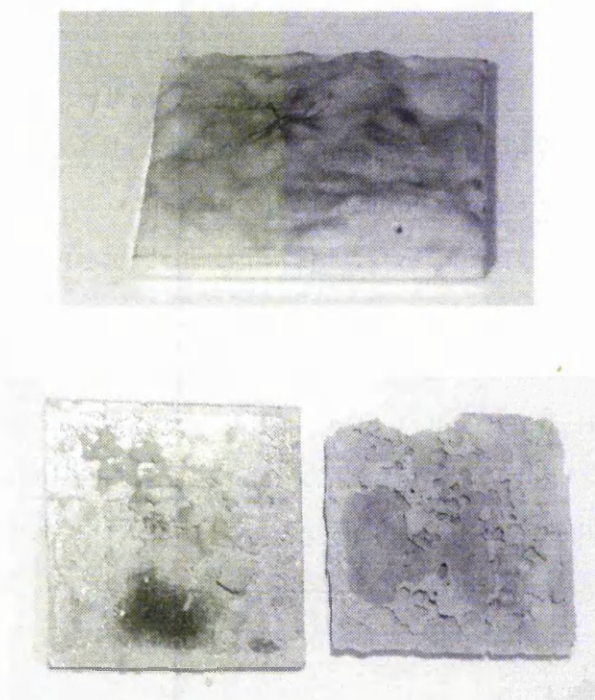


Fig. 5.3 *Examples of defects arising from too rapid debinding of the coatings*

5-3-3 Step Heating of the Coating Layer

Clearly an appropriate debinding cycle had to be devised to overcome the problems described in the previous section to produce macro-defect free samples. In general, it is necessary to use a well-defined combination of temperatures and times to give satisfactory debinding (German and Bose 1997). This is the case in the present study, where it was shown that it was necessary to investigate the depolymerization temperatures/times in more detail. Fig. 5.4 shows cracking defects arising from the use of an inappropriate debinding rate in a coating made of alumina powder (No.2). These cracks were formed when a debinding regime with no dwell time was used, i.e. continuous heating from room temperature to 220°C in ~2.5 hours. These kinds of defects would obviously result in poor mechanical properties in the final sintered coatings.

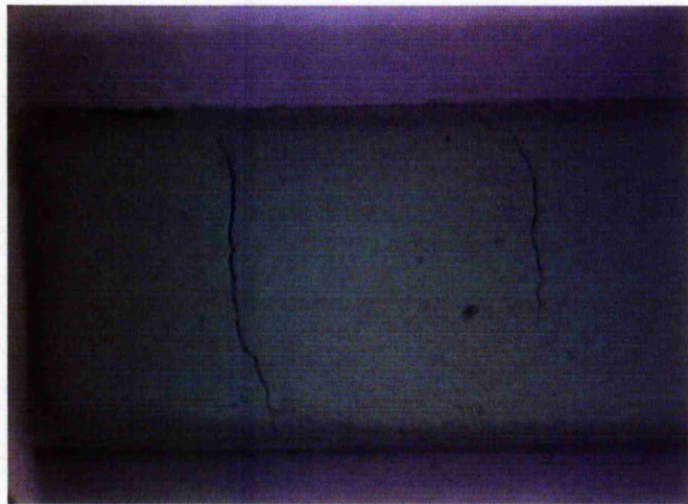


Fig. 5.4 Sample of cracking defect in coating layer

To study the slow heating of the samples in an oven, Newtonian heating theory (Eastop and McConkey 1993) was first used to determine a minimum effective heating rate for the debinding stage. This approach, also known as lumped capacity, may be used when the temperature within a body does not vary significantly as the body's average temperature changes with time due to exposure to a fluid at a different temperature. The equation can be written as:

$$\frac{t_f - \bar{t}}{t_f - t_i} = e^{-BiFo} \quad (5.1)$$

where t_f = oven set temperature
 t_i = initial sample temperature
 \bar{t} = average sample temperature
 Bi = Biot number
 Fo = Fourier number

In unsteady state heat transfer, the Biot number and Fourier number can be written as:

$$Bi = \frac{h.L}{k} \quad (5.2)$$

$$Fo = \frac{k.\tau}{\rho.C.L^2} \quad (5.3)$$

where in this case for a 1 mm thick coating containing 45 %v alumina then:

k = thermal conductivity of the compact = 1.5 (J/s.m.°C)
 h = heat transfer coefficient = 30 J/m².s.°C
 L = coating thickness = 1 mm
 τ = time (sec.)
 ρ = density of the compact = 2.392 g/m³
 C = heat capacity of the compact = 1188 J/kg.°C

Loctite data sheets (2004) and data supplied by Ng (2004) were used to derive the required properties and constants.

Hence,

$$BiFo = \frac{h.\tau}{\rho.C.L}$$

or; $\tau = \frac{\rho.C.L}{h}.BiFo \quad (5.4)$

Equation 5.4 can be used to estimate approximately the time needed for the coating interface to reach the furnace temperature.

In the present trials, the furnace set temperature was increased in 10 to 20 degree C steps throughout the active debinding temperature range, i.e. 100°C to 200°C (the oven temperature took between 4 and 6 minutes to equilibrate at each step, depending on the temperature). Now, it is reasonable to assume that equilibrium will have been nearly attained when the average temperature of the coating is within 1 deg C of the set temperature, i.e.

$$\frac{t_f - \bar{t}}{t_f - t_i} = \frac{1}{10} = 0.1 = e^{-BiFo}$$

$$\therefore e^{BiFo} = 10$$

$$\text{or } BiFo = 2.303 \quad (5.5)$$

$$\therefore \tau = \frac{2392 \times 1273 \times 0.001 \times 2.303}{30} = 234 \text{ sec.}$$

This approximate calculation shows that it takes nearly four minutes for the interface to reach the furnace temperature, with any subsequent holding time resulting in thermal debinding.

The calculation ignores any heat absorption and generation including heat absorbed by depolymerization of cyanoacrylate during thermal degradation. The result indicates that the average temperature in the compact is within 1°C of the furnace temperature. The result suggests that for heating in steps of 10°C sufficient time should be allowed for the oven to increase in temperature, the coating to increase in temperature and the debinding process at that temperature to proceed almost to completion. It was observed that the oven temperature increased in 4-5 minutes, depending on the temperature, the average coating temperature was calculated above to require ~4 minutes, with the time for depolymerization not known. It was therefore considered reasonable to use dwell times of ~30 minutes at the set temperature to determine if this would prove to be appropriate.

For the initial trials, aluminium powder was used to study the debinding behaviour of the coating mixtures. The coatings consisted of aluminium powder (No.5) and cyanoacrylate (Loctite 408) with a particle loading of 55%v. To study the effect of coating thickness, samples with either a 'thin' or 'thick' coating, i.e. 0.6 or 1 mm, respectively, were utilised since this covers the practical coating thickness range of most interest in this investigation. The substrate was pure aluminium plate in all cases. These samples were thermally debonded by increasing the temperature from room temperature to 150°C in one hour, and then step heating the coatings by heating for 45 minutes at each of the following temperatures; 150, 165, 180, 190, 200 and 220°C. Several identical samples were

placed together in the oven, and one sample quickly removed from the oven after each holding temperature, so that the weight loss could be determined at each stage. Fig. 5.5 shows the percentage weight loss of the cyanoacrylate binder phase as a function of the final hold temperature. It can be seen that the relative weight loss is slightly greater for the thinner layer, as might be expected, but that there is not a substantial difference. Further trials showed that further heating at higher temperatures did not increase the weight loss of the binder, indicating that using this particular combination of materials and debinding cycle, depolymerization is effectively completed at 220°C. It can also be noted from the results presented in Fig. 5.5 that there was some slight weight loss at even 150°C, and that most of the weight loss occurred in the temperature range 170°C to 190°C.

These results are in contrast to those presented in Figures 5.1 and 5.2 for the TGA and DSC, using smaller samples and more rapid heating rates, which indicated relatively little weight loss below 190°C.

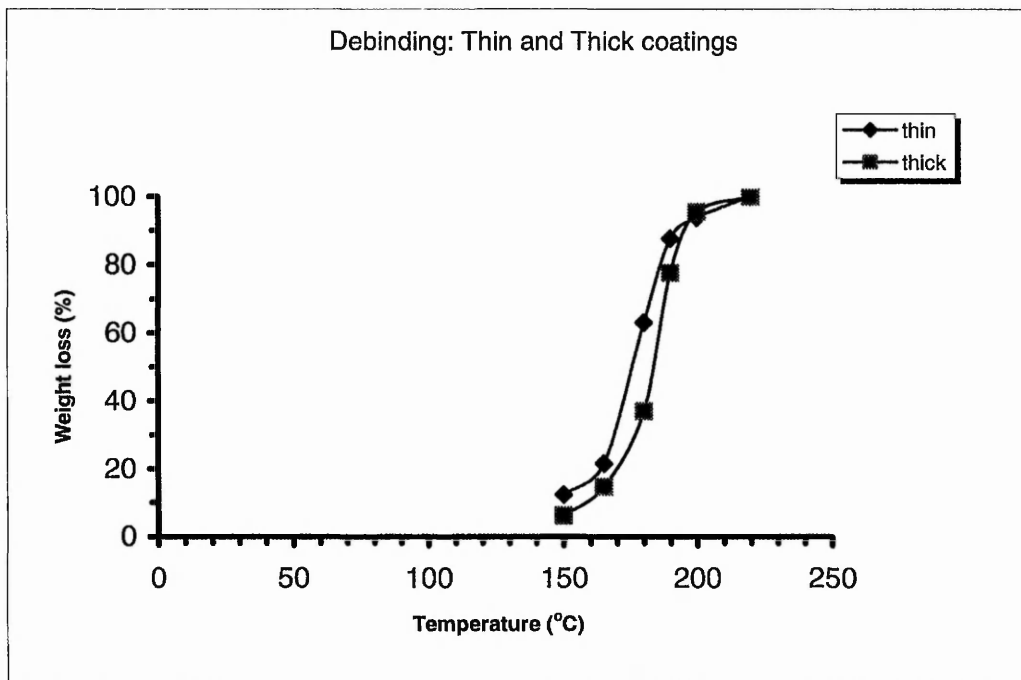


Fig. 5.5 Binder (cyanoacrylate) weight loss as a function of the final hold temperature for 0.6 and 1.0 mm thick coatings of a 55% Volume fraction of aluminium powder in Loctite 408 binder (45 minutes hold at each temperature)

On the basis of the calculation above and information obtained in the preliminary trials, a similar schedule using step heating in the oven was devised for the debinding of coating samples containing alumina powder. The samples were made of 45%v alumina powder (No.2) with thicknesses of 0.8 mm and Loctite 408 as binder, incorporating 2% PTS and 1% dissolved caffeine, on flat aluminium and alumina substrates. The specimens were placed in the oven at the same time and heated to 100°C in 60 minutes. The subsequent soak temperatures were 100, 120, 140, 150, 165, 180, 190, 200 and 220°C, with a dwell time of 30 minutes at each temperature.

Fig. 5.6 shows an example of the results obtained using this debinding schedule in the form of cumulative binder weight loss up to a given final dwell temperature. The results are very similar to those in Fig. 5.5, i.e. there is a small amount of weight loss at 120°C, and the major part of the weight loss occurs between 170°C and 190°C. Fig. 5.7 shows SEM micrographs of the surface of a debonded layer (alumina powder No.2). It can be seen that there are only the normal connected pore channels present, with no macrodefects.

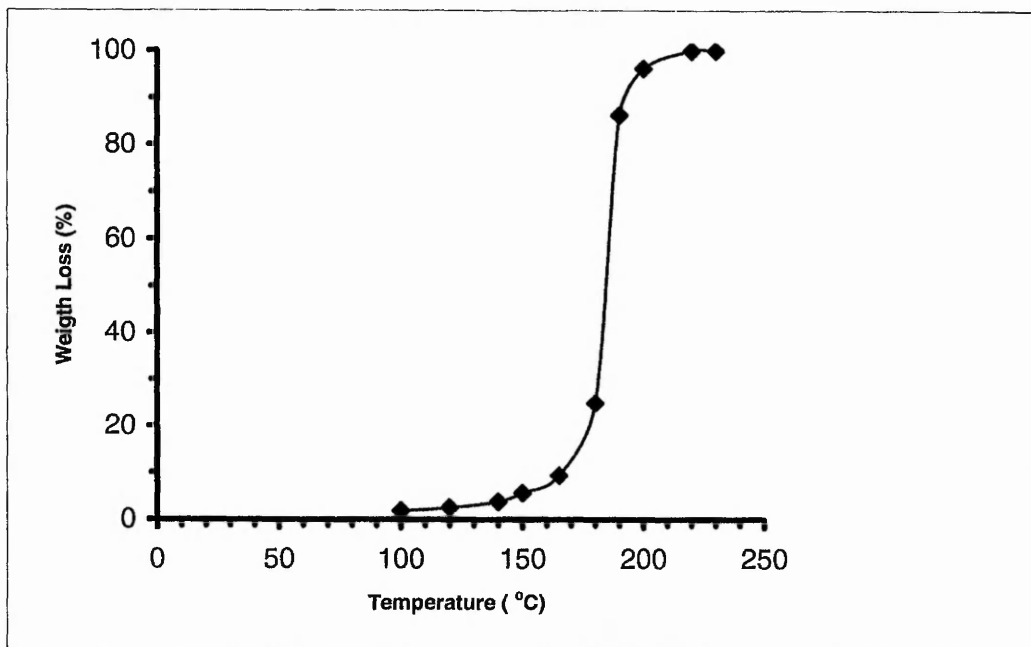


Fig. 5.6 Binder (cyanoacrylate) weight loss as a function of the final hold temperature for 0.8 mm thick coatings of a 45%v alumina powder (No.2) in LOCTITE 408 plus 2% acid, and 1% dissolved caffeine, with 30 minutes hold at each temperature.

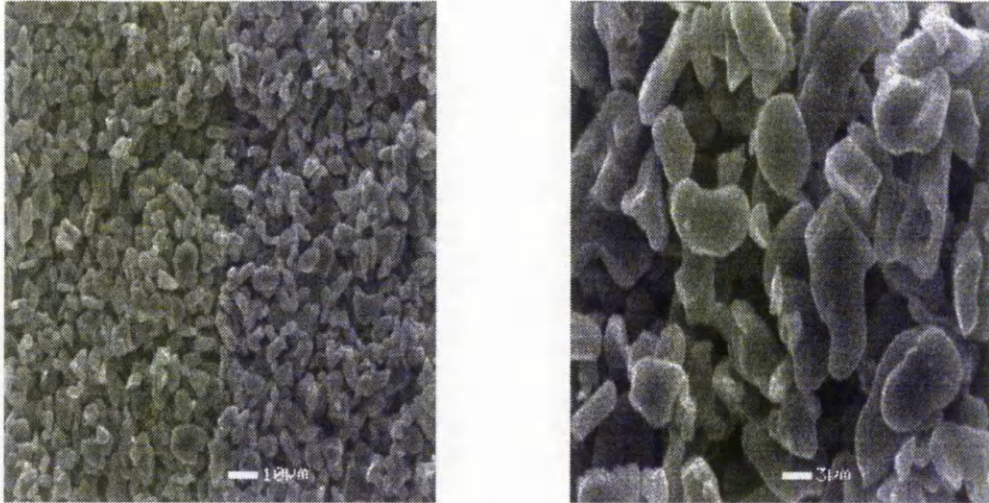


Fig. 5.7 SEM images of a fully debonded alumina powder(No.2)

It is clear that the type of the powder, solid loading and thickness of the coating will result in different rates of binder removal. Nevertheless, the formation process of connected pore channels will remain the same, regardless of the kind of packing structure or coating dimensions (Li et al 2003). During the thermal debinding cycle, the binder which fills the space between the powder particles evaporates gradually, resulting in a progressive pore opening mechanism. When the binder removal reaches a certain level, then the connected pore channels will form throughout the whole coating layer.

The next stage in this phase of the research was to investigate the applicability of this form of heating cycle to coatings containing a higher percentage of powder, i.e. 58%v alumina, which were prepared using a bi-modal powder mixture, as described in section 3-1-2. Several samples of 0.8 mm thick coatings were deposited onto flat alumina substrates.

Based on the previous observations, the heating schedule was slightly revised. This included inserting more holding steps between 165°C and 200°C, which is the temperature range where the major part of the weight loss was observed to occur. This helped to avoid possible defects such as cracking, which are more likely in compacts with a higher solid loading, such as the bi-modal compacts (58%v powder) compared to uni-modal powder compacts (45%v powder). The samples were heated to 120°C in 60 minutes. This was followed by soaking with a temperature sequence of 120, 135, 150, 165, 175, 180, 185, 190, 195, 200, and

220°C for dwell times of 30 minutes in all cases. Fig. 5.8 shows the cumulative binder weight loss as a function of the final dwell temperature. These results are very similar to the preceding ones, and the layers were again uniform and macrodefect free.

The results presented in this section demonstrate that a thermal debinding cycle has been developed which should be able to be successfully applied to all the coating layers made in this study.

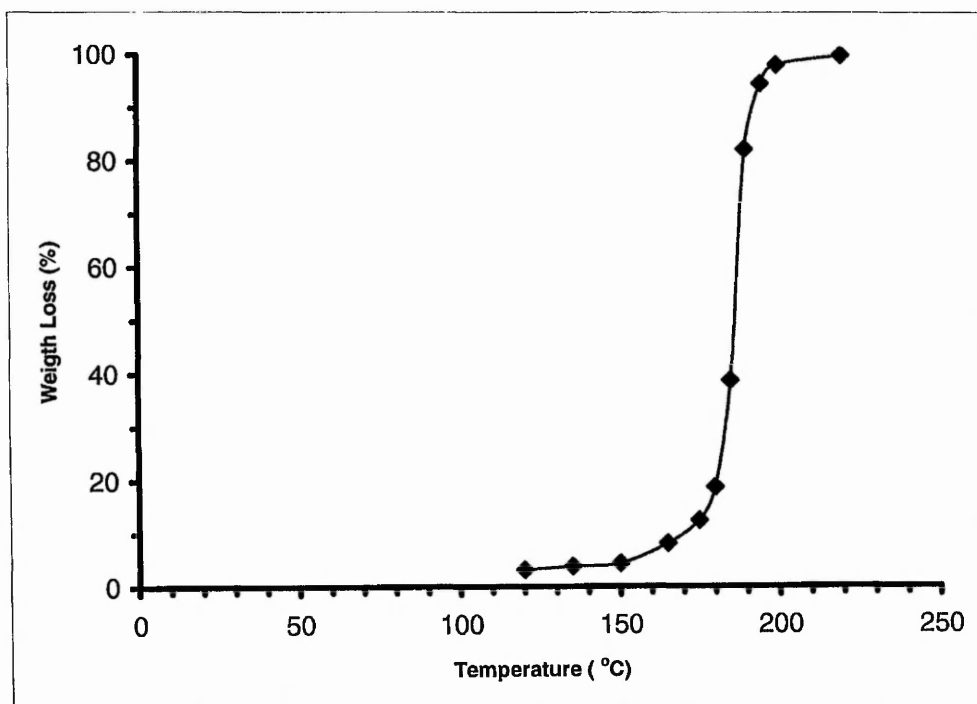


Fig. 5.8 Binder (cyanoacrylate) weight loss as a function of the final hold temperature for 0.8 mm thick coatings of a 58%v binary alumina powder in LOCTITE 408 plus 2% acid, and 1% caffeine binder (30 minutes hold at each temperature)

5-4 Debinding prior to full curing

As discussed previously, section 4-2-3, it is inevitable that there will be some gas released during curing of the cyanoacrylate, which leads to the formation of a small number of larger pores in the coating layers. This is clearly undesirable, and it was decided to investigate if a procedure could be developed to eliminate, or at least significantly reduce, these pores. It was noted that the gas voids appeared in the mixture at a very late stage in the curing, when the viscosity is very high. Consequently, it was decided that 1.0%w caffeine, or even as low as 0.5%w

(depending on the required time to cure), could be added to the mixture to control the curing rate, with subsequent debinding of the coating being able to be started when the viscosity of the coating is high enough for handling, but before the curing had been completed. It was found that using the combination of the step heating schedule outlined in section 5-3-3 with partially (>75%) cured mixtures produced the most satisfactory coatings. Fig. 5.9 shows that the gas bubbles can be significantly reduced, and effectively eliminated, by debinding the coatings before the final completion of curing.

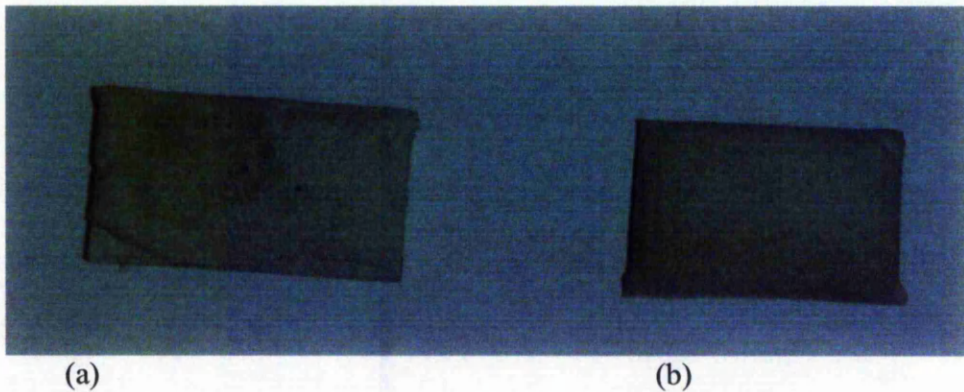


Fig.5.9 Surface of coating (a) fully cured and debonded sample
(b) partially cured and debonded sample

5-5 Summary

- Cured mixtures can be debonded using a thermal debinding technique,
- Although TGA and DSC analysis of cured mixtures showed that debonding of the mixtures is a simple process with just one peak at $\sim 230^{\circ}\text{C}$, the heating rate should be controlled to avoid defects during debinding,
- Step heating of the coating layers in air using a controlled time-temperature procedure can result in defect free debonded layers while maintaining coating integrity as well as its adhesion to the substrate,
- Step heating of unimodal alumina samples at 100, 120, 140, 150, 165, 180, 190, 200 and 220°C with a dwell time of 30 minutes at each temperature resulted in defect free debonded layers.
- It was noted that the debonding rate is maximum in the temperature range of 170°C to 190°C .

- For bi-modal alumina powder compacts with a higher solid loading the debinding cycle can be optimised by inserting more holding steps in the range of 165°C to 200°C into the debinding regime.
- Debonding of the non-fully cured layers can significantly reduce the formation of gas bubbles in the mixture prior to sintering.

6

Sintering

Introduction

The firing of the debonded ceramic coatings to sinter them is the last step in the production of PRIME coatings. Although sintering can be carried out as a continuation of binder burn out, i.e. heating in the same furnace, it is also common to use a two-stage process, i.e. debinding in a low temperature oven, and then transferring the components to another furnace for sintering. The second approach has been chosen in the present study to make the coatings.

It is worth noting that the sintering stage was not the main focus of the present research study. Alternative sintering processes, such as microwave or laser sintering, might be more appropriate to the sintering of a thick ceramic coating on a wider range of substrates.

The main objectives of this part of the present investigation were to:

- Sinter to full density alumina and zirconia ceramic coatings of controlled thickness within the range 0.1 – 1 mm within a reasonable time at temperature in a controlled and reproducible procedure
- Ensure the production of defect free coatings with good adhesion to a suitable ceramic or metallic substrate
- Study the microstructures of the coatings, substrate and substrate-coating interface

- Investigate the microhardness of the sintered coatings

The key activities in this section were:

- Pressureless solid state sintering of debonded alumina layers
- Pressureless liquid phase sintering of debonded alumina and zirconia layers
- Use of different substrates (pure alumina, 96% alumina, and Mo plate)
- SEM study of the coatings
- Vickers and Knoop Microhardness testing of the coatings

6-1 Equipment Used for Sintering

To study the sintering behaviour of the debonded ceramic layers, an induction heating furnace with a RF induction powder supply (Radyne, 15TQ50) was used. The generator worked at 50 kHz with a maximum power of 15 kVA.

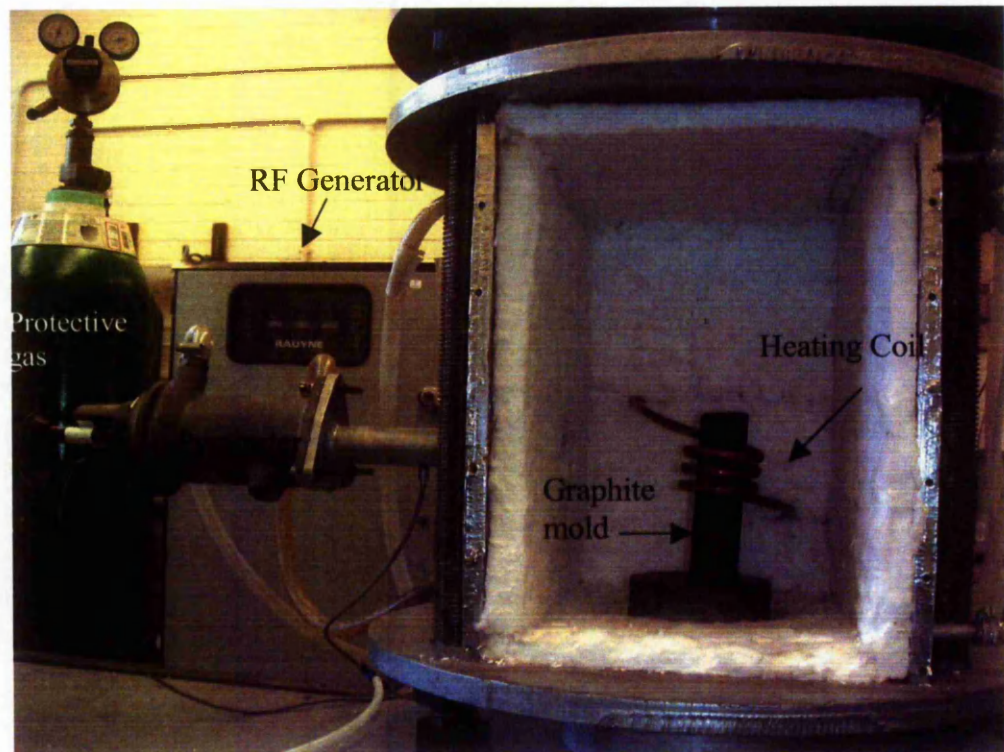
6-1-1 Induction Furnace

Although induction heating is normally generally used with metals or other conductive materials, non-conductive materials can be heated efficiently by using a conducting material as the susceptor. The susceptor is used to transfer heat to the target part through conduction or radiation. A RF heating system was already available to be utilised to undertake the sintering studies. Unfortunately, most of the equipment had not been used for some while, and substantial refurbishment and re-development was required before the system became operational again. Fig. 6.1(a) shows the equipment used to sinter the debonded layers. The external walls of the cuboidal chamber were water cooled. The internal walls were covered in Kaowool insulating fibre blanket. Although the chamber of the furnace was not gas-tight, sintering was performed using a slightly positive pressure of protective gas atmosphere (argon).

A graphite core was used as a susceptor in this study, since graphite offers suitable resistivity with a useful operating temperature range up to 3000°C, is relatively inexpensive, and can be machined.

A three turn copper induction coil had been designed and made to heat the graphite using induction heating. To ensure uniform heating, and to reduce heat loss due to water cooling of the inductor, the induction coil was covered with

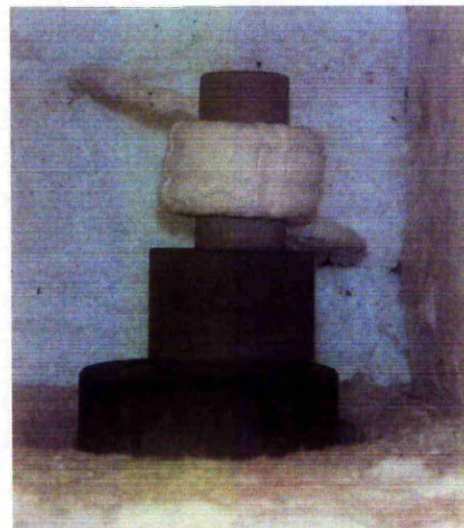
insulating paper. Fig. 6.1(b) shows a close-up of the graphite susceptor and induction coil covered with heat resistant paper. This arrangement was used to



(a)



(b)



(c)

Fig. 6.1 Equipment used for sintering (a) general set-up (b) a close-up of graphite susceptor and, (c) its fitting within the covered induction coil

heat components placed inside the graphite core by emitted radiation and conduction.

The sintering was performed using an inert gas environment, which was normally commercial purity argon gas, at a slight overpressure. Heat transfer to the internal chamber walls was also affected by the argon gas, which contributed to the heat losses.

6-1-2 *Temperature Measurement and Control*

Common ceramic oxides including alumina and zirconia can be sintered in air at temperatures up to 1700°C. Generally, the most convenient and accurate method of measuring temperatures in this range is to use a thermocouple. Consequently, thermocouple types S, R and B (Johnson Matthey) have been used to monitor the temperature during sintering. Using a high purity alumina shield, the tips of the thermocouples were placed at the top of the samples. A PC and A/D card (PICO-TC8) and associated software were used for measuring and storing the data. Table 6.1 shows the specification of the thermocouples.

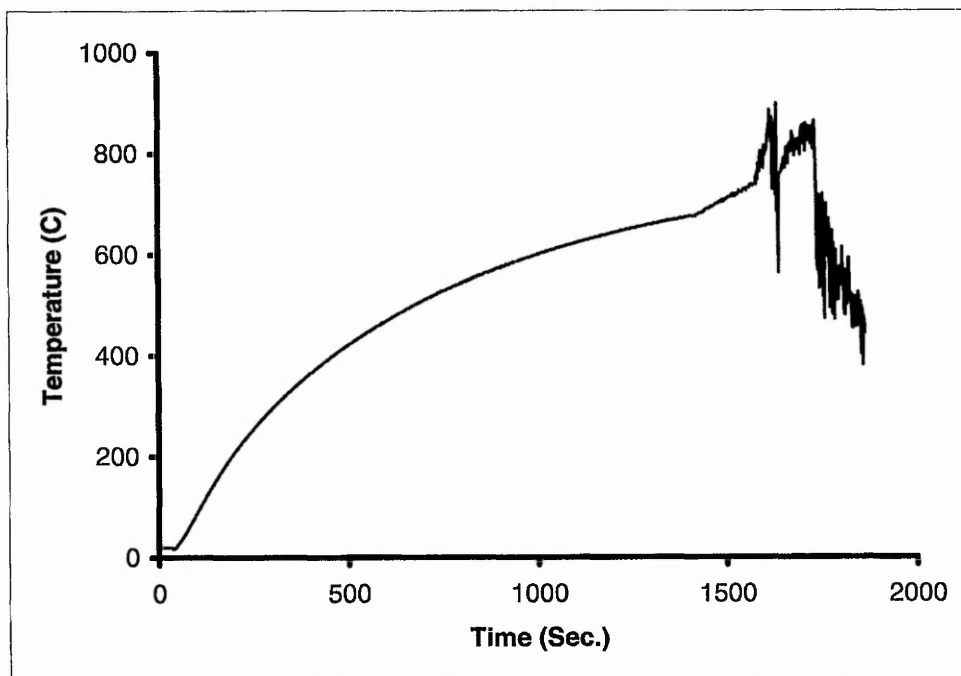
Although all of the thermocouples mentioned could withstand the high temperatures, a common problem arose on heating the chamber. On exceeding a specific temperature, dependent on the type of thermocouple, the temperature reading started to oscillate wildly. It was presumed that this probably occurred as a result of the increase in the strength of the magnetic field around the coil on increasing the power. Thus, the induced current in the thermocouple wires resulted in inaccurate temperature readings.

Table 6.1 *Specifications of thermocouples used*

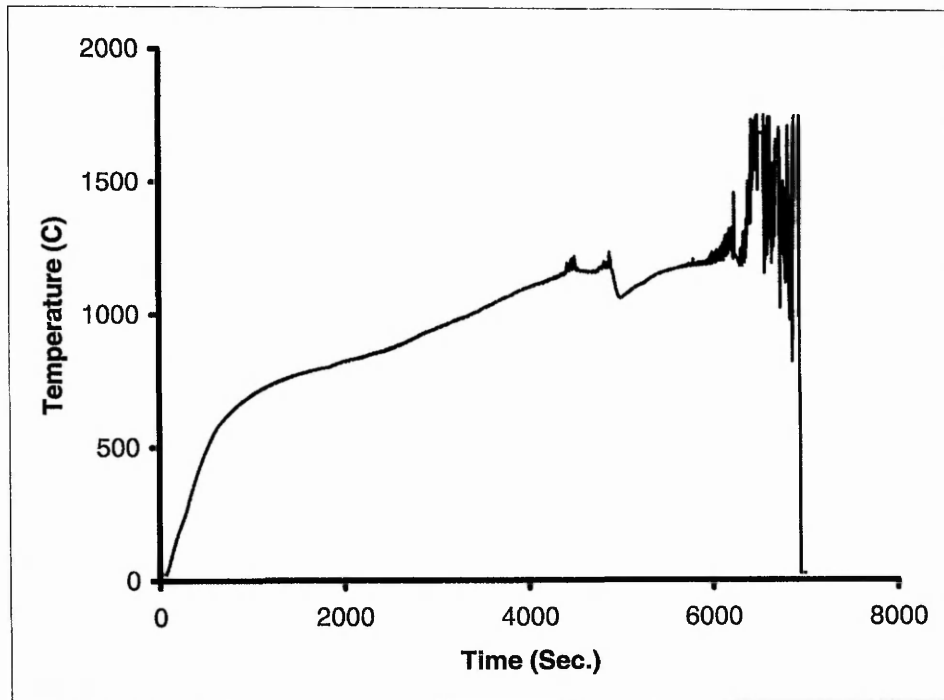
Thermocouple type	Materials	Working Temperature	
		Continuous use	Intermittent use
Type S	Pt-10% Rh/Pt	200-1500	200-1700
Type R	Pt- 13% Rh/Pt	200-1500	200-1700
Type B	20%Rh/Pt- 40% Rh/Pt	200-1700	200-1850

Figures 6.2 (a) and (b) show typical readings from type R and S thermocouples respectively. The rapid oscillations above $\sim 700^{\circ}\text{C}$ and $\sim 1100^{\circ}\text{C}$ respectively probably arise from coupling between the RF field and the thermocouple and are not representative of the actual chamber temperature. This meant that it was not possible to use a thermocouple to measure the temperature above $\sim 800^{\circ}\text{C}$.

As a result of these oscillations, it was not possible to use a thermocouple to monitor the sintering temperatures. Consequently, an alternative method of temperature reading was implemented. This alternative temperature measurement system consisted of a fixed on-line pyrometer (Land Radiation Thermometer-GP122) with the data being monitored and stored on a PC via an analogue to digital card. This pyrometer required the emitted electromagnetic waves to be in the visible region. Consequently, it could only be used for temperature readings when the temperature of the graphite core was above $\sim 800^{\circ}\text{C}$. To ensure a uniform heating and cooling rate below 1000°C , the temperature readings were taken using thermocouples inserted in the cavity of the graphite susceptor, with the same heating and cooling rates being used for all samples.



(a)



(b)

Fig. 6.2 Examples of temperature readings from thermocouples type (a) S and (b) R during sintering.

In all cases the heating and cooling rates were controlled manually, and the temperatures up to 1000°C measured using a thermocouple. Above this temperature the pyrometer was used. The maximum temperature that could be achieved under well-controlled conditions for this apparatus was 1850°C, although a temperature of 1700°C was considered to be the maximum useful temperature when holding at temperature for several hours.

6-1-3 Preparation of Samples for SEM Study and Mechanical Tests

For SEM study of the samples and microhardness testing, all samples were transversally sectioned and hot mounted. The samples were ground using water lubricated SiC papers 240, 400, 800, 1200 grades sequentially, and subsequently polished using 6, 3, and then 1 μm diamond paste for 30 minutes each. All samples were gold coated prior to study. This included the samples for hardness testing.

6-2 Solid State Sintering

The first step in the study of sintering of the debonded layers was undertaken using compositions and pressureless sintering conditions that were considered likely to result in solid state sintering.

6-2-1 Procedure for Making the Coating

For this purpose two different flat (~2mm thick) substrates were used: one metallic (molybdenum) and one ceramic (pure alumina). Alumina powder No.2 with an average particle size of 8 μm and cyanoacrylate (Loctite 408) were used to make the coating mixtures containing 45%v powder. 2%w acid was dissolved in the cyanoacrylate before mixing and 1% caffeine mixed with the mixture at the end of the mixing stage. Debinding was performed as described in chapter 5.

6-2-2 Sintering of the Coatings

As discussed in section 2-9-4, the temperatures used for pressureless sintering of pure alumina powders are generally in the range 1600 - 1700°C. Too low a temperature leads to incomplete densification, whereas too high a temperature results in excessive grain growth. Therefore for the preliminary sintering trials a 0.6 mm thick coating layer on a pure alumina substrate (99.99%) was sintered at 1600°C for 120 minutes. Fig. 6.3 shows the sintering cycle of the sample. The heating rate and cooling rate above 1000°C were 12 and 15°C/min, respectively. The furnace temperature increased from room temperature to 1000°C in 30 minutes. Also samples were generally removed from the furnace one and a half hours after passing the last reading by the pyrometer (1000°C) on cooling. The coating mixture consisted of 45 %v alumina powder (No.2) and cyanoacrylate, plus 2%w, PTS acid (as a proportion of the cyanoacrylate weight percent) as stabilizer. 1% caffeine (as a proportion of the cyanoacrylate weight percent) was added at the end of mixing and the semi-cured samples debonded up to 220°C as described in section 5-3-3.

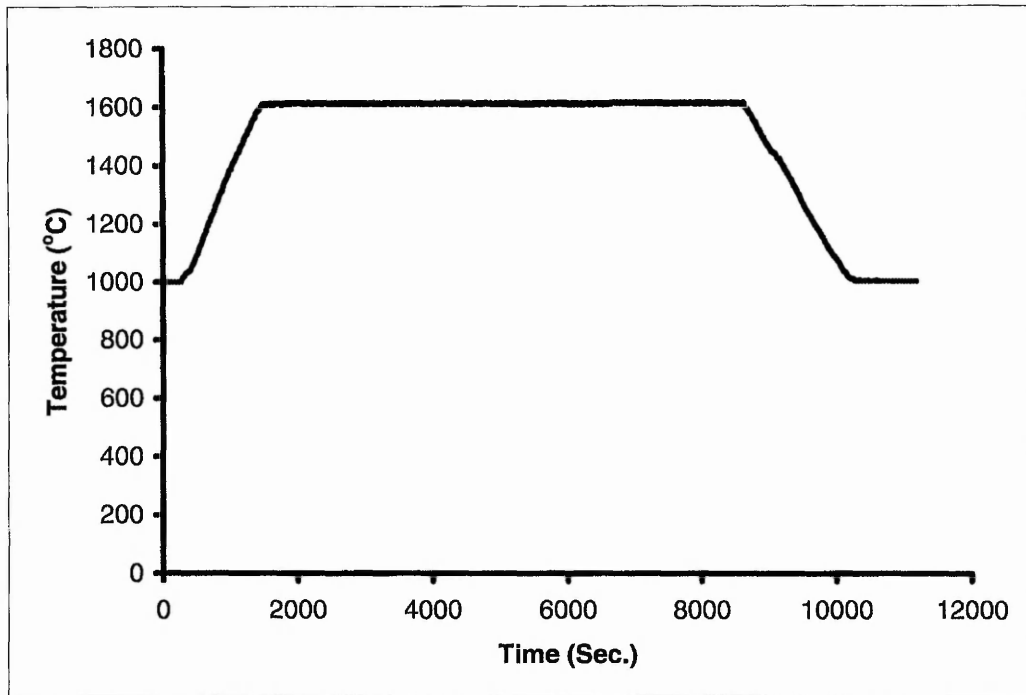


Fig. 6.3 Sintering cycle for alumina powder on pure alumina substrate

Initially, the samples were placed on the surface of the graphite susceptor and left open to the chamber atmosphere. It was found that this resulted in a dark discoloration of the surface and near-surface regions. Consequently, subsequent samples were placed in a cavity in the graphite core and covered with BN powder. This minimised the interactions between the substrate and/or coating materials, and the susceptor and gaseous phases to give conventional white/ivory surfaces.

As can be seen, Fig. 6.4, following sintering at 1600°C, there was an apparent lack of adhesion of the alumina coating to the substrate. These micrographs also demonstrate that there are voids between the sintered particles. The mechanical properties of the coating were studied by measuring the hardness of the sintered layers. Knoop microhardness tests using a Leitz Miniload with 0.3 kg normal load were performed on the samples. The tests were performed on the transverse section of as-sintered coatings, which had been debonded while only partially cured. The standard formulas (equations 2.3) were used to calculate the hardnesses of the coatings. The results are expressed as the Knoop hardness number under the stated load, and the units are kg/mm^2 . Although, as a general rule, the mean values are more reliable if the number of determinations is large,

the recommended practice is to use more than five randomly positioned macrohardness tests (Morrell 1985).

The hardness of this coating was measured to be 68 $\text{HK}_{0.3}$. These observations all indicate that the coating did not sinter to full density during this heating cycle.

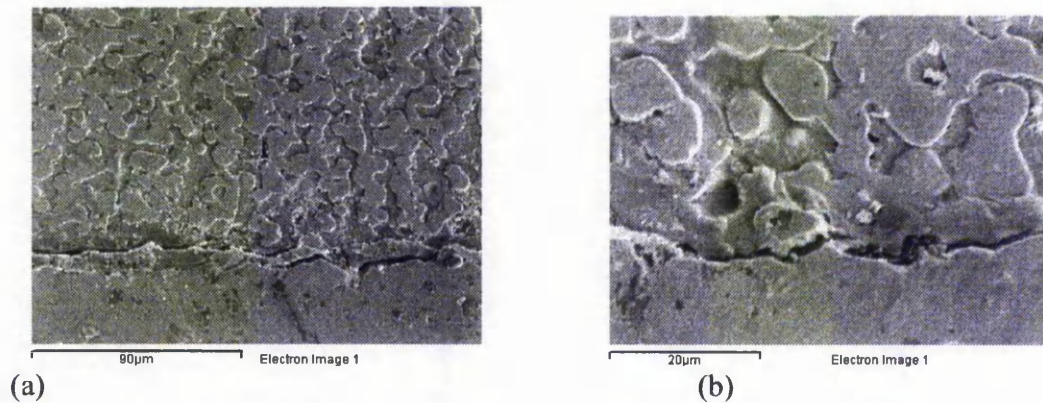


Fig. 6.4 SEM micrographs of transverse sections of an alumina coating sintered at 1600°C on a pure alumina tile.

Increasing the sintering temperature to 1675°C only improved the hardness of the coating to 140 $\text{HK}_{0.3}$, which is well below the substrate hardness, (which was measured as 1759 $\text{KH}_{0.3}$). Furthermore, there was still a lack of bonding between the substrate and coating, as well as the presence of voids (Fig. 6.5). This suggests that in the absence of applied pressure, or application of an interlayer, obtaining full densification and good adhesion would be quite difficult to achieve. Furthermore, the fairly coarse particle size of the alumina powder (8 μm) and relatively low solid particle loading made further practical improvement even more difficult.

These results were not surprising, since it has been observed by Smith & Messing (1984) and Taruta et al (1996) that alumina compacts sintered at 1600°C for two hours only attained up to 65% and 70% of the theoretical density using solid state sintering of fairly coarse alumina powders, i.e. 4-5 μm and >3 μm, respectively.

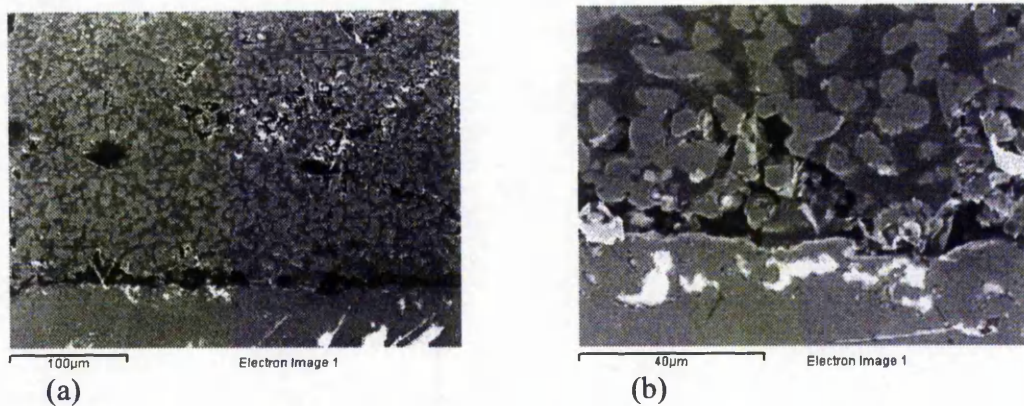


Fig. 6.5 SEM micrographs of transverse sections of an alumina coating sintered at 1675°C on a pure alumina tile

In order to investigate the possibility of using a metallic substrate, an alumina coating with the same composition as noted in section 6-2-1 was applied onto a molybdenum plate. One problem regarding using a molybdenum plate as a substrate is that it can couple with the RF magnetic field, and thus have an extra local induction heating effect in the substrate. This would mean that the actual temperature of the coating would be likely to be higher than the reading from the pyrometer.

Fig. 6.6 shows SEM micrographs of an alumina coated molybdenum sample. The nominal sintering conditions were 1520°C for 2 hours. Although there is an apparent adhesion to the substrate, the hardness of the coating was only 35 HK_{0.3}, i.e. lower than the results obtained previously on the alumina substrate. The micrographs in Fig. 6.6 both show that the coating had not sintered to full density. This suggested that it was necessary to consider other methods of sintering to improve the degree of densification and adhesion to the substrate. Thus the possibility of changing the system to obtain liquid phase sintering of the layers was studied.

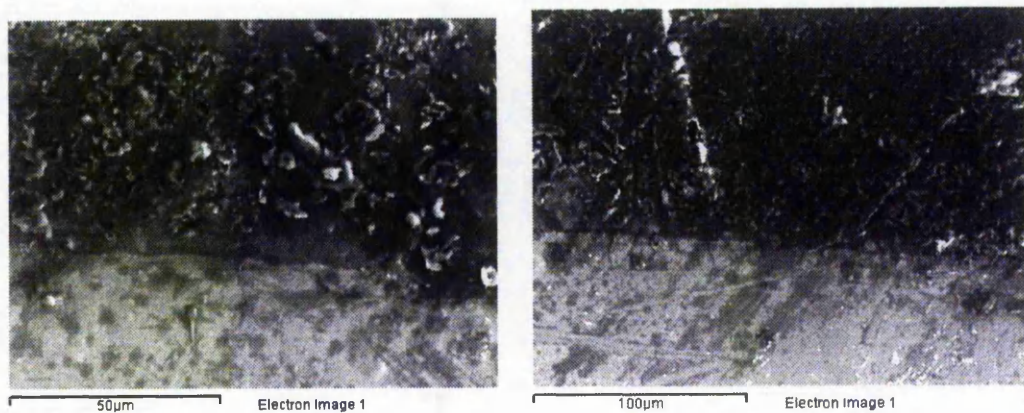


Fig. 6.6 SEM micrographs of transverse sections of an alumina coating sintered at nominal temperature of 1520°C on a molybdenum substrate

6-3 Liquid State Sintering

The sintering temperature and time for many commercial alumina products is lowered by the use of sintering aids (German 1985, Brydson et al 1998). Therefore, it was decided to modify the coating mixture composition to incorporate a sintering aid. There are many different sintering additives, e.g. MgO, TiO₂, MnO₂, Li₂O, ZrO₂ (Erkaifa et al 1998, Sathiyakumar and Gnanam 2003) and magnesium alumina silicates (Kwon and Messing 1990) that have been successfully used with alumina. Generally, such sintering aids enable the sintering temperature to be substantially lowered as a result of the formation of eutectic liquid phases. In this study a very fine powder of fumed silica powder with a surface area of 200 m²/g was used as an additive.

The reason behind using fumed silica powder as a liquid former was that because of its lower melting temperature, combined with its very fine particle size, alumina can react with the resulting liquid and the mass transfer could take place at intergranular channels to help the rearrangement and densification of the alumina particles.

6-3-1 Procedure for Making the Coatings

The sintering aid additive needs to be well mixed within the coating to enable it to be effective in use. Thus, the coating procedure for the ceramic layers, as described in section 3.2.2 was modified as follows;

1. Measured quantities of para-toluene-sulphonic acid and cyanoacrylate binder were dispensed into a small plastic cup.
2. The solution was heated at 45°C in a water bath for 30 minutes, whilst the acid dissolved in the cyanoacrylate monomer.
3. The cup was removed from the bath and a measured quantity of additives added to the solution (in small quantities) whilst mixing by hand.
4. A measured quantity of the main ceramic powder, i.e. alumina powder was added (in small amounts) into the solution, whilst continually stirring by hand.
5. Caffeine powder (1%w) was mixed into the mixture at the end of the process, i.e. after the addition of the appropriate amount of powder to the solution of binder, acid and sintering aid.

The incorporation of an additional ceramic powder into the mixture as a sintering aid introduces more surface area (and also different surface chemistry) into the cyanoacrylate. When fumed silica was added, it was found that 2%w acid was not sufficient to prevent premature polymerization of the cyanoacrylate during mixing and the desired amount of alumina powder, i.e. 45%v, could not be mixed into the solution. This meant that more acid was needed to stabilise the cyanoacrylate during the mixing stage. After several trials, it was found that, increasing the dissolved acid level to 4%w allowed up to 2.5%w silica (as a proportion of the powder weight percent) be added to the mixture. Further trials showed that a maximum of 6%w of acid could be used to enable 3.5%w fumed silica to be added to the coating mixture; increasing the amount of dissolved acid beyond this level did not enable the amount of sintering aid to be increased further.

6-3-2 *Sintering of Modified Coatings*

Coatings containing fused silica as sintering aid were applied onto pure alumina substrates and sintered at 1620°C for 2 hours. The sintering cycle is shown in Fig. 6.7.

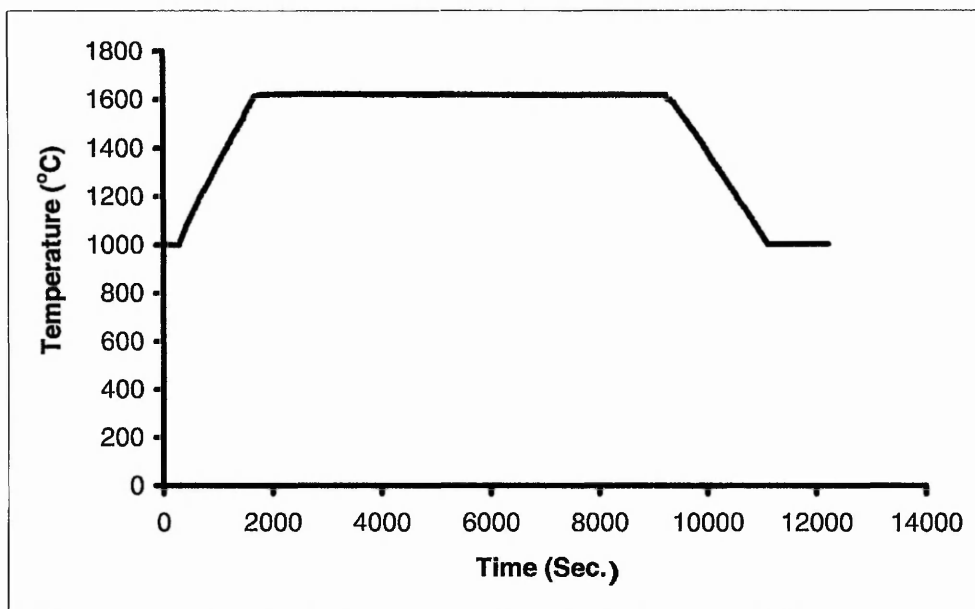


Fig. 6.7 Sintering cycle for an alumina coating containing SiO_2 sintering aid on pure alumina substrate

Fig. 6.8 shows macro- and micro-photographs of a transverse section of a sintered layer using fumed silica. As can be seen, there is no sign of large voids or lack of adhesion to the substrate, although the presence of interconnected pores indicates that full densification had not taken place. The hardness was measured as 123 $\text{HK}_{0.2}$ on samples with 2.5%w fumed silica. Increasing the amount of silica to 3.5 %w increased the hardness to 470 $\text{HK}_{0.3}$. Fig. 6.9 shows examples of Knoop microhardness measurements on the coating and pure alumina substrate.

It has been noted that the amount of additive can directly influence the volume fraction of liquid, and consequently affect the sintering rate and final microstructure of the sintered parts (German 1985, Kwon 1991). These observations would imply that by increasing the relative proportion of silica, greater densification, and thus higher hardness, could possibly be achieved. However, it was found that with the particular alumina and silica powder used in this study it was not possible to add a greater proportion of silica to the mixture, since this resulted in a lower proportion of main ceramic powder, i.e. alumina, that could be added at the later stage of the mixing.

Using 3.5%w fused silica and alumina powder No.2, pure molybdenum was tried as the substrate, but with limited success, since the adhesion of the coating to

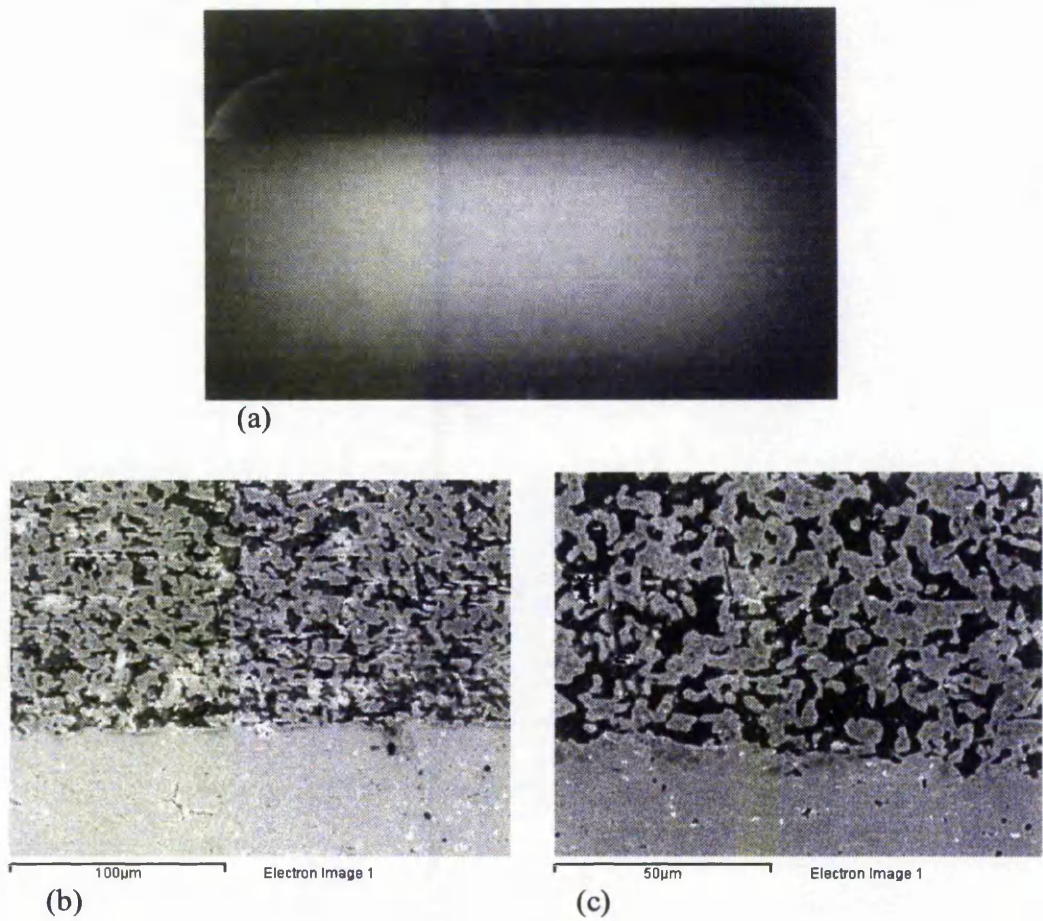


Fig. 6.8 (a) Macro- and (b) & (c) SEM micrographs of a sintered alumina coating on a pure alumina substrate using 2.5%w fumed silica as the sintering aid

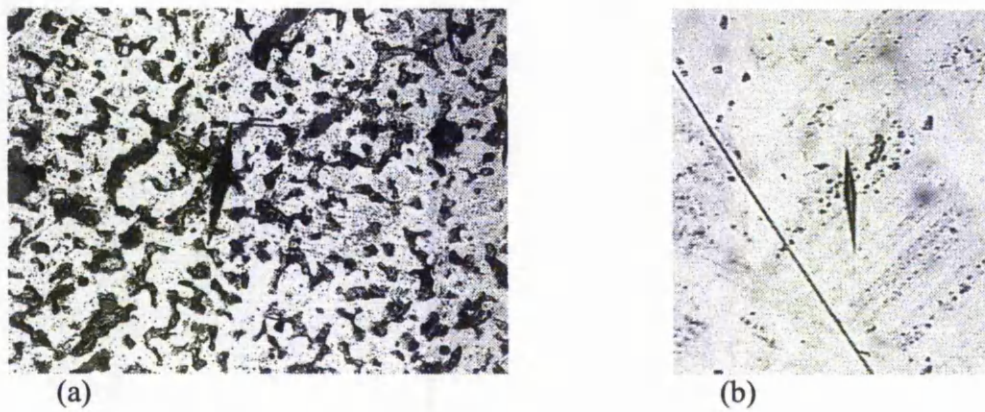


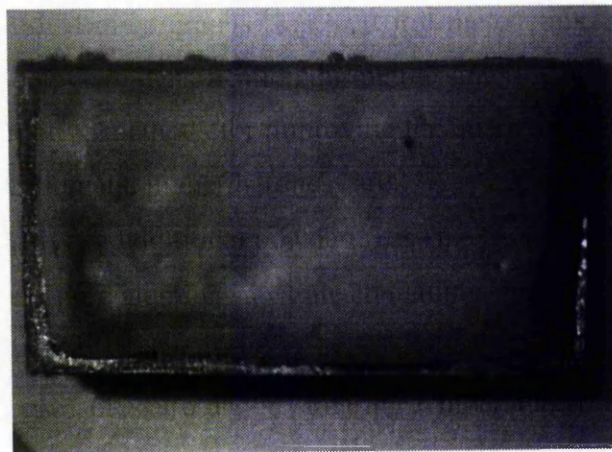
Fig. 6.9 Knoop microhardness impressions on (a) liquid phase sintered coating and (b) pure alumina substrate

substrate was limited. Fig. 6.10(a) shows the shrinkage of the coating after sintering at a nominal temperature of 1520°C. The surface of the molybdenum substrate was fully covered with the coating material before sintering, and the difference in measured coating length before and after sintering indicated that there is a linear shrinkage in the coating of ~5% after sintering. This observation, together with the SEM micrographs (Fig. 6.10) of the coating, suggest that there was a reasonable degree of densification during the sintering stage.

The possible alternative methods for improving the quality of the coating in terms of greater densification and higher hardness are:

- Use alternative or additional powder(s) as sintering aid(s)
- Use of a less pure alumina substrate containing sintering aid(s)
- Higher sintering temperatures
- Application of pressure at the sintering temperature (hot pressing or hot isostatic pressing), or
- Use of an interlayer.

It was decided to concentrate on the second alternative in the present study.



(a)

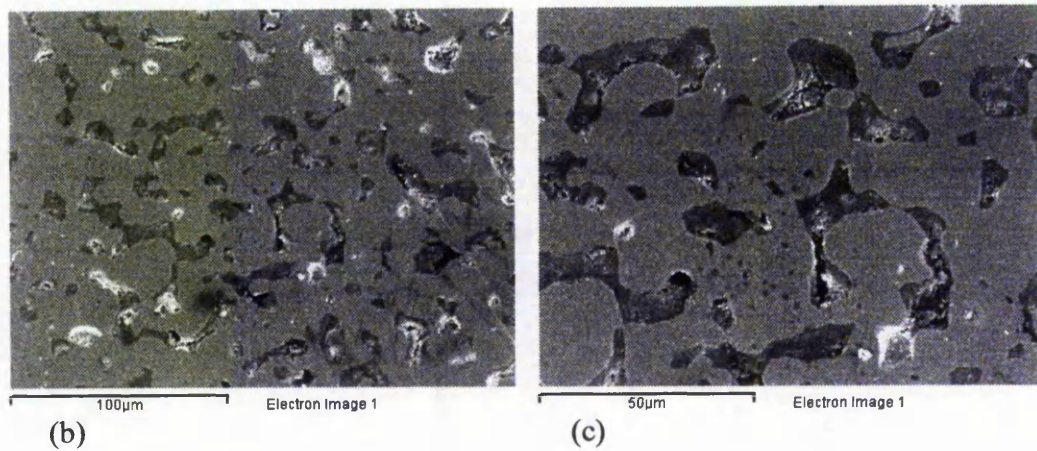


Fig. 6.10 (a) Macrograph of surface of liquid phase sintered coating on pure molybdenum substrate and (b) and (c) SEM micrographs of the coating in contact with the surface of the molybdenum substrate.

6-4 96 % Alumina Tile

To study the feasibility of achieving a sintered coating with reasonable properties, as well as good adhesion at the interface, a commercially produced alumina (96% Al_2O_3) tile, supplied by Ceramic Substrates & Components Ltd, was selected as an appropriate substrate. The key reason for this choice was that on firing the debonded layer-substrate system, the optimised glass in the alumina substrate could melt and penetrate into the pores/grain boundaries in the coating up to a reasonable distance from the interface. One possible drawback to this approach is that it might result in a gradient in the properties. The extent of penetration is likely to be a function of the starting glass type and amount of glass, as well as the bonding temperature and soaking time (Esposito and Bellosi 2001).

6-4-1 96% Alumina substrates

The 96% alumina formulation is relatively standard for fully dense substrates. Such alumina substrates are available from a number of suppliers. Although each supplier has its own proprietary formulation and manufacturing processes, which may account for minor differences, the substrates generally have a large proportion of grain boundary glass (Wirth 1991). The glassy phase must have a carefully controlled composition to produce the required densification and behaviour characteristics. In general, the formulations for the grain boundary glass consist of an aluminosilicate containing additional oxides such as CaO or MgO at

the grain boundary (Lee and Rainforth 1994) which is used as a densification aid and to bond the alumina crystals together. The glass phase also provides a bonding mechanism for adherence of the thick film or as a bonding agent when joining ceramics (Lee and Rainforth 1994). The microstructures generally show a uniform distribution of alumina crystals, completely separated by glass. Any pores are usually located at the grain boundaries within the glass phase (Chinn 2002).

The 96% alumina ceramics would generally be fabricated using a tape process or dry pressing, with the latter being more appropriate for thicker parts. The firing temperatures generally lie in the range 1520-1600°C (Wirth 1991). Typical thick-film alumina compositions fall in the ranges indicated in Table 6.2. These aluminas cannot be used in applications requiring very high temperature stability, but they have good thermal conductivities and are used in many cases for electrical insulation, such as fabrication of hybrid microelectronic circuits (Wirth 1991). The mechanical properties of glass containing alumina ceramics depend on the volume change during sintering, since this may induce microcracking, which degrades the fracture strength.

Secondary crystalline phases are usually present and can be revealed by XRD. The structure of these phases depends on the composition used, the firing temperature and the cooling rate. The phases produced are generally of the CaO-MgO-Al₂O₃-SiO₂ type. The ratio of CaO to MgO has a significant effect on mechanical and chemical properties of the substrates.

Table 6.2 Typical composition of alumina substrate (Wirth 1991)

Substrate	Composition, wt%
Al ₂ O ₃	96
SiO ₂	2.5-3
MgO	0.75-1.0
CaO	0.1-0.25
Na ₂ O	0.05-0.1 max
Fe ₂ O ₃	0.03-0.5
ZrO ₂	0-0.5

A polished specimen of one of the tiles used in this study was examined by SEM, (Fig. 6.11). There is a noticeable amount of well dispersed residual porosity, which is located at grain boundary junctions.

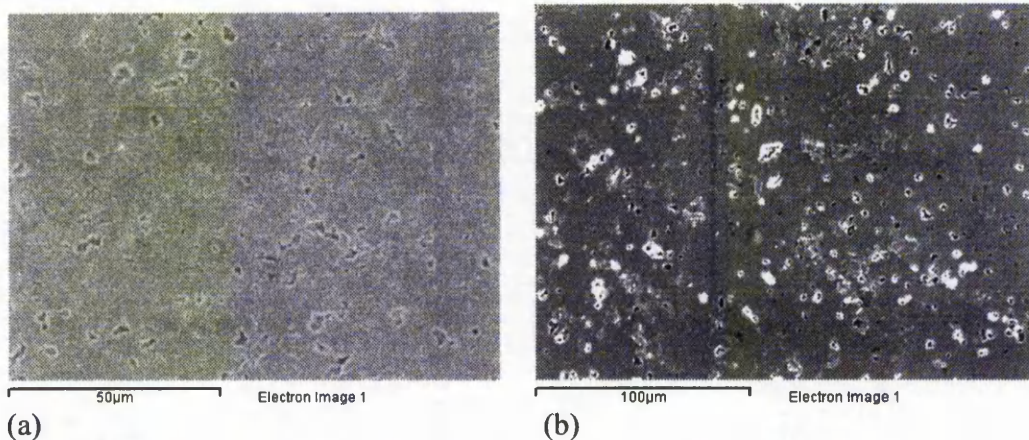


Fig. 6.11 SEM micrographs of a transverse section of the 96% alumina substrate

The hardness of the 96% alumina substrate was measured by two methods; using (a) the microscope fitted to the microhardness tester or (b) a Leitz optical microscope equipped with a digital camera. All the measurements were made on transverse sections of polished samples and the scale on the optical microscope was calibrated before taking any readings. Fig. 6.12 shows examples of the appearance of Knoop hardness impressions in the alumina substrate. Table 6.3 summarises the results of seven readings using the two above-mentioned methods. As can be seen, there was no significant difference in the readings using the two methods; although the standard deviation is less for the optical microscope. Consequently further measurements were made using the optical microscope.

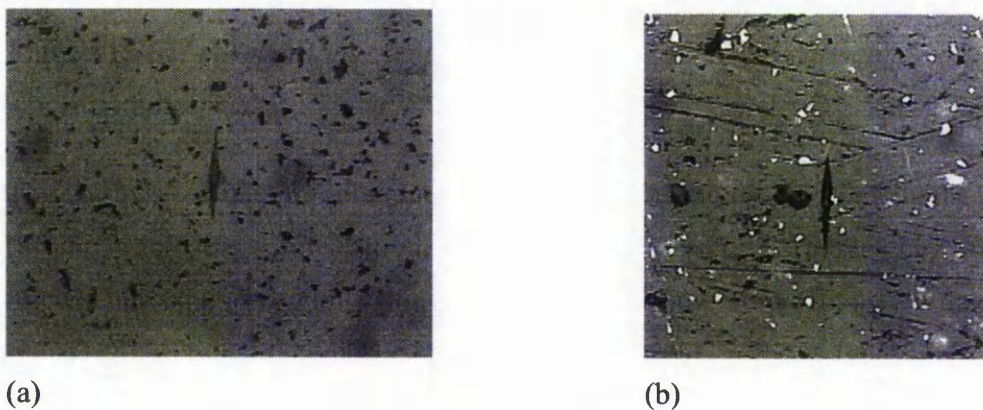


Fig. 6.12 Sample Knoop (300gr) impressions on 96% alumina substrate

Table 6.3 Comparison between two reading methods for Knoop microhardness tests on 96% alumina substrate

	Microhardness Tester		Microscope	
	Length of Diagonal (μm)	Hardness ($\text{HK}_{0.3}$) Kg/mm^2	Length of Diagonal (μm)	Hardness ($\text{HK}_{0.3}$) Kg/mm^2
Average	52.6	1535.8	51.8	1598.3
Standard Deviation	1.06	77.67	0.95	57.35

It was also noted that the microstructure, and consequently the hardness, of the substrate might be affected by the sintering cycle used for the coating. As a result, one of the 96% alumina tiles was heated at 1500°C for 15 minutes. The microhardness, $\text{HK}_{0.3}$, after exposure to this temperature was measured as $1472 \pm 108 \text{ kg/mm}^2$, based on nine readings. Although the mean value after exposure is somewhat less than the original value, Table 6.3, the difference is considerably less than the standard deviation, and is therefore not considered to be statistically significant. In addition, there was no obvious change in the microstructure.

6-4-2 Procedure for Making the Coating

Uni-modal and bi-modal aluminas and stabilized zirconia powders were used to make coating mixtures onto 96% alumina tiles. In all cases, alkoxyethyl cyanoacrylate (Loctite 408) was used as the binder.

For uni-modal mixtures, 45%v alumina powder (No.2) with average particle size of 8 μm , and 43%v stabilized zirconia have been used to make the coating mixtures. The amount of dissolved acid was 2 or 4%w, respectively. For bi-modal mixtures, a mixture of 70%w coarse alumina (No.2) and 30%w fine alumina (No.3) was used to make a mixture containing 58%v powder. 4%w acid was dissolved in the cyanoacrylate to stabilize it in the bi-modal system.

1%w caffeine was added to the final mixtures in most cases and the non-fully cured samples debonded by step heating up to 220°C as described in chapter 5. In order to compare the effect of gas release during curing on the sintered samples,

some samples were fully cured before debinding by adding 3% caffeine to the mixture. After some preliminary experiments, and considering the maximum working temperature of the substrate (1550°C), the sintering temperatures were fixed at 1500°C and 1300°C for the alumina and zirconia powders, respectively. The holding time at maximum temperature was either 15 or 20 minutes.

6-4-3 Study of the Coatings

6-4-3-1 Uni-modal Alumina Powder coating

The sintering of debonded uni-modal alumina coating mixtures deposited onto a 96% alumina tile was performed at 1500°C for 15 minutes. The thickness of the coatings was 0.6 mm. Fig. 6.13 illustrates a sample sintering cycle.

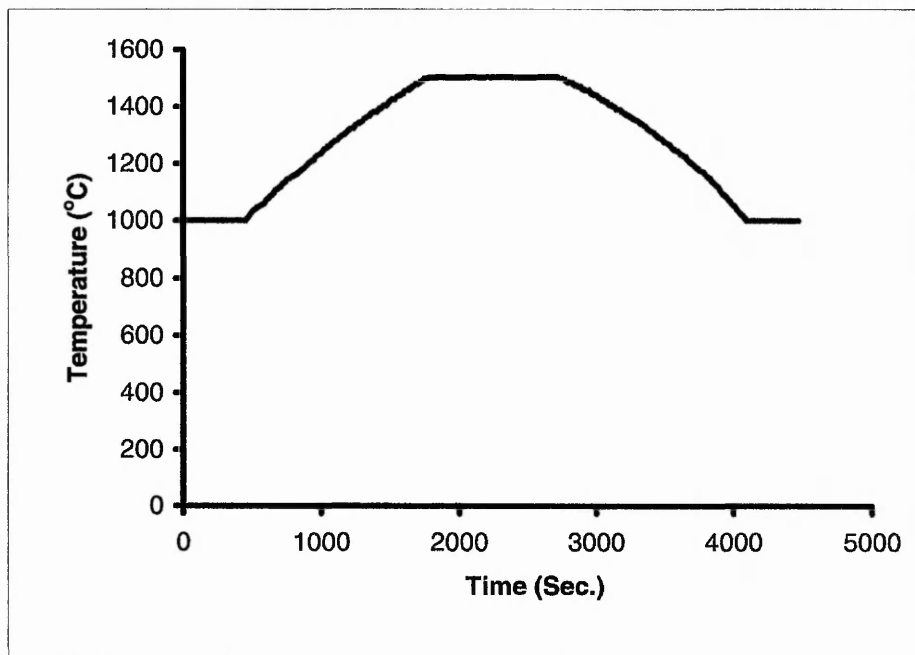


Fig. 6.13 Sintering cycle of the coating using 96% alumina as substrate

Fig. 6.14 shows optical and SEM images of polished transverse sections of a sintered coating on a 96% alumina substrate, sintered at 1500°C for 20 minutes. There was no apparent cracking or lack of adhesion to the substrate. The interface can be determined by the increase in the amount of porosity in the coating, as compared to the substrate (Fig. 6.14(b)).

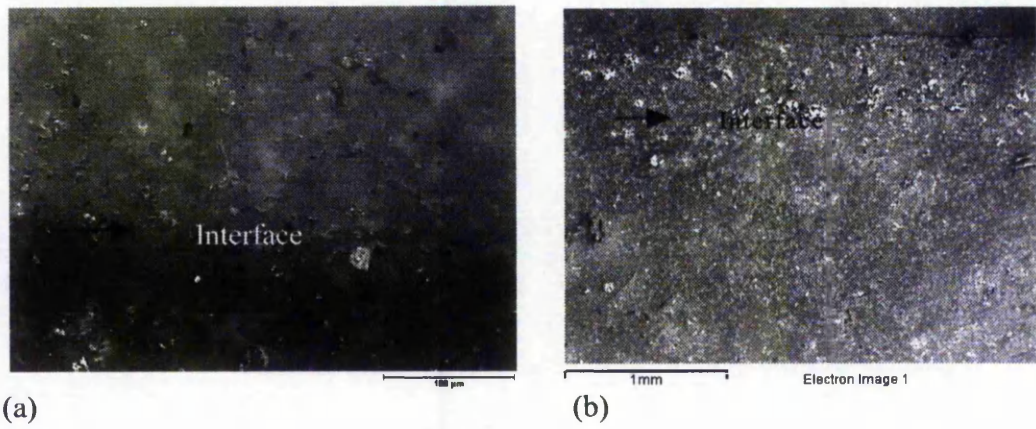
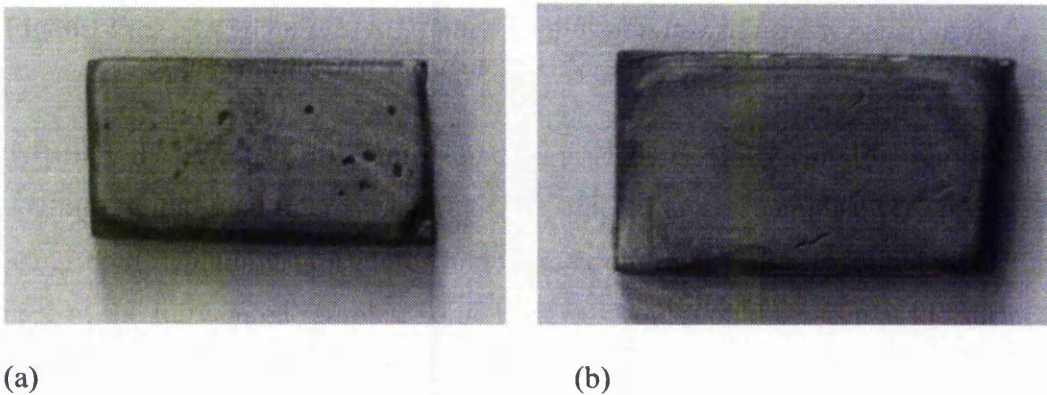
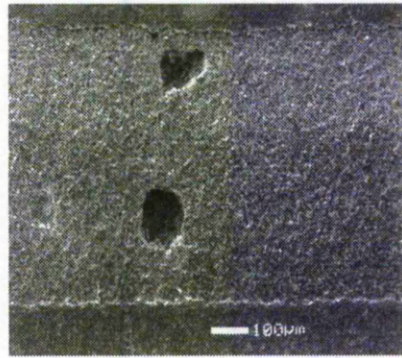


Fig. 6.14 (a) optical and (b) SEM micrographs of polished transverse sections of the coating and substrate

To study the effect of different debinding procedures (fully cured or semi-cured coating) on the final microstructure of the sintered layers, samples were prepared using both debinding procedures and sintered at 1500°C for 15 minutes. In the case of the fully cured samples, some large gas voids could be seen at the surface of the coating (Fig. 6.15 (a)) and were found to be present throughout the thickness of the coating (Fig. 6.15 (c)). Samples in which the debonding cycle was started whilst the coatings were only partially cured did not show these kinds of defects, as can be seen in Fig. 6.15(b).

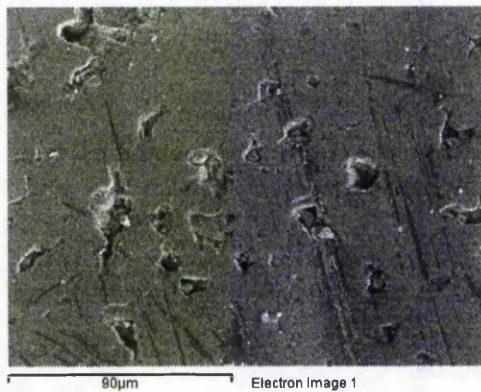




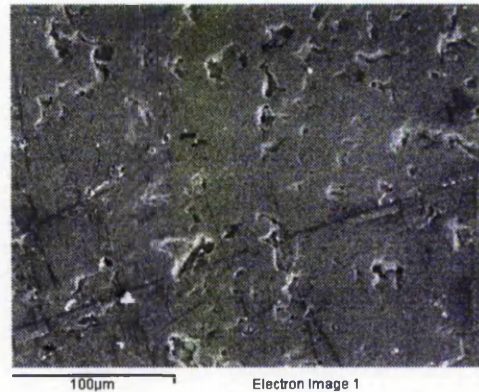
(c)

Fig. 6.15 Surface of (a) fully cured and (b) partially cured sample, and (c) gas voids in a cross sectioned fully cured coating

The SEM micrographs in Fig. 6.16 are polished transverse sections of a coating after sintering at 1520°C for 20 minutes. These show that sintering proceeded more into the intermediate stage (solution–precipitation stage) in the sintered layers compared to the ones that have been described in section 6-3-2 using fumed silica as an additive. Densification in the intermediate stage depends on mass flow through the liquid phase (which is easier in the optimised glass used in 96% alumina substrate) and results in pore shrinkage (German 1985).



(a)



(b)

Fig. 6.16 SEM micrograph of a polished transverse section of a sintered unimodal alumina layer onto 96% alumina substrate

The coatings were generally very homogenous. However, occasionally defects were observed in polished transverse sections of the coatings. Fig. 6.17 (a) and (b) show a pocket of an early stage of the solution–precipitation stage in the coating,

while figures 6.17 (c) and (d) show the largest void observed and a non-densified defect, which probably occurred as a result of agglomeration in the mixture.

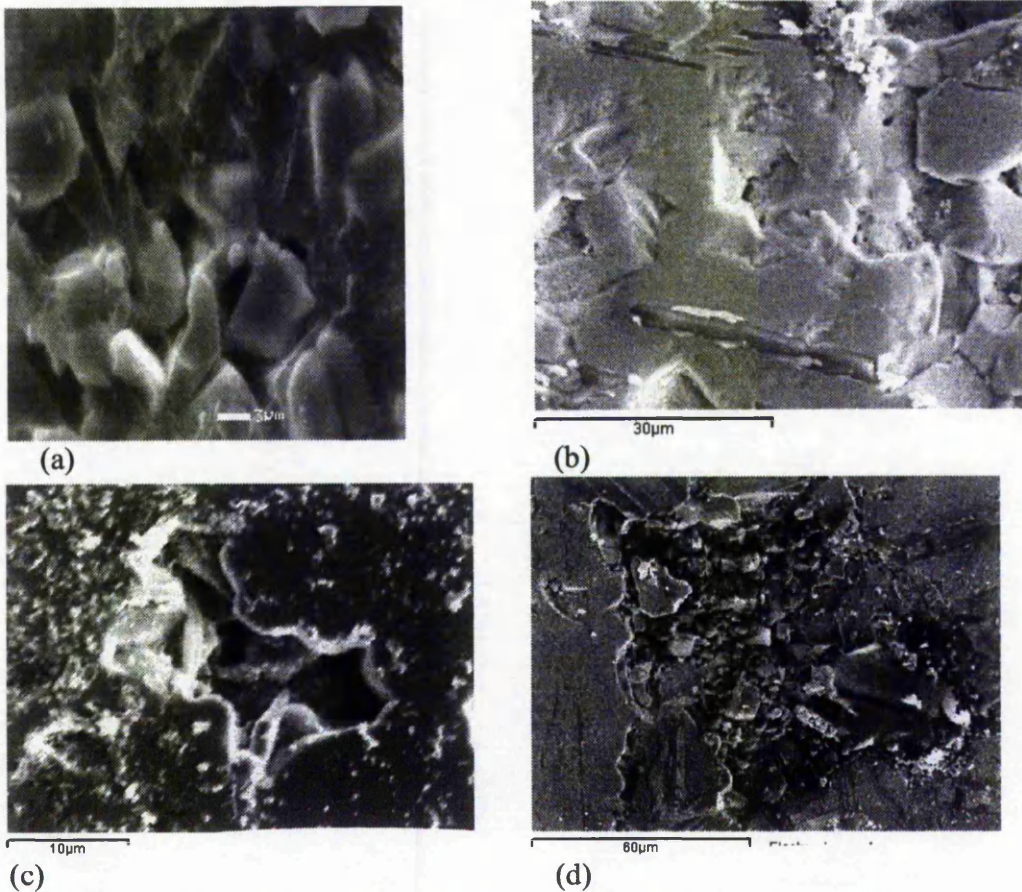


Fig. 6.17 *Some defects in polished transverse sections of sintered layers*

A conventional Vickers macrohardness test, with a 2.5 kg normal load, and Knoop microhardness tests with 0.3 kg normal load were performed on the samples. The tests were performed on the transverse section of as-sintered coatings on 96% alumina substrates, which had been debonded while only partially cured and sintered at 1530°C for 20 minutes. Again, the standard formulas (equations 2.2 and 2.3) were used to calculate the hardnesses of the coatings. Table 6.4 summarizes the measured hardness values.

Table 6.4 Average hardness of uni-modal alumina sintered coating

	Uni-modal Alumina Sintered Coating	
	Hardness (HK 0.3) Kg/mm²	Hardness (HV 2.5) Kg/mm²
Average Hardness	1337.2	1017.5
Standard Deviation	232	136

The average hardness of seven readings for a uni-modal alumina sintered coating was 1017.5 HV_{2.5} (Kg/mm²) with a standard deviation of 136. The equivalent Knoop value was determined as 1337.2 KH_{0.3} (Kg/mm²) with a standard deviation of 232 (for eleven readings). Fig. 6.18 shows an example of a Knoop impression on the polished coating cross section. The scatter in the results arises normally as a consequence of the presence of multiphases and pores in the structure. It is not uncommon to obtain coefficients of variation of 10% in macrohardness measurements and 20% in microhardness measurements (Morrell 1985).

The difference between the two average values is probably a result of indenter size, shape and load, which affect the readings. The hardness of the coating layers was not quite as high as the substrate (Table 6.3), but the absence of any kind of cracking or other major defects at the interface, and the achievement of a reasonable hardness value compared to the other thick coating methods, such as flame spray, show that it is possible to use the PRIME technique to obtain good quality ceramic coatings.

For example, Saravanan et al. (2000) and Sarikaya (2005) studied the influence of the process variables on the quality of detonation gun sprayed and air plasma sprayed alumina coatings. The hardness was found to lie between 951 and 1363 HV_{0.2}. Erikson et al (2001) reported a hardness of 6.6 to 10.2 HK (GPa) [660 to 1020 Kg/mm²], for alumina plasma sprayed coatings using a 10N load.

Comparing the above data with the hardness measured in this study, it can be concluded that a good hardness has been achieved using the present process. It is

also quite likely that further development of the sintering cycle would enable even better properties and uniformity to be achieved.

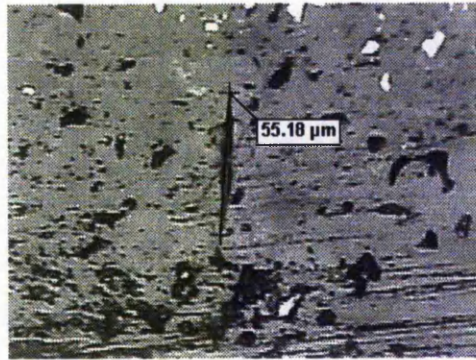


Fig. 6.18 Sample Knoop Indentation on polished transverse coating layer using 96% alumina as substrate

6-4-3-2 Bi-modal Alumina Powder coating

A powder mixture with a bi-modal particle size distribution, i.e. one which contains two powders having quite different particle sizes, enables a higher packing density in green state to be obtained. The procedure in this study for making such coating mixtures was given in section 6-4-2. The non-fully cured coatings, with a thickness of 0.6 mm, were sintered at 1500°C for 20 minutes

Fig. 6.19 shows an optical and SEM micrographs of polished transverse sections of this coating. No cracks or lack of adhesion was observed at the interface, although a comprehensive examination of the coating cross sections occasionally resulted in finding some defects in the coating, such as the possible incomplete sintering shown in Fig. 6.20.

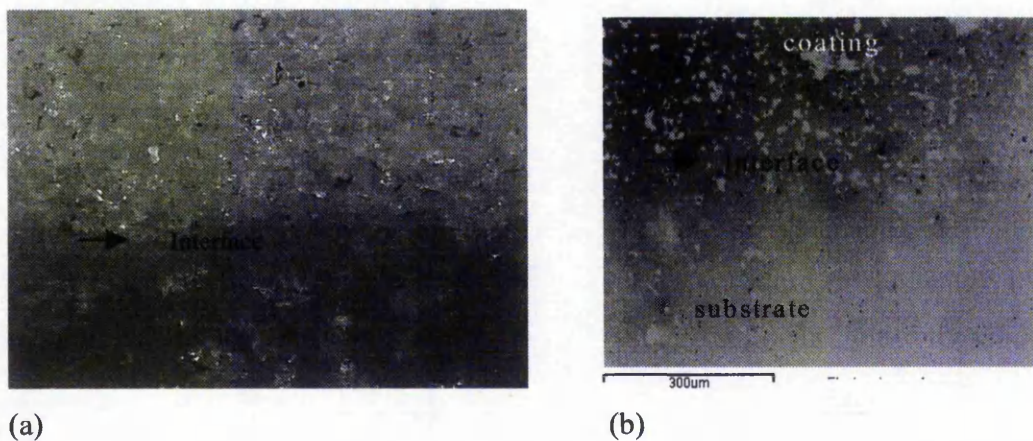


Fig. 6.19 (a) Optical and (b) SEM micrographs of polished transverse sections of sintered coating prepared from bi-modal particle size alumina

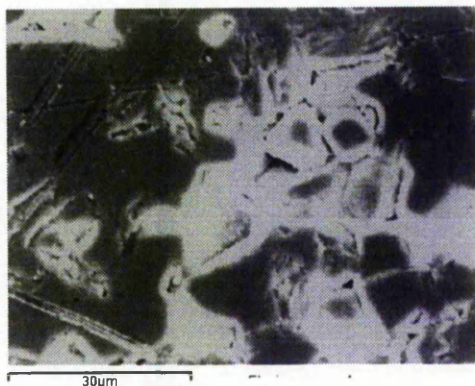


Fig. 6.20 SEM micrograph sample of a defect (initial stage of solution-precipitation) in the polished transverse section of sintered bi-modal alumina coating

The average of eleven Knoop microhardness readings on the coating cross section gave a value for $HK_{0.3}$ of 1309.2 ± 112 (Kg/mm^2). This value is effectively the same hardness as that measured on the coatings made using uni-modal alumina powder. This good hardness level has been achieved despite the fact that the sintering cycle for the coating has not been optimised, as well as the fact that the molten glass would be expected to experience some difficulties as it percolates through the debonded structure of the coating. However, the standard deviation is lower, which would indicate that a more uniform structure had been developed.

Surface cracks generated by a Vickers indentation can be used to estimate the critical stress intensity factor. Fig. 6.21 shows a sample Vickers indentation impression on a transverse section of a polished substrate and coating. The indentation fracture technique is commonly used at room temperature to determine fracture toughness, in spite of the discrepancy between the value calculated by this method and fracture toughness measured by conventional methods, such as the single edge notch beam (Gong 2002). The indentation toughness was calculated for substrate and coating using the equation proposed by Anstis et al (1981):

$$K_{Ic} = 0.0226 (E P)^{1/2} (a_V/c_V)^{3/2} \quad (6.1)$$

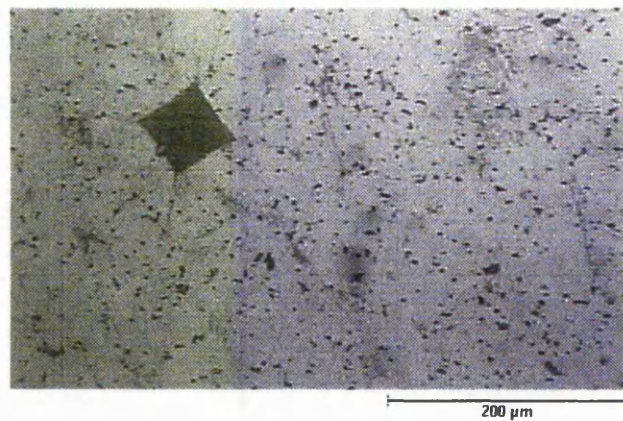
where P is the applied load (N), E the Young's modulus (GPa), c_v half the average length of the crack (m), a_v half the indentation diagonal length and K_{Ic} is the critical stress intensity factor ($\text{MPa m}^{1/2}$).

Assuming Young's modulus to be 303 GPa for 96% alumina (Chinn 2002), Table 6.5 summarizes the calculated values for the indentation fracture toughness for the substrate and coating after sintering at 1500°C for 20 minutes.

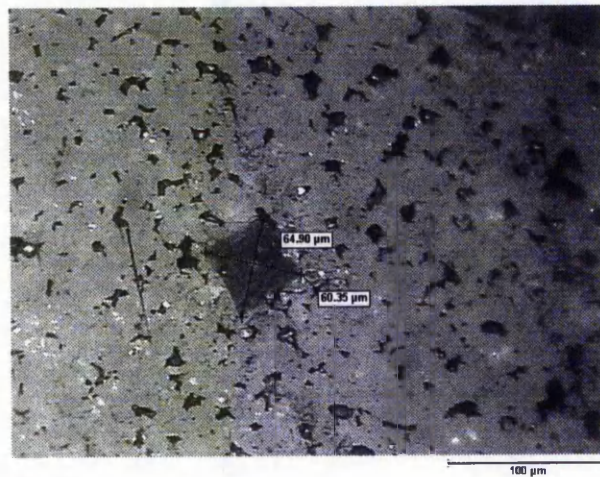
The average fracture toughness of the coating and substrate were calculated as 3.61 and 3.93 $\text{MPa m}^{1/2}$, respectively. Although the toughness of the coating is slightly lower, the measured values show less variation than for the substrate.

Table 6.4 Measured values and calculated toughnesses for bimodal alumina coating and 96% alumina substrate after application of the sintering cycle

		Load (Kg)	a_v (μm)	c_v (μm)	K_{Ic} ($\text{MPa m}^{1/2}$)
<i>Coating</i>	<i>CF1</i>	2.5	31.3	68.2	3.41
	<i>CF2</i>	2.5	32.6	64.8	3.85
	<i>CF3</i>	2.5	30.8	65.4	3.58
<i>Substrate</i>	<i>SC1</i>	5.0	41.1	79.0	5.09
	<i>SC2</i>	5.0	38.4	92.6	3.75
	<i>SC3</i>	2.5	27.6	69.6	2.99
	<i>SC4</i>	2.5	28.2	53.8	3.90



(a)



(b)

Fig. 6.21 Vickers hardness impressions on (a) the substrate and (b) sintered alumina coating made of bi-modal powder

6-4-3-3 Stabilized Zirconia Powder coating

To study the effect of using a different coating material on the 96% alumina substrate, stabilized zirconia was used as a coating material. 4%w PTS acid (as a proportion of the cyanoacrylate percent) was dissolved in cyanoacrylate as stabilizer and a coating mixture containing 43%v yttrium-stabilized zirconia mixed with 1%w caffeine (as a proportion of the cyanoacrylate) was prepared before applying on a 96% alumina tile. Non-fully cured samples were thermally debonded up to 220°C with a heating regime as described in section 5-3-3. Sintering was carried out at 1300°C for 20 minutes.

Fig. 6.22 illustrates SEM images of a polished transverse section of one of these samples, which shows a good adhesion between the coating and the substrate.

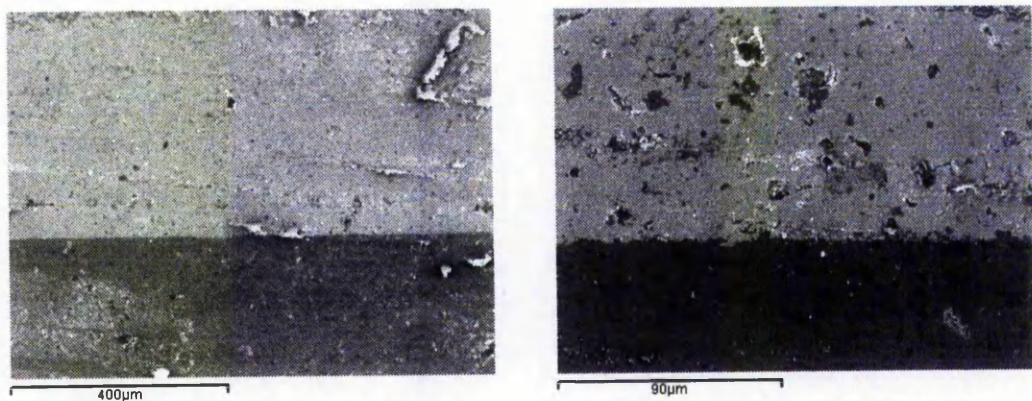


Fig. 6.22 SEM micrographs of polished transverse section of stabilized zirconia on alumina (96%) substrate

The average Knoop microhardness of the sintered stabilized zirconia coating was measured as $995 \text{ HV}_{0.3}$ (Kg/mm^2), with a standard deviation of 69 based on eleven readings. The SEM observations, plus the measured hardness for the sintered coatings, suggests that the sintering cycle resulted in the transfer of glassy phase from the substrate through the coating thickness.

This is consistent with studies of Esposito and Bellosi (2001). Using a silicate glass ($\text{CaO}-\text{Al}_2\text{O}_3-\text{SiO}_2$), they reported that when joining alumina-20% zirconia to 3% mole Y_2O_3 -zirconia parts, the existing glassy interlayer flowed through the interface driven by the capillary pressure and penetrates the grain boundaries of the zirconia up to a distance from the interface to a depth that is a function of the starting glass amount, bonding temperature and soaking time.

Although the hardness of the coating is comparable to zirconia coatings deposited by the flame spray method, various forms of inhomogeneities were observed in the present sintered stabilised zirconia laminates. These included cracks and crack like defects (horizontal and vertical), which were relatively common (Fig. 6.22). These defects in film-substrate systems might have been produced as a result of localised stresses. One source of stress is the mismatch in thermal expansion between the layers (alumina has a lower thermal expansion than zirconia), which occurs during the sintering and cooling stages, and results in different densification kinetics (Cai et al 1997). The extent of cracking could be reduced or eliminated by decreasing the mismatch stress. This could be done by reducing the heating and/or cooling rates, or by adding alumina into the zirconia layers.

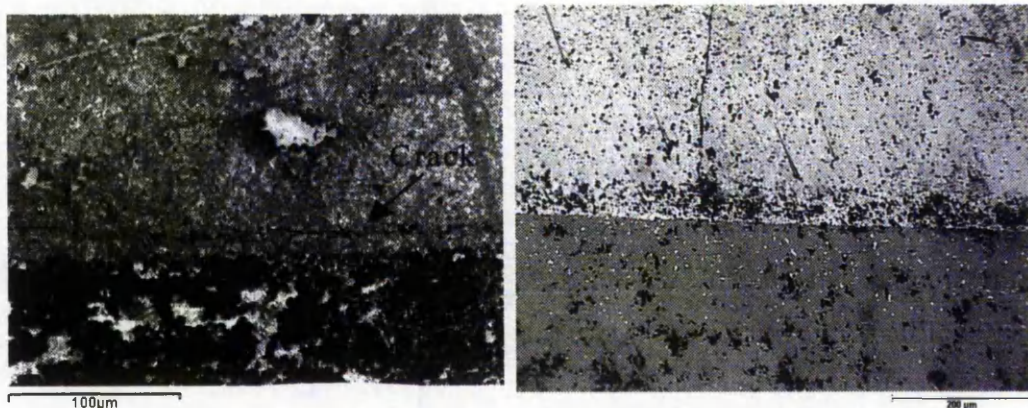


Fig. 6.23 Samples of defects observed in stabilized zirconia coatings after sintering

Finally, Table 6.6 summarizes the average hardness values and their standard deviations for the three different coatings on a 96% alumina substrate. The hardness results for coatings of alumina uni-modal and bi-modal powders are practically the same, although with a smaller standard deviation for the coating from the bi-modal powder. The coating made of stabilized zirconia has satisfactory hardness with a much lower standard deviation.

Table 6.6 Comparison of the average hardness values for different coatings made by PRIME method on 96% alumina substrate

	<i>Hardness (Kg/mm²)</i>		
	Uni-modal alumina powder (No.2)	Bi-modal alumina powder	Stabilized zirconia Powder
<i>Average</i>	<i>1337.2</i>	<i>1309.2</i>	<i>995.0</i>
<i>Standard Deviation</i>	<i>232</i>	<i>112.6</i>	<i>69.3</i>

6-5 Summary

- Different substrates (pure alumina, molybdenum and 96% alumina), coating materials (uni-modal and bi-modal alumina powders, stabilized zirconia powder) and sintering methods (pressure-less solid state and liquid phase) were investigated in order to sinter the debonded layers,
- It was found that pressureless solid state sintering did not produce fully densified adherent coatings using RF heating. Sintering of a debonded layer of uni-modal alumina powders at 1675°C for two hours resulted in a coating with a low hardness, i.e. 140 HK_{0.3},
- Liquid phase sintering of the coatings was investigated using fine fumed silica powder as a sintering aid. Adding 3.5%w fumed silica powder to the coating mixture and sintering at 1620°C for 2 hours improved the hardness of the coating to 470 HK_{0.3},
- Further increase in fumed silica proportion in the mixture was not possible because of its side effect in reducing the proportion of the ceramic powder in the mixture due to the increased viscosity of the mixture,

- It was found that using fumed silica was not an entirely satisfactory sintering aid, and that the evaluation of further potential sintering aid compositions was beyond the scope of the present study,
- A substrate made of 96% alumina was selected to use on the basis that its optimised glassy phase could melt and penetrate into the pores/grain boundaries in the coating up to a reasonable distance from the interface, therefore assisting with the sintering of the debonded coating,
- Sintering of coatings containing uni- and bi-modal alumina powders at 1530°C for 20 minutes resulted in hardnesses of 1337 and 1309 HK_{0.3}, respectively,
- Coatings exhibiting good densification, a hardness comparable with the commercial alumina used as substrates (1536 HK_{0.3}), and apparently good adhesion could be achieved for both uni-modal and bi-modal alumina powders,
- Applying stabilized zirconia coatings onto 96% alumina substrates by sintering at 1300°C for 20 minutes, resulted in a good hardness (995 HV_{0.3}) and apparently good adhesion to the substrate, but cracks were observed in the sintered coating, presumably arising as a result of the difference in thermal expansion coefficients of zirconia and alumina
- It has been demonstrated that the PRIME technique as developed in this study could be used as an alternative fabrication method for producing thick coatings.

7

Summary & Discussion

Introduction

Ceramic coatings cover a wide range of techniques and applications. However there is always the potential to develop new techniques to address the shortcomings of current methods and/or improve the properties for a specific application.

As noted at the beginning of this dissertation, the present study has investigated the possible application of powder reaction injection moulding to form a novel thick ceramic coating, i.e. PRIME surface coating. The research reported in this study has been concerned with the development and refinement of the initial ideas and translating them into practice. The preceding chapters present the procedures and experimental information leading to the manufacture of the novel coatings. There has been a discussion of the findings, and a short summary, within each chapter. Some of the main points of the research linking across the specific developments described in the respective preceding chapters are discussed in this chapter and the developed procedures and technology can be assessed overall.

The initiative for the project was based on the idea of combining the concept of ceramic injection moulding with using a new type of binder to develop a new thick ceramic coating method.

The main aim of this research was to develop a processing chain from powder and binder selection and mixing, to deposition, debinding and sintering of the coating layers.

Several types of powders, cyanoacrylates, substrates and additives as well as various curing and sintering methods were investigated. Furthermore, experimental techniques have been used to study the mixture properties and the resultant cured and sintered coatings. Combining the results together, an overview of the process and the effects of the more important variables can be presented.

7-1 Materials Processing & Mixing

The first step in making the mixture was to find a suitable cyanoacrylate formulation. Binders for injection moulding are generally recommended to have a viscosity lower than 10000 cP at the moulding temperature and pressure, otherwise, when a powder is included, the combined viscosity would be too high (German and Bose 1997). In the present technique, it has been observed that in addition to the effect of the viscosity of the binder, it is also very important to take into account the outgassing characteristics of the cyanoacrylates during mixing and curing.

Therefore, several candidate binders with low viscosities were selected for study. From the binders investigated Alkoxyethyl cyanoacrylate, with a viscosity of 7 cP was chosen for this investigation. This selected binder has a range of features, including lowest possible viscosity combined with low blooming and outgassing effects, as well as the best technical compatibility with the coating aims.

According to German (1997) and Reed (1995) an ideal PIM powder should have a particle size between 0.5 and 20 μm , and that for bi-modal powders the size ratios must be greater than 7. Based on these recommendations, and the observations in the SEM studies, a fairly coarse alumina powder with D_{50} of 8 μm and a fine stabilized zirconia powder, with an average particle size of 1.1 μm , were selected to produce coatings containing uni-modal powders. A simple paddle type mixer was made for blending 70%w coarse (8 μm) and 30%w fine (0.45 μm) alumina powders to make a bi-modal powder mixture.

Several factors may affect the critical solid loading in the mixture, including the viscosity of the binder and the powder characteristics. The viscosity of the

mixture increased rapidly with increasing solids concentration near the critical point and the optimal volume fraction for the powders was chosen to be slightly less than the critical value. The volume fraction of powders was fixed at ~45% for uni-modal and 58% for bi-modal powders. The powders were all dried for two hours at 220°C immediately prior to being used.

It was noted that it was not possible to mix a high concentration of powder into the cyanoacrylate since the mixture rapidly became too viscous and unworkable. This was hypothesised as occurring as a result of the initiation of polymerization from the surface of the particles, either due to their inherent chemistry or surface water vapour. Although it was not possible to monitor the pH of the mixture during curing, based on the observations on the curing behaviour of pure cyanoacrylate, i.e. polymerization occurring at pH >5.5 (Cook and Allen 1993), the acidity of the binder had to be increased to inhibit the initiation of significant polymerization at any time during the mixing, handling and application of the coating. This was achieved by the addition of a controlled concentration of p-toluene sulphonic acid being dissolved into the cyanoacrylate before mixing with the powder. This prevented any significant polymerization whilst mixing the powder and binder, and also during the application stage. It was noted that different concentrations of acid were needed to inhibit polymerization during mixing, dependent on the composition of the powder (in particular its surface chemistry) and the surface area. The present studies showed that dissolving only small amounts of acid in the cyanoacrylate did not effect sufficient inhibition to enable a sufficiently fluid mixture to be obtained after the addition of a high volume fraction of powder.

It was also determined in the mixing trials that for a specific powder, the inhibition period was a function of the solids concentration in the mixture, and it decreased with increasing powder concentration. This finding supported the contention that the powder surface can play a significant role on the start of localized polymerization. This premature polymerization presumably initiates on, or adjacent to, the surface of the powders, with a resultant rapid increase in the viscosity of the mixture. On the other hand, once a sufficient concentration of acid had been added to inhibit the polymerization, there was no further

improvement observed on increasing the acid concentration above this level. Thereafter the viscosity increased only due to increasing the solid particle content. These observations indicated that there was a good potential for using rapidly polymerized cyanoacrylate as a carrier to make homogenous coating mixtures containing ceramic powders.

The use of processing aids, such as surfactants, has also been investigated using either an anionic (DISPEX) or a non-ionic (Alkyl ethoxylate) surfactant. It was found that despite DISPEX being a polycarboxylic acid it acts as an initiator rather than an inhibitor as might have been expected, and the cyanoacrylate containing the dissolved acid started to cure locally as soon as the DISPEX was added. Alkyl ethoxylate, was added in small amounts ranging from 0.17 to 0.38%w. Although it was found to lower the viscosity of a cyanoacrylate-45%v alumina mixture, the cured coated layers were brittle and contained cracks. There was also an apparent lack of adhesion to the substrate after curing. Considerable further development would be required to enable an appropriate surfactant, and the required concentration in the mixture, to be identified. Therefore, it was decided not to use a surfactant in the mixture in the present study.

To determine the optimum acid concentration, different concentrations of acid were dissolved in the cyanoacrylate at 45°C for 30 minutes prior to mixing. Based on the findings from this study, the effective acid level was fixed at 2%w for coarse alumina and 4%w for fine zirconia and bi-modal alumina powders.

However, the monomer was inhibited to such an extent to ensure sufficient time for thorough mixing and controlled application of the mixture to the substrates that curing of the coating layer after application took longer than would be feasible in practice. Therefore, several methods of increasing the polymerization rate in the coating after application were investigated. The effectiveness of water vapour, steam, and caffeine, either incorporated into the coating mixture or applied to the surface of the substrate, were examined. It was found that although steam was effective in increasing the polymerization rate, the resulting cured layers contained internal pores and signs of localised cracking. There are several alternative initiating chemicals reported in the literature (Lee 1981, Birkinshaw et al 1996, Scheenberg 1990, Dombroski and Weemes 1976), with caffeine being one of the more readily available and least hazardous. From this investigation it

was determined that dissolving caffeine in cyanoacrylate could provide a suitable method for controlling the onset of the polymerization reaction in a cyanoacrylate-powder-acid mixture. On this basis, caffeine was selected as the initiator that was generally used. It was dissolved in the cyanoacrylate for 30 minutes at 45°C, after the acid addition and before introducing the powder(s) into the mixtures.

Once the types of powder and cyanoacrylates to be used, and the maximum feasible percentage of powder in the mixture, had been fixed, the rheological behaviour and coatability of the mixtures were controlled by the relative amounts of the para-toluene sulphonic acid and caffeine additives.

Due to a combination of the abrasive nature of the ceramic powders and adhesive qualities of the cyanoacrylate binders it was decided not to use the available standard rheometers to measure the viscosities of the mixtures. Instead, a relatively straightforward method utilising a pressurised plastic syringe was designed and constructed. This was not suitable for all the mixtures that were made, but it was appropriate for those mixtures with appropriate viscosities. Using this apparatus, the effect of dissolved caffeine and acid (C/A) was investigated for three different ratios, i.e. 0.8, 1.0, 1.2. It was found that for a given cyanoacrylate binder, powder type and concentration, and acid concentration that increasing the caffeine concentration effectively lowers the viscosity of the mixtures.

Furthermore, in order to compare the effect of the binder composition on the viscosity of the mixtures (containing 45%v alumina powder No. 2), three different cyanoacrylates (Loctite 420, 408 and 406), with one percent pre-dissolved acid were investigated. These results indicate that the lower the original viscosity of the cyanoacrylate, the lower is the viscosity of mixture with the same amount of powder and C/A ratio.

7-2 Application & Curing

When the basic practical properties of the materials and mixtures were understood, a simple PTFE mould was made to apply the coating mixture onto flat substrates. It was observed that two major problems happened during the curing of the coating mixtures. The first one was the release of gas, which would become entrapped in the mixture at the later stage of curing, as a result of the high

viscosity. The second major problem encountered during the curing stage was the formation of a thin layer of pure cyanoacrylate at the interface between the coating and the substrate.

A variety of curing methods were studied with a view to eliminating the porosity occurring as a result of gas evolution during curing. It was considered that these voids were undesirable and would almost certainly result in defects after debinding and sintering. Although caffeine was selected as an appropriate initiator, several techniques for using the initiator were investigated. These involved for example applying caffeine solution at the surface of the substrate (surface activation), or dissolving caffeine in the cyanoacrylate and adding it to the mixture of cyanoacrylate and powder at the end of the mixing stage just prior to the application of the coating.

The hypothesis behind trying surface activation was to try directional curing from the substrate outwards towards the external surface of the coating to eliminate or reduce the trapped gas bubbles. This method showed only limited success. The reason for this was that there was too much acid in the coating mixture to be neutralized by substrate surface activation alone.

From the methods investigated, it was found that the best procedure involved adding caffeine to the mixture at the end of the process, i.e. after the addition of the appropriate amount of powder to the binder. It was noted that although this method required more caffeine, it had several advantages over pre-dissolving caffeine prior to mixing, including better control of the viscosity and curing time of the mixture, and reproducibility of the process.

In order to investigate the effect of caffeine concentration in the mixture on the curing behaviour, four samples were made with the same amount of cyanoacrylate, powder and acid and different amounts of caffeine (1, 2, 3 or 4%w) incorporated at the end of the mixing stage. The extent of the polymerization was judged by measuring the temperature increase over the curing time. It was noted that as the concentration of caffeine increased, the curing started sooner and took place more quickly. Furthermore, it was observed that with the addition of more than 3% caffeine, curing started while mixing, which could adversely affect the viscosity, and thus 'coatability', of the mixture.

The results of these studies suggested that the concentration of caffeine can be optimised to prevent premature curing during mixing and application of the

coating on one hand, and avoiding long curing times to meet manufacturing requirements on the other hand. As a result, a small amount of caffeine, depending on the required time to cure, could be incorporated into the mixture to provide a suitable controlled curing rate.

The advantage of using this curing method was that it enabled the debinding of the coating to be commenced while the viscosity of the coating was high enough for handling, but crucially before curing had been fully completed. This procedure was found to be very successful, and it was possible to eliminate virtually all the voids resulting from gas release during curing.

The second major problem concerned the formation of a thin layer of pure cyanoacrylate at the interface between the coating and the substrate. This was considered to be undesirable since it was anticipated that it could adversely affect the coating properties after subsequent thermal treatment. It was also demonstrated that this layer could affect the adhesion strength of the coatings onto the substrate. It was found by practical investigation that devising appropriate compatibility between the coating mixture and the substrate surface eliminated this layer. For example, applying an alumina powder containing mixture onto an aluminium substrate could leave a pure cyanoacrylate layer (2-3 μm) at the interface, while mechanical polishing of the substrate prior to application eliminated this layer. Furthermore, applying the same mixture onto stainless steel substrates did not result in a cyanoacrylate-only layer at the interface.

It was also noted that, as well as affecting the viscosity and coatability of the mixture, the C/A ratio could affect the strength of the adhesive bond between the substrate and the cured layers, with a lower shear strength being obtained for the higher C/A ratios.

The hardnesses of the coatings were measured to be in the range 26.4 to 30.1 $\text{HV}_{0.2}$ (Kg/mm^2) for uni-modal alumina powder (No.2) and 33.0 to 37.1 $\text{HV}_{0.2}$ (Kg/mm^2) for bi-modal alumina (70%w powder No.2 and 30%w powder No.3) mixtures.

Limited studies were also made to ensure that the coatings could be applied successfully onto non-flat substrate geometries. These generally had the same appearance and quality as coatings applied to flat substrates.

7-3 Debinding

Debinding was required to remove the binder from the coating mixture to enable an uncontaminated sintered coating to be obtained at a later stage.

It was found using TGA and DSC (Birkinshaw, 2003) that the thermal decomposition of the cyanoacrylate binder in the mixtures exhibited only a single exothermic peak, with the main heat output occurring at $\sim 230^{\circ}\text{C}$, although it was noted that the decomposition actually commenced at a much lower temperature, i.e. between 100°C and 150°C . It was also observed that relatively rapid heating of cured coatings, i.e. ~ 5 degrees C/minute resulted in swelling of the coatings and the surface became porous. Furthermore, there was no adhesion at the interface after debinding at this rate.

Based on these observations, slow heating of samples was investigated using step heating in an oven. The time needed for the coating interface to reach the furnace temperature was estimated to assist with the formulation of an appropriate temperature-time profile. This approximate calculation showed that it should take about four minutes for the interface to reach the furnace temperature (for a 10 degree temperature difference between the oven and interface temperatures) with any subsequent holding time resulting in thermal debinding. It was therefore considered reasonable to use dwell times of 30 minutes at the set temperatures to determine if this would prove to be appropriate. SEM studies after debinding showed there were only the normal connected pore channels present in the coating layer, with no macrodefects.

It was observed that the type of the powder, solid loading and thickness of the coating would result in different rates of binder removal. Nevertheless, the formation process of connected pore channels remains the same, regardless of the kind of packing structure or coating dimensions (Li et al 2003). As a result, although measurements of the weight loss of the samples for various time-temperature sets were evaluated, the debinding cycle which was finally selected was optimised to suit the higher solid volume fraction coatings made of bi-modal alumina powders. Hence, the samples were heated to 120°C in 60 minutes followed by soaking with a temperature sequence of 120, 135, 150, 165, 175, 180, 185, 190, 195, 200, and 220°C for dwell times of 30 minutes in all cases. The

oven temperature increased in 4-6 minutes between temperature holds, depending on the temperature.

As was mentioned earlier, debonding of the partially cured layers can significantly reduce the formation of gas bubbles in the mixture prior to sintering. These samples did not crack or show any sign of slumping or trapped gases and the heating parameters were considered to be adequate for this stage of the investigation.

7-4 Sintering

Sintering was the final stage of the development of the new coating process. This was undertaken using a low frequency induction-heating furnace with graphite being used as the susceptor to heat the components placed inside the induction coil under the protection of argon gas. The investigations of the quality of the sintered coatings was undertaken using microstructural studies, mainly on polished transverse sections using SEM, with hardness, and K_{IC} by indentation, being used to evaluate the mechanical behaviour.

In the first phase, pressureless solid state sintering of the debonded layers on pure alumina or molybdenum substrates was investigated. Sintering the samples at 1675°C for two hours resulted in porous rather than fully dense coatings, with the appearance of limited adhesion to the substrates. The reason for this was probably that for this combination of temperature, pressure and time, the rate of solid state diffusion in the alumina coating was too slow, and only the initial phase of sintering could be achieved. The relatively low solid loading would also contribute to this slow densification rate.

As a result, it was decided that liquid phase sintering of the layers needed to be investigated. On this basis, a sintering aid (fine fumed silica powder) was added to the cyanoacrylate before mixing with the alumina powder. It was found that this required the concentration of para-toluene sulphonic acid inhibitor to be increased from 2 to 6%w to compensate for the additional large powder surface area. Various concentrations of sintering aid were studied, with the final mixture having 45%v alumina powder and 1.58%v fumed silica. The mixtures were debonded and sintered for 2 hours at 1620°C. This produced an improvement in the interparticle bonding in the coating to give a hardness value of 470 HK_{0.3}.

This demonstrated that by increasing the relative proportion of sintering aid(s) greater densification, and thus higher hardness was potentially achievable. However, with the particular alumina and silica powder used in this study it was not possible to add a greater proportion of silica to the mixture, since this resulted in lower proportion of main ceramic powder, i.e. alumina, that could be added at the later stage of mixing.

The potential alternative methods for producing a coating with close to full density that were considered were: to modify the sintering aid(s), to increase the sintering temperature and/or hold time and/or the application of pressure. Practically, the most attractive alternative was to modify the sintering aid. It was decided that the most effective approach to finding a suitable solution was to investigate the use of a different, lower purity, alumina substrate which already contained an appropriate composition of sintering aids.

Therefore, it was decided that to investigate the feasibility of achieving a sintered coating with reasonable properties, as well as good adhesion at the interface, using a commercially produced alumina (96%) tile, as the substrate. The key reason for this choice was that on firing the debonded layer-substrate system, the optimised glass phase in the alumina substrate could melt and penetrate into the pores/grain boundaries in the coating up to a reasonable distance from the interface.

Uni-modal and bi-modal alumina coating mixtures were applied on the 96% alumina substrate and the debonded layers were sintered at 1500°C with a hold time of either 15 or 20 minutes.

After sintering, the layers were observed to have good adhesion to the substrate. SEM study showed no apparent cracking in the coating or at the coating-substrate interface. The position of the interface was determined by the increase in the amount of porosity in the coating, as compared to the substrate.

In samples in which the cyanoacrylate was fully cured prior to debonding and sintering it was observed that occasional large gas voids could be found at the surface and throughout the thickness of the coatings. Samples in which the debonding cycle was started whilst the coatings were only partially cured did not show these kinds of defects.

The sintered coatings were between 0.5 and 0.7 mm thick and were observed to be generally very homogenous. However, occasional defects were observed in polished transverse sections of the coatings. It was hypothesised that these mainly

formed as a result of some agglomeration in the mixtures and/or the non-fully optimised sintering cycle.

The average hardness readings for uni-modal and bi-modal alumina sintered coatings were determined as 1337.2 ± 232 and 1309.2 ± 112 HK_{0.3} respectively.

The indentation fracture toughness of coatings was also measured. The average fracture toughness of the coating and substrate were calculated to be 3.61 and 3.93 MPa m^{1/2}, respectively. Although the toughness of the coating is slightly lower, the measured values showed less variation than for the substrate.

These good mechanical properties are comparable with the properties for other methods of applying thick ceramic coatings. It is important to emphasise that these properties have been achieved despite the fact that the sintering cycle for the coating has not been optimised, as well as the fact that the molten glass would be expected to experience some difficulties in percolating through the debonded structure of the coating.

A different coating material from the substrate (stabilized zirconia) was also investigated. 4%w PTS acid (as a proportion of the cyanoacrylate) was dissolved in the cyanoacrylate as stabilizer and a coating mixture containing 43%v yttria-stabilized zirconia mixed with 1%w caffeine (as a proportion of the cyanoacrylate) was applied to a 96% alumina tile. Non-fully cured samples were thermally debonded using a step heating cycle up to a maximum of 220°C. Sintering was carried out at 1300°C for 20 minutes.

The average Knoop microhardness of the sintered stabilized zirconia coating was measured as 995 HV_{0.3} with a standard deviation of 69. The SEM observations, plus the measured hardness for the sintered coatings, suggests that the sintering cycle resulted in the transfer of glassy phase from the substrate through the coating thickness.

Although the hardness of the coating is acceptable compared to zirconia coatings deposited by the flame spray method, various forms of inhomogeneities were observed in the sintered stabilised zirconia laminates including cracks and crack like defects presumably caused by localised stresses. One source of such stress is the mismatch in thermal expansion between the substrate and coating, which occurs during the sintering and cooling stages. Adjusting the heating and/or cooling rates, or adding alumina into the zirconia layers would reduce this.

7-5 Summary

This investigation has demonstrated that a novel thick ceramic coating can be made from the PRIME process using a cyanoacrylate binder and the novel coating technique produced a coating with properties at least as good as conventionally deposited thick ceramic coatings.

The binder has introduced a different coating practise in comparison to the standard ones with factors including mixing, application and curing and debinding behaviour. Because of these differences, there are many conclusions that can be drawn from this research, which are listed in the next chapter.

8

Conclusions & Recommendations for Further Research

Introduction

This chapter presents the conclusions of this investigation, and an outlook for further research. It has been shown that the novel PRIME coating technique as developed in this study could be used as an alternative fabrication method for producing thick coatings. With in-situ experiments it would be possible to achieve an improved understanding of the mixing behaviour and improve the sintering behaviour. An outlook is presented on the possible future research and applications based on this novel coating method.

8-1 Conclusions

As a result of the work conducted in this study on the investigation and production of a novel coating many conclusions can be drawn specifically associated with the research reported in this thesis. On this basis, the following sections summarise the main conclusions arising from this study.

8-1-1 *Materials Processing & Curing*

- Rapidly polymerized cyanoacrylate can be used as a carrier to make homogenous coating mixtures containing alumina and zirconia powders.
- Para-toluene sulphonic acid can be used effectively as an inhibitor in a mixture of powder and cyanoacrylate to prevent premature polymerization during mixing and handling of the coating mixture.
- The effective concentration of the acid required to perform as an effective inhibitor depends on the powder concentration, composition and surface area.
- Bi- (58%v) and uni-modal (45%v) alumina powders used in the study required 4%w and 2%w PTS acid to stabilize the binder, respectively. For mixtures containing 43%v stabilized zirconia powders, the acid level for efficient stabilisation of the cyanoacrylate during mixing was 4%w.
- Initiation of the polymerization reaction of the cyanoacrylate in the mixture can be effectively controlled by adding the appropriate amount of caffeine (1-2%w of cyanoacrylate used) to the mixture.
- For a fixed concentration of acid, adding more caffeine to the mixture resulted in faster initiation of curing and shorter curing time.
- The caffeine can either be pre-dissolved in the cyanoacrylate, or mixed directly into the coating mixture at the end of the mixing stage and before application of the coating.
- Mixing caffeine with the coating mixture has some advantages over pre-dissolving, including, better control of the viscosity and cure time of the mixture and reproducibility of the process.
- The viscosity of the coating mixture, as well as the strength of the adhesive bond between the substrate and the cured layers, was affected by the concentrations of dissolved acid and caffeine (C/A).
- It was found that a chemical compatibility between the coating mixture and the substrate surface (cyanoacrylate-powder-substrate system) is needed to produce a layer free interface, which would generally be expected to affect the coating properties after subsequent thermal treating,

- A process procedure for mixing cyanoacrylate and particulates for deposition as a coating onto flat, or irregular, substrates and subsequent curing was successfully investigated and established.
- It was found that mixtures comprising Loctite 408 with powder volume fractions ~45%v (uni-modal alumina), or ~58%v (bi-modal alumina), can be effectively inhibited with acid concentrations of 2%w and 4%w (of the binder) respectively and using 1%w caffeine powder as initiator.
- The hardnesses of the coatings were measured to be in the range 26.4 to 30.1 HV_{0.2} for uni-modal alumina powder (No.2) and 33.0 to 37.1 HV_{0.2} for bi-modal alumina (70%w powder No.2 and 30%w powder No.3) mixtures
- The curing time of the coating can be controlled by selecting an appropriate ratio of acid and caffeine in the mixture.
- The proposed method for the mixing and application of the coating could be satisfactorily performed on metallic and ceramic substrates over a period of time in a manner that the mixing, handling, deposition and reproducibility goals of the process could be achieved.

8-1-2 *Debinding*

- Cured mixtures can be debonded using a thermal debinding technique.
- TGA and DSC analysis of cured mixtures showed that debonding of the mixtures resulted in just one exothermic peak around 230°C.
- Isothermal heating at lower temperatures showed that debonding could be started and taken to completion at lower temperatures than apparent from the TGA and DSC, albeit at lower rates.
- It was noted that the debonding rate is maximum in the temperature range 170°C to 190°C.
- Step heating of the coating layers in air, using a controlled time-temperature procedure (to control the heating rate), can result in macro-defect free debonded layers, while maintaining coating integrity as well as the adhesion to the substrate.
- Step heating of uni-modal alumina samples carried out at 100, 120, 140, 150, 165, 180, 190, 200 and 220°C with a dwell time of 30 minutes at each

temperature, while the heating regime was revised for bi-modal alumina powder compacts (with a higher solid loading) by inserting more holding steps in the range 165°C to 200°C.

- It was found that the debonding of partially cured layers could significantly reduce the formation of gas bubbles in the mixture prior to sintering.

8-1-3 *Sintering*

- It was found that pressureless solid state sintering of debonded layers on either a pure alumina or molybdenum substrate did not produce fully densified adherent coatings using RF heating. Sintering of a debonded layer of uni-modal alumina powders at 1675°C for two hours resulted in a low hardness, i.e. 140 HK_{0.3}.
- Fine fumed silica powder was investigated as a sintering aid; this necessitated variations in the concentrations of PTS acid and caffeine required to inhibit and initiate the polymerization, and did not result in the sintering to full density of the alumina coatings. Experiments showed that the hardness of uni-modal alumina compacts was only increased to 470 HK_{0.3} using 3.5%w fumed silica powder addition to the coating mixture and sintering at 1620°C for 2 hours
- Using 96% Al₂O₃ alumina as the substrate resulted in good densification, a hardness comparable with the commercial alumina used as the substrate, and appropriate adhesion could be achieved for both uni-modal and bi-modal alumina powders.
- Sintering coatings containing uni- and bi-modal alumina powders at 1530°C for 20 minutes resulted in hardnesses of 1337 and 1309 HK_{0.3}, respectively,
- Applying stabilized zirconia coatings onto 96% alumina substrates resulted in a good hardness (995 HV_{0.3}) and apparently good adhesion to the substrate, but cracks were observed in the sintered coating, presumably arising as a result of the difference in thermal expansion coefficients of zirconia and alumina.

8-2 Recommendations for Further Research

The further work that could be undertaken subsequent to this project would probably be primarily concerned with the investigation of process improvements and properties of the layers, as well as studying new applications for this novel coating method. This involves producing new techniques for analysing parameters that are particular to this project.

8-2-1 Process developments

- Development of a model that describes cyanoacrylate polymerization when mixed with metallic and ceramic powders. Such a model would need to include parameters such as inhibition and initiator concentrations, powder surface area, and powder surface activity.
- Development of a mixing method or machine so that mixtures and coatings can be formed within much more controlled parameters. This would be an aid to investigating working parameters such as the rheology of the mixture or thickness of the coating.
- Detailed studies of the debinding behaviour (such as on-line measuring of mass loss whilst debinding) to help optimise the debinding stage.
- A very interesting aspect would be the use of local sintering methods, such as laser sintering.
- Another interesting area for study would be the incorporation of an appropriate interlayer to improve the adhesion of the coating.

8-2-2 Property measurements

Mechanical testing of the coating mixture, cured mixtures and layers, as well as the sintered layers to measure the relevant properties, such as tensile strength, Young's modulus, fracture toughness and adhesion would be invaluable in the characterisation and improvement of the coatings.

8-2-3 Applications

The examples of coatings shown in this thesis only touch the surface of the broad possible applications of this novel PRIME based coating method. Some further applications are as follows,

- The coatings created in this study were single layer, using multilayer coatings could be a challenging and worthwhile next step.
- The work was aimed specifically at producing fully densified coatings. However, there are applications where there are many possibilities for using porous ceramic layers, such as filters or medical implants.
- Nano-size powders and composite powders are now critical in many applications and essential to the production of new coatings and films. Investigation of the use of such powders would be another field of interest.

References

- Albano, M.A., & Garrido, L.B.,** (2005), "Influence of the Slip Composition on the Properties of Tape-Cast Alumina Substrates", *Ceramic International*, **31**, pp. 57-66
- Ai, Y., Liu, Y., Cui, T., & Varahraman, K.,** (2004), "Thin Film Deposition of a n-type Organic Semiconductor by Ink-Jet Printing Technique", *Thin Solid Film*, **450**, pp. 312-315
- Ainsley, A., & Gong, H.,** (1999), "Precision Sintering of Slip Cast Components", *Journal of Materials Processing Technology*, **95**, pp.201-209
- Anstis, G.R., Chantikul, P., Lawn B.R., & Marshall, D.B.,** (1981), "A Critical Evaluation of Indentation Techniques for Measuring Fracture Toughness: I, Direct Crack Measurements", *J. Amer. Ceram. Soc.*, **64**, pp. 533-538
- ASTM standard:** (2001) Standard Test method for: Apparent Shear Strength of Single-Lap-Joint Adhesively Bonded Metal Specimens by Tension Loading (Metal-to-Metal), Designation: D 1002-99, Vol. 15.06
- Axen, N., Hogmark, S., & Jacobson, S.,** (2000), "Friction and Wear Measurement Techniques", *Modern Tribology Handbook*, Ed. Bhushan, B., CRC, USA
- Barriere, Th., Liu, B., & Gelin, J.C.,** (2003), "Determination of the Optimal Process Parameters In Metal Injection Moulding From Experiments and Numerical Modeling" *Journal of Materials Processing Technology*, **143-144**, pp.634-644
- Binner, J.G.P.,** (1990), "Advanced Ceramic Processing and Technology", William Andrew Publishing, Noyes
- Birkinshaw, C.,** (2003), Private Communication, the University of Limerick
- Birkinshaw, C., Buggy, M., & O' Neill, A.,** (1996), "Reaction Moulding of Metal and Ceramic Powders", *J. Chem. Biotechnol.*, **66**, pp.19-24
- Birkinshaw, C., & Pepper, D.C.,** (1986), "The Thermal Degradation of Polymers of n-Butylcyanoacrylate Prepared Using Tertiary Phosphine and Amine Initiators", *Polymer Degradation and Stability*, **16**, pp. 241-259

- Blazell, P.F., & Evans, J.R.G.**, (2000), "Application of a Continuous Ink Jet Printer to Solid Freeforming of Ceramics", *Journal of Materials Processing Technology*, **99**, pp. 94-102
- Brookes, C.A., Zhang, L.Y., & May, P.W.**, (1997), "On the Mechanical Integrity Ratio of Diamond Coatings", *Diamond and Related Materials*, **6**, pp.348-352
- Brydson, R., Chen S.C., Riley, F.L., & Milne, S.J.**, (1998), "Microstructure and Chemistry of Intergranular Glassy Films in Liquid-Phase-Sintered Alumina", *J. Amer. Ceram. Soc.*, **81**, pp. 369-379
- Bull, S.J.**, (2001), "Can the Scratch Adhesion Test Ever Be Quantitative?", *Adhesion Measurement of Films and Coatings*, Ed. Mittal, K.L., Vol.2, pp. 107-130, VSP, USA
- Bull, S.J., Berasetegui, E.G., & Page, T.F.**, (2004), "Modelling of the Indentation Response of Coating and Surface Treatments", *Wear*, **256**, pp.856-866
- Bunshah, R.F.**, (2001), "Handbook of Hard coating", Noyes/William Andrew Publication
- Burnett, P.J., & Page, T. F.**, (1987), "The Friction and Hardness of Ion-Implanted Sapphire", *Wear*, **114**, pp. 85-96
- Cai, P.Z., Green, D.J., & Messing, G.L.**, (1997), "Constrained Densification of Alumina/Zirconia Hybrid Laminates, I:Experimental Observation of Processing Defects", *J. Amer. Ceram. Soc.*, **80**, pp. 1929-1939
- Calvert, P. & Cima, M.**, (1990), "Theoretical Models for Binder Burnout", *J. Amer. Ceram. Soc.*, **73**, pp.575-579
- Chinn, R.E.**, (2002), "Ceramography- Preparation and Analysis of Ceramic Microstructures", ASM International, Ohio, USA
- Choy, K.L.**, (2003), "Chemical Vapour Deposition of Coatings", *Progress in Materials Science*, **48**, pp.57-170
- Christofieldes, C., McHugh, P.E., Forn, A., & Picas, J.A.**, (2002), "Wear of a Thin Surface Coating: Modelling and Experimental Investigations", *Computational Materials Science*, **25**, pp.61-72
- Cook, B., & Allen, A.**, (1993), "Cyanoacrylates and Their Acid Values", *Int. J. Adhesion and Adhesives*, **13**, pp.73-76

- Dean, G., & Duncan, B.,** (1998), "Preparation and Testing of Bulk Specimens of Adhesives", Measurement Good Practice Guide, No.17, NPL, UK
- Denchev, Z.Z., & Kabaivanov, V.S.,** (1993), "Thermal Behaviour and Adhesive Properties of Some Cyanoacrylate Adhesives with Increased Heat Resistance", Journal of Applied Polymer Science, **47**, pp.1019-1028
- Dombroski, J.R., & Weemes, D.A.,** (1976), "2-Cyanoacrylate Adhesive Composition", US Patent, No.745757
- Eastop, T.D., & McConkey, J.,** (1993), "Applied Thermodynamics for Engineering Technologist", Ed.5, Longman Scientific & Technical, Hong Kong
- Edirisinghe, M.J.,** (1991), "Binder Removal from Moulded Ceramic Bodies in Different Atmospheres", J. Mater. Sci. Lett., **10**, pp.1338-1341
- Edirisinghe, M.J., & Evans, J.R.G.,** (1987), "Rheology of Ceramic Injection Moulding Formulation", Br. Ceram. Trans. J., **86**, pp.18-22
- Erickson, L.C., Hawthorne, H.M., & Troczynski, T.,** (2001), "Correlation Between Microstructural Parameters, Mechanical Properties and Wear Resistance of Plasma Sprayed Ceramic Coatings", Wear, **250**, pp. 569-575
- Erkaifa, H., Misirili, Z., & Baykara, T.,** (1998), "The effect of TiO₂ and MnO on Densification and Microstructural Development of Alumina", Ceramics International, **24**, pp.81-90
- Esposito, L., & Bellosi, A.,** (2001), "Joining of Ceramic Oxides by Liquid Wetting and Capillarity", Scripta Materialia, **45**, pp. 759-766
- Foresight, Report of Advanced Ceramic Task Force,** (2000), "Engineering our Future through Ceramics", The UK Office of Science and Technology, London
- Freitag, D.W & Richerson, D.W,** (1998), "Opportunities for Advanced Ceramics to Meet the Needs of the Industries of the Future", US Advanced Ceramics Association
- Furnas, C.C.,** (1928), Relation Between Specific Volume, Voids and Size Composition in Systems of Broken Soilds of Mixed Sizes", U.S. Bur. Mines Rep. Invest., No.1894
- Galusek, D., & Riley, F.L.L.,** (2002), "The Influence of Sintering Additives on the Indentation Response of Liquid-Phase-Sintered Polycrystalline Aluminas" Philosophical Magazine A, **82**, pp.2041-2057
- Garvie, R.C.,** (1970), "Zirconium Dioxide and Some of its Binary Systems", High Temperature Oxides, Part II, Ed. Alper, A.M., Academic Press, UK

- German, R.M.**, (1985), "Liquid Phase Sintering", Plenum Press, USA
- German, R.M.**, (1991), "Fundamentals of Sintering", Engineered Materials Handbook, Vol.4, Ceramic and Glasses, ASM, Ohio, USA
- German, R.M.**, (1996), "Sintering Theory and Practice", John Wiley & Sons, USA
- German, R.M., & Bose A.**, (1997), Injection Mouldings of Metals and Ceramics, Metal Powder Industries Federation, USA
- German, R.M., Farooq, N.S., & Kipphut, C.M.**, (1988), "Kinetics of Liquid Phase Sintering", Materials Science and Engineering, **105/106**, pp.215-224
- German, R.M., & Hens, F.H.**, (1991), "Key Issues in Powder Injection Moulding", American Ceramic Society Bulletin, **70**, pp.1294-1302
- Gitzen., W.H., & Louis, S.L.**, (1970), "Alumina as a Ceramic Material", The American Ceramic Society, Special Publication No.4.
- Goncalves, A.C.**, (2001), "Metallic Powder Injection Molding Using Low Pressure", Journal of Materials Processing Technology, **118**, pp.193-198
- Gong, J.**, (2002), "Indentation Toughness of Ceramics: a Statistical Analysis", Ceramic International, **28**, pp. 767-772
- Goswami, A.P., & Das G.C.**, (2000), "Role of Fabrication Route and Sintering on Wear and Mechanical Properties of Liquid-Phase- Sintered Alumina", Ceramics International, **26**, pp.809-819
- Guessasma, S., Montavon, G., & Coddet, C.**, (2005), "Velocity and Temperature Distributions of alumina-titania in -Flight Particles in the Atmospheric Plasma Spray Process", Surface & Coating Technology, **192**, pp.70-76
- Guillou, M-O., Henshall, J.L., & Hooper, R.M.**, (1993), "Indentation Cyclic Fatigue of Single-Crystal Magnesium Oxide", J. Amer. Ceram. Soc., **76**, pp.1832-1836
- Haber, A.H., & Smith, A.**, (1991), "Overview of Traditional Ceramics", Materials Handbook, Ceramics and Glasses, Vol. 4, ASM, Ohio, USA
- Hayakawa, S., & Sekida, S.**, (1989), "Chemical Properties" Advanced Technological Ceramics, Ed. Somiya, S., Chapter 9, Academic Press, UK
- Henshall, J.L., Guillou, M-O., & Hooper, R.M.**, (1995), "Point Contact Surface Fatigue in Zirconia Ceramics", Tribology International , **28**, pp.363-376

- Hiraga, T.**, (1989), "Magnetic Properties" Advanced Technological Ceramics, Ed. Somiya, S., Chapter 7, Academic press, UK
- Horn, R.G.**, (1995), "Particle Interactions in Suspensions", Ceramic Processing, Eds. Terpstra, R.A. et al., Chapman & Hall, UK
- Hull, J.B., Birkinshaw, C., & Buggy, M.**, (1996), "Novel Binder/Carrier System: Powder Reaction Injection Moulding Engineering (PRIME)", US Pat No.9615698.9
- Hwang, K.S., & Hsieh, Y.M.**, (1996), "Comparative Study of Pore Structure Evolution During Solvent and Thermal Debinding of Powder Injection Molded Parts", Metallurgical and Materials Transaction A, 27A, pp.245-253
- Inamori, K.**, (1989), "Biological Application", Advanced Technological Ceramics, Ed. Somiya, S., Chapter 11, Academic press, UK
- Janney, M.A.**, (1995), "Plastic Forming of Ceramics: Extrusion and Injection Moulding", Eds. Terpstra, R.A. et al., Chapman & Hall, UK
- Jantunen, H., Hu, T., Usimaki, A., & Leppavuori, S.**, (2004), "Tape Casting of Ferroelectric, Piezoelectric and Ferromagnetic Materials", Journal of the European Ceramic Society, 24, pp.1077-1081
- Jung, Y., Lee, J., Lee, J.H., & Kim, D.**, (2003), "Liquid- Phase Redistribution During Sintering of 8 mol% Ytria- Stabilized Zirconia", Journal of the European Ceramic Society, 23, pp. 499-503
- Kadolkar, P., & Dahotre, N.B.**, (2003), "Effect of Processing Parameters on the Cohesive Strength of Laser Surface Engineered Ceramic Coating on Aluminium Alloys", Materials Science and Engineering, A342, pp.183-191
- Kawakubo, T., & Yamamoto, N.**, (1989), "Thermal Properties", Advanced Technological Ceramics, Ed. Somiya, S., Chapter 8, Academic press, UK
- Kim, H.S.**, (2000), "On the Rule of Mixtures for the Hardness of Particle Reinforced Composites", Materials Science and Engineering, A289, pp. 30-33
- Kim, H., & Kim, T.**, (2002), Measurement of Hardness on Traditional Ceramics", Journal of the European Ceramic Society, 22, pp.1437-1445
- Kim, H., Lee, J., & Kim, J.**, (2000), "Densification Behaviors of Fine –Alumina and Coarse –Alumina Compacts During Liquid Phase Sintering With the Addition of Talc", J. Amer. Ceram. Soc., 83, pp.3128-3134
- King, A.G.**, (2002), "Ceramic Technology and Processing -A Practical Working Guide", William Andrew Publishing, USA

- Klien, L.C.**, (1988) "Sol-Gel Technology for Thin Films, Fibers, Preforms, Electronics and Specialty Shapes", USA
- Kosmos, A.S., Belch, L.I., & Susnik, D.**, (1996) "Additives in Coarse Grain Alumina Ceramics For Metallization", *Fizika A*, **5**, pp. 85-90
- Kotzev, D.L., Ward, T.C., & Dwight, D.W.**, (1981), "Assessment of the Adhesive Bond Properties of Allyl 2- Cyanoacrylate", *Journal of Applied Polymer Science*, **26**, pp.1941-1949
- Kwon, O.**, (1991), "Liquid Phase Sintering", *Engineering Materials Handbook*, Volume 4, Ceramic and Glasses, ASM, Ohio, USA
- Kwon, O., & Messing, G.L.**, (1990), "Kinetic Analysis of Solution-Precipitation During Liquid-Phase Sintering of Alumina", *J. Amer. Ceram. Soc.*, **73**, pp. 275-281
- Lance, D., Valdivieso, F., & Geouriot, P.**, (2004), "Correlation Between Densification Rate and Microstructural Evolution for Pure Alpha Alumina", *Journal of the European Ceramic Society*, **24**, pp. 2749-2761
- Laberty-Robert, C., Ansart, F., Delget, C., Manuel Gaudon, M., & Rousset, A.**, (2003), " Dense Yttria Stabilized Zirconia: Sintering and Microstructure", *Ceramics International*, **29**, pp.151-158
- Latella, B.A., & O'Conner, B.H.**, (1999), "Effect of Porosity on the Erosive Wear of Liquid-Phase Sintered Alumina Ceramics", *J. Amer. Ceram. Soc.*, **82**, pp. 2145-2149
- Laux, T., Killinger, A., Auweter-Kurtz, M., Gadow, R., & Wilhelmi, H.**, (1998), "Functionally Graded Ceramic Materials for High Temperature Application for Space Planes", *Proceedings, 5th International Symposium on Functionally Graded Materials*, Dresden, Germany
- Lawn, B.R.**, (1998), "Indentation of Ceramics with Spheres: A Century After Hertz", *J. Amer. Ceram. Soc.*, **81(8)**, pp.1977-1994
- Lee, H.**, (1981), "Cyanoacrylate Resins- The Instant Adhesives", Henry Lee Pasadena Technology Press, USA
- Lee, S.**, (2004), "Sintering Behaviour and Mechanical Properties of Injection – Moulded Zirconia Powder" *Ceramic International*, **30**, pp. 579-584
- Lee, W. E., & Rainforth, W.M.**, (1994), "Ceramic Micostructures- Property Control by Processing", Chapman & Hall, UK

- Lewis, J.A., & Galler, M.A.**, (1996), "Computer Simulation of Binder Removal From 2-D and 3-D Model Particulate Bodies", *J. Amer. Ceram. Soc.*, **79**, pp.1377-1388
- Li, J.F., Li, L., & Stott, F.H.**, (2004), "Multi-layered Surface Coatings of Refractory Ceramics prepared by Combined Laser and Flame Spraying", *Surface and Coating Technology*, **180-181**, pp. 500-505
- Li, Y., Jiang, F., Zhao, L., & Huang, B.**, (2003), "Critical Thickness in Binder Removal Process for Injection Molded Compacts", *Materials Science and Engineering*, **A362**, pp. 292-299
- Lii, D.**, (1998), "Thermal Effects of Atmosphere on the Thermal Debinding of Injection Moulding Si₃N₄ Components", *Ceramics International*, **24**, pp.99-104
- Liu, D., & Tseng, W.J.**, (1999), "Binder Removal from Injection Moulded Zirconia Ceramics", *Ceramics International*, **25**, pp. 529-534
- Loctite Company**, (2004), Data Sheets, Available at: http://www.loctite.com/int_henkel/loctite_uk/index.cfm?pageid=268&layout=1 (Accessed 20 February 2005)
- Maerky, C.**, (1997), PhD Thesis, "Analysis of The Soft Impresser Techniques With Application on The Fatigue of Engineering Ceramics", University of Exeter.
- Matsumoto, R.**, (1991), "Mechanical Consolidation", *Engineering Materials Handbook*, Volume 4, Ceramics and Glasses, ASM, Ohio, USA
- Matsusue, K.**, (1989), "Mechanical Properties", *Advanced Technological Ceramics*", Edi. Somiya, S., Chapter 12, Academic press, UK
- Maxwell, A.S.**, (2001), "Review of Test Methods For Coating Adhesion", Report MATC(A)49, National Physical laboratory, London
- McColm, I.J.**, (1990), "Ceramic Hardness", Plenum Press, USA
- Meneve, J., Ronkainen, H., & Anderson, P.**, (2001), "Scratch Adhesion Testing of Coated Surfaces-Challenges and New Directions" *Adhesion Measurement of Films and Coating*, Vol.2, Ed. Mittal, K.L., pp.79-106, VSP, USA
- Millet, G.H.**, (1981), "Properties of Cyanoacrylates- An overview", *Adhesive Age*, **24**, pp.10-27
- Miranzo, P., Tabernero, L., Moya, J., & Jurado, J.**, (1990), "Effect of Sintering atmosphere on the Densification and Electrical Properties of Alumina", *J. Amer. Ceram. Soc.*, **73**, pp. 2119-2121

- Miyayama, M., (1991),** "Engineering Properties of Single Oxides", Engineering Materials Handbook, Volume 4, Ceramics and Glasses, ASM, Ohio, USA
- Morrell, R., (1985),** "Handbook of Properties of Technical Ceramics, Part 1; An Introduction For Engineer And Designer", National Physical Laboratory, London
- Morrell, R., (1987),** "Handbook of Properties of Technical Ceramics, Part 2; Data Review, Section I; High- Alumina Ceramics", National Physical Laboratory, London
- Morrell, R., (1997),** "Flexural Strength Testing of Ceramics and Hardmetals", Measurement Good Practice Guide No.7, National Physical Laboratory, London
- Mott, M., & Evans, J.R.G., (1999),** "Zirconia /Alumina Functionally Graded Material Made by Ceramic Ink Jet Printing", Materials Science and Engineering, A271, pp. 344-352
- Mutsuddy, B.C., (1991)** "Coalescence of Particles", Engineering Materials Handbook, Volume 4, Ceramics and Glasses, ASM, Ohio, USA
- Mutsuddy, B.C., (1991),** "Injection Molding", Engineering Materials Handbook, Volume 4, Ceramics and Glasses, ASM, Ohio, USA
- Mutsuddy, B.C., & Ford R.G., (1995),** "Ceramic Injection Molding", Chapman & Hall, UK
- Negulescu, I.I., Calugaru, E., & Vasile, C., (1987),** "Thermal Behavior of Poly (α - Cyanoacrylate)s", Journal of Macromolecular Science Chemistry, 124, pp. 75-83
- Ng, S.H., (2004),** Private Communication
- Ng, S.H., Hull, J.B., & Henshall, J.L., (2003),** "Machining of a Novel Alumina/Cyanoacrylate Green Ceramic Compact", Proceeding of the 12th International Scientific Conference- Achievements in Mechanical & Material Engineering, Poland, pp. 645-648
- Ng, S.H., Hull, J.B., & Henshall, J.L., (2004),** "Manufacture of a Novel Alumina/Cyanoacrylate Advanced Ceramic Material", 3rd Materials Research Conference, London
- Nunomura, S., Nakayama, J., Hirosh, A., Kamigatio, O., Takahara, K., & Petrie, E.M., (1996),** "Joining of Plastics, Elastometers, and Composites", Handbook of Plastics, Elastometers, and Composites, 3rd Edition, C.A. Harper, Mc Grawhill
- Petrie, E.M., (2000),** "Handbook of Adhesives and Sealants", McGraw-Hill.

- Petrie, E.M.**, (1996), "Joining of Plastics, Elastomers, and Composites", Handbook of Plastics, Elastomers, and Composites, 3rd Edition, C.A. Harper, Mc Grawhill
- Petrie, E.M.**, (2000), "Handbook of Adhesives and Sealants", McGraw-Hill.
- Psyllaki, P.P., Jeandin, M., & Pantelis, D.I.**, (2001), "Microstructure and Wear Mechanisms of Thermal-Sprayed Alumina Coatings", *Materials Letters*, **47**, pp.77-82
- Quinn, G.D.**, (1998), "Hardness Testing of Ceramics", *Advanced Materials and Processing*, **154**, pp.23-27
- Redway, K.**, (2002), Private Communication, Loctite Company
- Reed J.S.**, (1995), "Principles of Ceramics Processing", Second edition, John Wiley & sons, Inc
- Rice, R.W., Wu, C.C., & Borchelt, F.**, (1994), "Hardness-Grain-Size Relations in Ceramics", *J. Amer. Ceram. Soc.*, **77**, pp. 2539-2553
- Richerson, D.W.**, (1992), "Modern Ceramic Engineering", 2nd edition, MarcelDekker, Inc.
- Rickerby, D.**, (1996), "Measurement of Coating Adhesion", *Metallurgical and Ceramic Protective Coatings*, Ed. Stern, K.H., Chapman&Hall
- Ridgway, J.S.**, (2000), Thesis, "Development of Novel Ceramic Processing Techniques for Manufacture of Heart Valves", Nottingham Trent University
- Ridgway, J.S., Hull, J.B., & Gentle, C.R.**, (1997), "Development of a Novel Binder System for Manufacture of Ceramic Heart Valve Prostheses", *Proc. Conf. AMME'97*, Wisla, Poland, pp.165-169
- Ridgway, J.S., Hull, J.B., & Gentle, C.R.**, (1998), "Design for Powder Reaction Moulding Ceramic Conduct Heart Valves", *Proc. Conf HC Tech*, Bulgaria
- Ridgway, J.S., Hull, J.B., & Gentle, C.R.**, (2001), "Development of a Novel Binder System for Manufacture of Ceramic Heart Valve Prostheses", *Journal of Materials Processing Technology*, **109**, pp. 161-167
- Ridgway, J.S., Hull, J.B., & Gentle, C.R.**, (2003), "A PRIME Approach for the Moulding of Conduit Ceramic Parts", *Journal of Materials Processing Technology*, **133**, pp. 181-188
- Robinson, S.K., & Paul, M.R.**, (2001), "Debinding and Sintering Solutions for Metals and Ceramics", *MPR*, June, pp.24-34

- Saravanan, P., Selvarajan, V., Rao, D.S., Joshi, S.V., & Sundararajan, G.,** (2000), "Influence of Process Variables on the Quality of Detonation Gun Sprayed Alumina Coatings", *Surface and Coating Technology*, **123**, pp.44-54
- Sarikaya, O.,** (2005), "Effect of Some Parameters on Microstructure and Hardness of Alumina Coating Prepared by Air Plasma Spraying Process", *Surface and Coating Technology*, **190**, pp.388-393
- Sato, T., Besshi, T., & Matsui, M.,** (1998), "A New Near Net-Shape Forming for Alumina", *Journal of Materials Processing Technology*, **79**, pp. 125-132
- Sathiyakumar, M., & Gnanam, F.D.,** (2003), "The Influence of additives on Density, Microstructure and Mechanical Properties Of Alumina", *Journal of Materials Processing Technology*, **133**, pp.282-286
- Schoenberg, J.E.,** (1990), "Cyanoacrylates", *Engineering Materials Handbook Vol.3, Adhesives and Sealants*, ASM international, Ohio, USA
- Shengjie, Y., Lam, Y.C., Chai, J.C., & Tam, K.C.,** (2004), "Simulation of Thermal Debinding: Effects of Mass Transport on Equivalent Stress", *Computational Materials Science*, **30**, 496-503
- Sharafat, S., Kobayashi, A., Chen, Y., & Ghoneim N.M.,** (2002), "Plasma Spraying of Micro-Composite Thermal Barrier Coatings", *Vacuum*, **65**, pp. 415-425
- Shaw, N.J., & Brook, R.J.,** (1986), "Structure and Grain Coarsening During the Sintering of Alumina", *J. Amer. Ceram. Soc.*, **69**, pp. 107-110
- Shi, Z., & Guo, Z.X.,** (2004), "Kinetic Modeling of Binder Removal in Powder-Based Compacts", *Materials Science and Engineering*, **A365**, pp.129-135
- Singh, H., Puri, D., & Prakash, S.,** (2005), "Some Studies on Hot Corrosion Performance of Plasma Sprayed Coatings on a Fe-Based Superalloy", *Surface & Coating Technology*, **192**, pp. 27-38
- Smallman R.E., & Bishop R.J.,** (1999), "Modern Physical Metallurgy and Materials Engineering", Elsevier Butterworth-Heinemann, UK
- Smith, J.P., & Messing, G.L.,** (1984), "Sintering of Bimodally Distributed Alumina Powders", *J. Amer. Ceram. Soc.*, **64**, pp.238-242
- Somiya, S.,** (1989), "Types of Ceramics", *Advanced Technological Ceramics*, Ed. Somiya, S., Chapter 2, Academic Press, UK
- Stevens, R.,** (1986), "An Introduction to Zirconia- and Zirconia Ceramics", Magnesium Elektron Ltd., UK

- Stevens, R.**, (1991), "Engineering properties of Zirconias", Engineering Materials Handbook, Volume 4, Ceramics and Glasses, ASM, Ohio, USA
- Supati, R., Loh, N.H., Khor, K.A., & Tor, S.B.**, (2000), "Mixing and Characterization of Feedstock for Powder Injection Molding", Materials Letters, **44**, pp. 109-114
- Svancarek, P., Glusek, D., Calvert, C., Loughran, F., Brown, A., Brydson, R., & Riley, F.L.**, (2004), "A Comparison of the Microstructure and Mechanical Properties of Two Liquid Phase Sintered Alumina Containing Different Molar Ratios of Calcia-Silica Sintering Additives " Journal of the European Ceramic Society, **24**, pp. 3453-3463
- Szeto, Y.S.**, (1989), Thesis, "The Chemistry of Poly (alkyl a-cyanoacrylate)s", Queen's University of Belfast.
- Taruta, S., Takano, T., Takusagawa, N., Okada, K., & Otsuka, N.**, (1996), "Liquid Phase Sintering of Bimodal Size Distributed Alumina Powder Mixtures", Journal of Materials Science, **31**, pp. 573-579
- Trunec, M., & Cihlar, J.**, (1997), "Thermal Debinding of Injection Moulded Ceramics", Journal of the European Ceramic Society, **17**, pp.204-209
- Trunec, M., & Cihlar, J.**, (2002), "Thermal Removal of Multicomponent Binder from Ceramic Injection Mouldings", Journal of the European Ceramic Society, **22**, pp.2231-2241
- Tseng, W.J.**, (2000), "Influence of Surfactant on Rheological Behaviour of Injection-Moulded Alumina Suspensions", Materials Science and Engineering, **A289**, pp.116-122
- Tseng, W.J., & Hsu, C.**, (1999), "Cracking Defect and Porosity Evolution During Thermal Debinding in Ceramic Injection Moulding", Ceramics International, **25**, pp.461-466
- Ullner, C., Germak, A., Doussal, H.E., Morrell, R., Reich, T., & Vandermeullen, W.**, (2001), "Hardness Testing on Advanced Technical Ceramics", Journal of the European Ceramic Society, **21**, pp.439-451
- Wachtman, J.B., & Haber, R.A.**, (1993), "Ceramic Films and Coatings", William Andrew Publishing, USA
- Waddington, C.P., Zhang, L.Y., Brookes, E.J., & Brookes, C.A.**, (1997), "Methodology For Measuring Contact Pressure to Cause Failure of Ceramics and Coating Using Softer Blunt Cones", Surface Engineering, **13**, pp.199-203

- Wakino, K.**, (1989), "Electrical and Electronic Properties", Advanced Technological Ceramics, Ed. Somiya, S., Chapter 6, Academic press, UK
- Wei, W., Tsai, S., & Hsu, K.**, (1998), "Effects of Mixing Sequence on Alumina Prepared by Injection Molding", Journal of the European Ceramic Society, **18**, pp. 1445-1451
- Wirth, D.G.**, (1991), "Ceramic Substrate", Engineered Materials Handbook, Vol.4, Ceramic and Glasses, ASM, Ohio, USA
- Yeh, T., & Sacks, M.**, (1988), "Effect of Particle Size Distribution on the Sintering of Alumina", J. Amer. Ceram. Soc., **71**, C484-487
- Zeng, W., Gao, L., Gui, L., & Guo, J.**, (1999), "Sintering Kinetics of α -Al₂O₃ Powder", Ceramics International, **25**, pp. 723-726
- Zhao, J., & Harmer, M.**, (1987), "Sintering of Ultra- High- Purity Alumina Doped Simultaneously with MgO and FeO", J. Amer. Ceram. Soc., **70**, pp. 860-866